Analysis and Optimization Methods for Centralized Processing of Chassis

February 2017

A Research Report from the National Center for Sustainable Transportation

Anastasios Chassiakos, California State University, Long Beach
Hossein Jula, California State University, Long Beach
Timothy VanderBeek, California State University, Long Beach
Matt Shellhammer, California State University, Long Beach
Samnang Dona An, California State University, Long Beach

National Center for Sustainable Transportation

METRANS Transportation Center
USC CSULB

About the National Center for Sustainable Transportation

The National Center for Sustainable Transportation is a consortium of leading universities committed to advancing an environmentally sustainable transportation system through cutting-edge research, direct policy engagement, and education of our future leaders. Consortium members include: University of California, Davis; University of California, Riverside; University of Southern California; California State University, Long Beach; Georgia Institute of Technology; and University of Vermont. More information can be found at: ncst.ucdavis.edu.

U.S. Department of Transportation (USDOT) Disclaimer

Acknowledgments

This study was funded by a grant from the National Center for Sustainable Transportation (NCST), supported by USDOT through the University Transportation Centers program. The authors would like to thank the NCST and USDOT for their support of university-based research in transportation, and especially for the funding provided in support of this project.

NCST

Analysis and Optimization Methods for Centralized Processing of Chassis

A National Center for Sustainable Transportation Research Report

February 2017

Anastasios Chassiakos, Ph.D., College of Engineering, California State University, Long Beach

Hossein Jula, Ph.D., College of Engineering, California State University, Long Beach

Timothy VanderBeek, College of Engineering, California State University, Long Beach

Matt Shellhammer, College of Engineering, California State University, Long Beach

Samnang Dona An, College of Engineering, California State University, Long Beach

NCST

[page left intentionally blank]

TABLE OF CONTENTS

LIST OF FIGURES iii
LIST OF TABLES v
LIST OF ACRONYMS & ABBREVIATIONS vi
LIST OF SYMBOLS vii
ABSTRACT ix
1 Introduction 1
2 Background and Literature Review 3
2.1 POLB and POLA Complex 3
2.2 Typical Transaction Types for Container Transport 4
2.3 Problems Present at the POLB and POLA 6
2.4 Chassis Leasing and the Gray Chassis Pool 7
2.5 Centralized Processing of Chassis 8
3 Problem Description 8
3.1 Problem 8
3.2 Objectives 9
3.3 Expected Outcomes 10
4 Analytical Models and Optimization 10
4.1 Import-Only Transactions with Unlimited Chassis Processing Facility Usage 11
4.2 Import-Only Transactions with Limited Chassis Processing Facility Usage 13
4.3 Import and Export Formulation 15
5 Case Study Set-Up 19
5.1 Marine Terminals 20
5.2 Trucking Companies 22
5.3 Central Processing Facilities 22
5.4 Travel Time Between Locations 24
6 Results of the Case Study Simulations 24
6.1 Parameter P: Additional Processing Time 25
6.2 Import-Only Transactions with Unrestricted CPF Usage 25
6.3 Import-Only Transactions with Restricted CPF Availability 38
6.4 Import/Export Integer Linear Formulation with the Full Model 41
6.5 Linear Program Sensitivity Analysis 50
7 Discrete Event Simulation Model (DESM) 56
7.1 Validation of the discrete event simulation model 57
7.2 Comparison of Optimal Solution to the Baseline Case using the DESM 60

NCST

7.3 Heuristic Methods 62
7.4 Simulations with Varying Traffic Conditions Using the DESM 67
7.5 Preliminary Model for Calculations of CO2 Emissions 68
8 Conclusions 70
9 References 72
Appendix A-1

LIST OF FIGURES

Figure 1. Annual TEU throughput at POLA & POLB (1997-2016) 3
Figure 2. Annual change in TEU throughput for the combined ports (2012-16) 4
Figure 3. Description of container transaction types at marine terminals 5
Figure 4. Chassis ownership in the POLA/POLB area 7
Figure 5. Schematic of centralized processing of chassis concept 9
Figure 6. Node locations for the full model used in the simulation 20
Figure 7. POLB & POLA marine terminal locations 21
Figure 8. Example of chassis stacking layout within a CPF 23
Figure 9. Schematic of centralized processing of chassis concept (6-node case) 27
Figure 10. Optimum transaction routing vs. parameter *P* (6-node case) 29
Figure 11. Optimum transaction routing vs. parameter *P* (10-node case) 33
Figure 12. Number of transactions routed through CPFs at optimality, as a function of *P* 34
Figure 13. Evaluation of Optimal Solution: Difference in the Number of Transactions 36
Figure 14. Evaluation of Optimal Solution: Percent difference in the Value of the Objective Function 37
Figure 15. Evaluation of Optimal Solution: Percent Difference in Computational Time 38
Figure 16. Optimum transaction routing vs. parameter *P*: one CPF available 39
Figure 17. Optimal value of the objective function vs. parameter *P*: one CPF available 40
Figure 18. Number of CPFs used vs. total travel time 42
Figure 19. Map of the optimal CPF locations (*P* = 1200 sec) 43
Figure 20. Map of the optimal CPF locations (*P* = 1200 sec) 44
Figure 21. Ranking of CPF candidate locations (*P* = 600 sec) 49
Figure 22. Percent change in total travel time vs. ratio of (export/import) transactions 55
Figure 23. Discrete event simulation model of the transaction routing process 56
Figure 24. Average number of transactions routed through each CPF 58
Figure 25. Percent difference in the value of the objective function between the DESM and the analytical model plotted for each simulation run 59
Figure 26. Running average of the percent difference in the value of the objective function between the DESM and the analytical model, plotted over 100 simulations 59
Figure 27. DSEM for baseline case 60
Figure 28. Comparison between the optimal solution and direct routing to MTs 61
Figure 29. Running average of percent difference between optimal solution and direct routing to MTs 61
Figure 30. Percent increase in the value of the objective function between Heuristic H1 and the optimal solution 64

Figure 31. Percent increase in the value of the objective function between Heuristic H2 and the optimal solution 65
Figure 32. Comparison of Heuristics H1 & H2 67
Figure 33. Total travel time with varying traffic conditions at optimality 68

APPENDIX

Figure A-1. Chassis racks A-1
Figure A-2. Specialized hydraulic stacker lifting a chassis A-2
Figure A-3. Example of vertical chassis storing A-2
Figure A-4. Port of Virginia arrangement of chassis storage A-3
Figure A-5. (Top View) Chassis rack with 16 vertically stacked chassis A-4
Figure A-6. Chassis rack (front view) with 20ft chassis (left) and 40ft chassis (right) A-5
Figure A-7. Schematic of a generic chassis storage Model 1 ..... A-6
Figure A-8. Schematic of a generic chassis storage Model 2 ..... A-7
Figure A-9. Schematic of a generic chassis storage Model 3 ..... A-8
Figure A-10. Example of chassis storage Model 3 (Google Earth) A-9
Figure A-11. Schematic of a generic chassis storage Model 4 (wheeled containers) A-10

LIST OF TABLES

Table 1. Notation for analytical model (Type 2 transactions) 11
Table 2. Notation for analytical model (Type 1 & Type 2 transactions) 15
Table 3. Locations of POLB and POLA marine terminals used in the case study 20
Table 4. POLB and POLA import and export statistics for 2015 21
Table 5. Potential CPF locations and capacities for chassis storage 23
Table 6. Travel times (in seconds) from TCs to CPFs without traffic congestion (6-node case) ... 26
Table 7. Travel times (in seconds) from CPFs to TCs without traffic congestion (6-node case) ... 26
Table 8. Travel Times (in seconds) from TCs to MTs without traffic congestion (6-node case) ... 27
Table 9. Optimal transaction routing (6-node case) 28
Table 10. Travel times (in seconds) from TCs to CPFs without traffic (10 node case) 30
Table 11. Travel times (in seconds) from CPFs to TCs without traffic (10 node case) 31
Table 12. Travel times (in seconds) from TCs to MTs without traffic (10 node case) 31
Table 13. Optimal transaction routing (10-node case) 32
Table 14. CPF capacity utilization (*P*=1200 sec) 35
Table 15. Ranking of potential CPF locations if only CFP is available 41
Table 16. Top CPF ranking vs. number of CPFs used: *P* = 1200 sec 44
Table 17. Top CPF ranking vs. number of CPFs used: *P* = 600 sec 46
Table 18. Top CPF ranking for import / export transactions 50
Table 19. CPF rankings vs CPF capacity: import transactions only 51
Table 20. CPF rankings vs CPF capacity: import and export transactions 53
Table 21. CPF rankings vs total number of transactions: import and export transactions 54
Table 22. CPF routing with the DESM (*P* = 1200 sec) 57

APPENDIX

Table Appendix A-1. CPF capacity estimates for different stacking configurations A-11

LIST OF ACRONYMS & ABBREVIATIONS

API	Application Program Interface
APL	American President Lines
CET	Chassis Exchange Terminal
CGM	Compagnie Générale Maritime
COSCO	China Ocean Shipping Company
CPF	Chassis Processing Facility
CRB	Chassis Rack Block
DCLI	Direct Chassis Link, Inc.
DESM	Discrete Event Simulation Model
FEU	Forty-Foot Equivalent Unit
ft	foot, feet
GDM	Google Distance Matrix
GGS	Global Gateway South
I-710	California Interstate 710
ID	Identification, Identity, Identifier
LBCT	Long Beach Container Terminal
LBCT	Lot Block
LLC	Limited Liability Company
min	Minute; minutes
MT	Marine Terminal
OOCL	Orient Overseas Container Line
PeMS	Performance Measurement System (CalTrans)
POLA	Port of Los Angeles
POLB	Port of Long Beach
POP	Pool of Pools
RP	Resource Pool
sec	second; seconds
SMA	Swedish Maritime Association
SSA	Stevedoring Services in America
TC	Trucking Company
TEU	Twenty-Foot Equivalent Unit
TRAPAC	Trans-Pacific
TTI	Total Terminals International
US	United States of America
WBCT	West Basin Container Terminal

LIST OF SYMBOLS

C_0	Proportion of number of chassis initially stored at CPF$_j$ with respect to capacity $C_0 = N_{ACj}(0) / C_{ACj}$ %
C_k	Cost of establishing and maintaining CPF k
C_{ACj}	Capacity of CPF$_j$
CPF_k	The k^{th} chassis processing facility $k \in [1, \dots, K]$
$C_{T_jF_k}$	Cost of transactions between TC_j and CPF_k
$C_{F_kM_l}$	Cost of transactions between CPF_k and MT_l
$C_{T_jM_l}$	Cost of transactions between TC_j and MT_l
C_{cpf}	Maximum cost allowable for establishing and maintaining CPFs
e_a^b	$a-th$ standard basis vector of size b
J	Number of TCs collaborating with the CPFs
K	Number of potential sites for CPFs
L	Number of participating MTs
MT_l	The l^{th} destination point $l \in [1, \dots, L]$
m_{jl}	Number of export transactions from TC_j to MT_l
$\mathbb{N}^0$	Set of nonnegative integer numbers
$N_{ACj}(t)$	Number of available chassis at CPF$_j$ at time t
N_{cpf}	Maximum number of allowable CPFs
n_{jl}	Number of transactions from TC_j to MT_l
P	Additional time required for chassis retrieval at a marine terminal, as compared to retrieval time at a CPF: $P = T_{MT} - T_{CPF}$
$\mathbb{R}$	Set of real numbers
$rep_b(a)$	Vector of size b with all components equal to a
T_{MT}	Average chassis retrieval time at a marine terminal
T_{CPF}	Average chassis retrieval time at a chassis processing facility
TC_j	The j^{th} origin point $j \in [1, \dots, J]$
T_{ICR}	Computational time when the integer constraint is relaxed

T_{ICP}	Computational time when the integer constraint is present
T_{DR}	Total travel time for direct routing to marine terminals
T_{OPT}	Total travel time for optimal solution routing through CPFs
T_{H1}	Total travel time when heuristic H1 is used
T_{H2}	Total travel time when heuristic H2 is used
U_k	Total storage capacity of chassis at CPF_k
$U_{k,0}$	Initial available storage capacity of chassis at CPF_k
x_{jkl}	Number of transactions from TC_j to MT_l routed through CPF_k
y_{jl}	Number of transactions routed directly from TC_j to MT_l
$\mathbb{Z}$	Set of integers
α_{jkl}	Number of export transactions from TC_j to MT_l routed through CPF_k
β_{jl}	Number of export transactions routed directly from TC_j to MT_l
Δ	Percent difference in computational/travel time
$\mathbf{0}_b$	Vector of size b with all components zero
$\mathbf{1}_b$	Vector of size b with all components one

Analysis and Optimization Methods for Centralized Processing of Chassis

ABSTRACT

The twin ports of Long Beach (POLB) and Los Angeles (POLA), consisting of fourteen individually gated terminals, combine to create the largest container port complex in the US. In 2015, the combined ports handled 15.4 million 20-foot equivalent units (TEUs), a 56% increase since 2000, expected to grow higher in the future. This large number of containers and the associated trips to/from the ports, result in traffic congestion, noise pollution, and greenhouse gas emissions in the vicinity of the ports. The current project studies the concept of "Centralized Processing of Chassis," and the possibility of using it to mitigate some of these problems. This concept revolves around an off-dock terminal (or several off-dock terminals), referred to as Chassis Processing Facilities (CPFs). A CPF is located close to the port, where trucks will go to exchange chassis, thereby reducing traffic at the marine terminals, resulting in reduced travel times and reduced congestion. The current project develops the required analytical framework for modeling and optimization of the CPF use. The developed analytical model is applied to a case study in the Los Angeles/Long Beach port area. The case study identifies sixteen locations in the vicinity of the ports that can be potentially used as CPFs, and examines several scenarios of container pickup/drop-off transactions. The study presents comparisons between the case when chassis exchanges occur at the CPFs versus the case when chassis exchanges occur at the marine terminals. It is shown that a reduction of up to 20% in total travel time can be achieved when using the CPFs, as compared to using only the marine terminals. The study also shows that using up to three of the potential sixteen CPFs provides significant improvements to total travel time, but using more than three CPFs will have insignificant additional benefits. Moreover, a discrete event simulation model is developed and used for detailed simulation scenarios, as well as for examining and evaluating the performance of heuristic methods.

Keywords: Chassis Exchange Terminal, Linear Programming, Transportation Optimization, Port of Long Beach, Port of Los Angeles

1 Introduction

The twin ports of Long Beach (POLB) and Los Angeles (POLA), consisting of fourteen individually gated terminals, combine to create the largest container port complex in the US. In 2015, the combined ports handled 15.4 million 20-foot equivalent units (TEUs) [1], [2]. This number represents a 56% increase since 2000 and is expected to grow even higher in the future. Since most of the containers in use are 40-foot units (FEU), the figure of 15.4 million TEUs corresponds to approximately 8.3 million individual container units (the conversion factor most widely used in the industry is: One Individual Container = 1.85 TEU, [3]).

This large volume of container trips results in traffic congestion, noise pollution, and greenhouse gas emissions in the areas around and within the ports [3]. Traffic congestion, in turn, impacts the local economy by decreasing reliability of delivery time for the imported goods, which forces local businesses to use more operators, equipment, distribution centers and inventory in order to deliver their end-products on time. One metric that can be used to assess the overall effectiveness of a proposed solution is the total travel time for trucks transporting goods from/to the ports during a given time period. This metric is correlated strongly with all of the items outlined above. Therefore, any concept which could minimize this total travel time can be expected to have a positive effect on all of these areas [4], [5], [6], [7]. One such concept which could have a positive impact on total travel time is the concept of Centralized Processing of Chassis.

The main objective of this project is to study and develop an analytical framework for modeling and optimization of the concept of Centralized Processing of Chassis around marine container terminals, with application to the Los Angeles/Long Beach port area, which will be used as a particular case study of interest. This concept revolves around an off-dock terminal (or several off-dock terminals), which in this project will be referred to as Chassis Processing Facilities (CPFs). A CPF is located close to the port, where trucks will go to exchange chassis, thereby reducing traffic at the marine terminals, resulting in reduced travel times for trucks and the potential of reduced emissions. The methodologies developed herein could contribute to improving the traffic conditions in the areas surrounding the ports, by modifying the patterns of truck trips to the ports. They have the potential to reduce traffic congestion on the roads to the terminal gates, air pollution and economic loss that would result from unnecessary delays and truck waiting times.

A detailed example of the application of the methodology developed in this project is presented through a case study, which focuses on the ports of Los Angeles and Long Beach, and on the areas in the vicinity of the ports. The case study considers the locations of all existing container marine terminals in the POLB/POLA complex, the locations of a number of existing trucking companies in the greater Los Angeles/Long Beach geographical area, and a set of potential locations for Chassis Processing Facilities. The developed methodology is used to study and analyze the optimal CPF locations, and to evaluate the potential benefits of the Centralized Processing of Chassis concept. The analytical models and optimization are first defined for import-only transactions under the assumption that any of the potential CPF

locations are available and can be used. This model is then expanded to include import and export transactions, using only a small number of CPFs, which have storage capacity limitations. The expanded model, which optimizes the chassis exchange process with a smaller number of CPFs allows for policy makers to make decisions for optimal solutions while taking into account budgetary constraints.

Analysis based on the simulation results, shows that the total travel time can be improved up to 20% when using CPFs to store and retrieve chassis as compared to the baseline situation where the chassis are retrieved directly from the marine terminals. In addition, optimal locations and CPF combinations are recommended, and a sensitivity analysis is performed. The sensitivity analysis explores the impact on the optimal solution that can result from limitations on CPF capacities, the total numbers of transactions, and the ratio of import to export transactions.

Furthermore, a discrete simulation model has been developed which serves as a tool for performing more detailed studies, taking into account items not included in the analytical model, such as daily traffic variations, queuing at the marine terminals, and other random variations, representing a more realistic environment.

The rest of the report is organized as follows:

- Section 2 provides the project background, current practices, and motivation.
- Section 3 describes the problem objectives, problem set up, and expected outcomes.
- Section 4 presents the development of the mathematical analysis including the optimization approach.
- Section 5 describes the case study scenarios.
- Section 6 presents the results of the analytical case study simulations and sensitivity analysis.
- Section 7 provides the discrete event model simulations and results.
- Section 8 presents a summary of the report, conclusions, and suggestions for future work.

2 Background and Literature Review

2.1 POLB and POLA Complex

As mentioned previously, the combined twin ports of Los Angeles and Long Beach create the largest container port complex in the US. Figure 1 shows the annual TEU throughput at the POLA and POLB for the period 1997-2016 [1], [2]. Although the explosive growth of the first ten years exhibited a slowdown after the recession of 2008, it has achieved quite a healthy recovery in the last five years reaching or surpassing its pre-recession levels. The numbers in Figure 1 include both loaded and empty units, destined for import or export. Figure 2 shows the change in total annual TEU throughput for the combined ports. The yearly change over the last five years is positive. The total container throughput (import and export) through the POLA and POLB is expected to grow in the future, correlated with population increase, domestic demand for inexpensive manufactured goods, as well as global demand for US products, and improving competitiveness of US industry. Handling a large number of the necessary container transactions requires intensive management of operations, changes in transportation policy and modernized equipment.

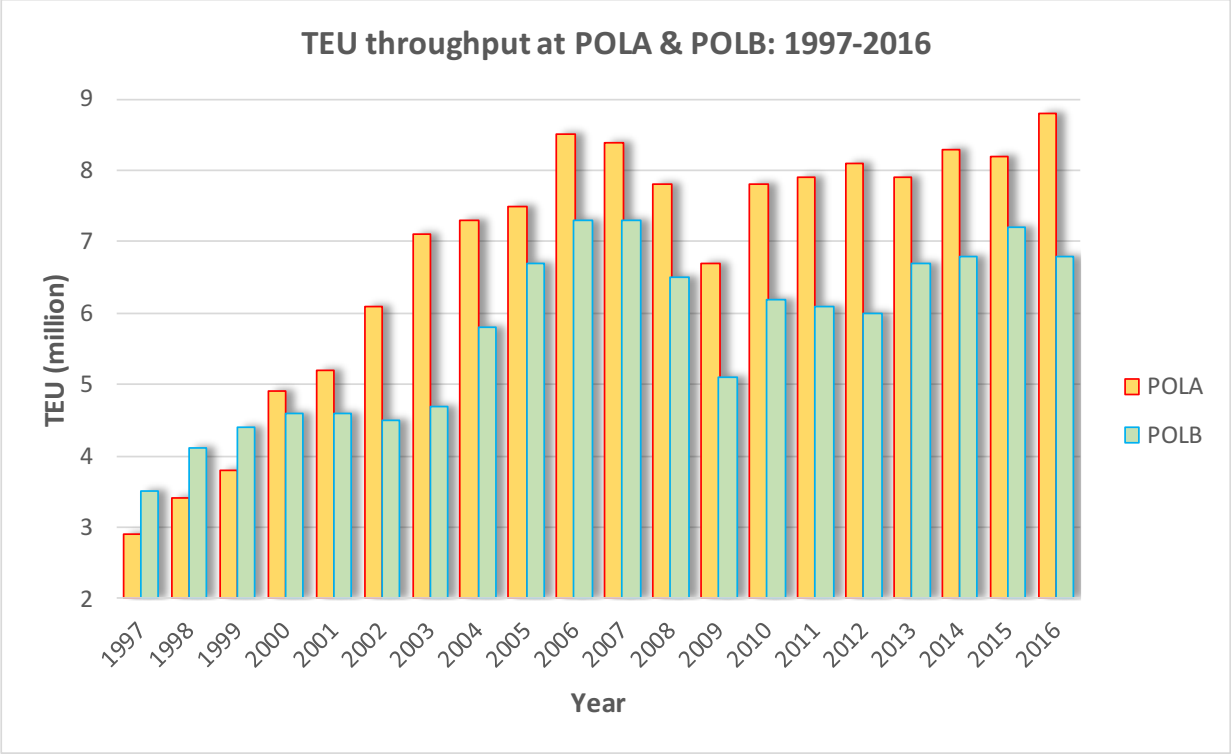

Figure 1. Annual TEU throughput at POLA & POLB (1997-2016)

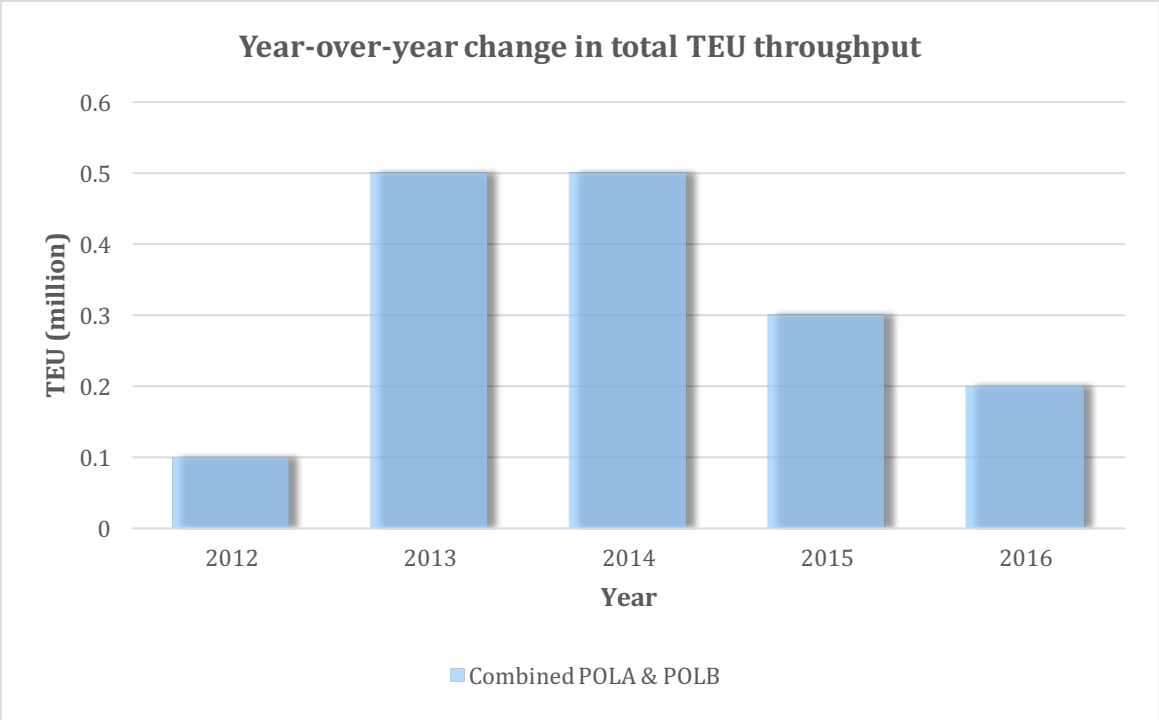

Figure 2. Annual change in TEU throughput for the combined ports (2012-16)

2.2 Typical Transaction Types for Container Transport

In order to complete the export/import operations for containers to/from marine terminals the transporting trucks will perform a series of steps including: dropping off export containers; dropping off empty chassis used for exports; picking up chassis for imports; picking up import containers; and traveling between any locations necessary to complete these tasks [8], [9]. The most common transaction types for trucking companies at marine terminals are listed below.

Type 1: Single transaction export
Type 2: Single transaction import of grounded container (i.e. container not loaded on a chassis)
Type 3: Single transaction import of wheeled container (i.e. container already loaded on chassis)
Type 4: Dual transaction export / import of grounded import
Type 5: Dual transaction export / import of wheeled import

Figure 3 shows the flow of bobtails, chassis and containers for transaction types 1-5 described above. The flows presented in Figure 3 depict the operations taking place between the in-gate and out-gate of the marine terminal. The truck's point of origin or its final destination, which could be for example a warehouse or a parking space at the trucking company, are not depicted

in the figure. The following list provides a detailed explanation of the operations taking place for each type of the five transactions.

- **Type 1: Single transaction export**. The bobtail leaves the trucking company (or its point of origin) with a chassis on which an export container is loaded. It arrives at the in-gate; enters the terminal; drops off the export container and the chassis in the marine terminal; passes through the out-gate and arrives at its final destination as a bobtail.
- **Type 2: Single transaction import of grounded container**. The bobtail arrives at the in-gate; picks up a chassis at the marine terminal; picks up an import container; passes through the out-gate and arrives at its final destination as a bobtail with a chassis and a container.
- **Type 3: Single transaction import of wheeled container**. The bobtail arrives at the in-gate; picks up a chassis which has already been loaded with an import container; passes through the out-gate and arrives at its final destination as a bobtail with a chassis and a container.
- **Type 4: Dual transaction export / import of grounded import**. The bobtail arrives at the in-gate with a chassis on which an export container is loaded; enters the terminal; drops off the export container; loads an import container to the chassis; passes through the out-gate and arrives at its final destination as a bobtail with a chassis and a container.
- **Type 5: Dual transaction export / import of wheeled import**. The bobtail arrives at the in-gate with a chassis on which an export container is loaded; enters the terminal; drops off the export container; drops off the chassis; picks up a chassis which has already been loaded with an import container; passes through the out-gate and arrives at its final destination as a bobtail with a chassis and a container.

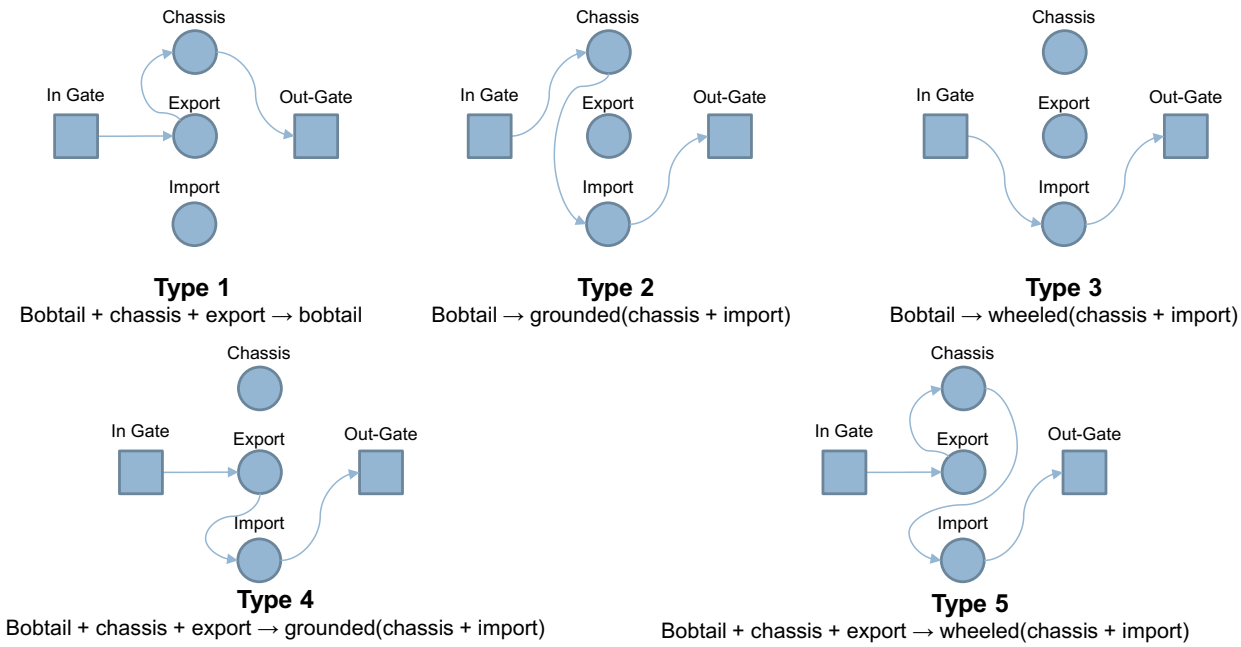

Figure 3. Description of container transaction types at marine terminals.

2.3 Problems Present at the POLB and POLA

Two of the key hurdles to overcome in managing POLB and POLA container imports and exports include chassis shortages and heavy traffic surrounding the port.

2.3.1 Shortage of Chassis

In the POLB and POLA, there are approximately 100,000 chassis available for leasing and transporting containers to and from warehouses, stores, factories, rail yards and container terminals [10]. Among these 100,000 chassis available to the trucking companies there are chassis supplied by various third party chassis leasing companies. However, terminals within the ports do not always have chassis available from each company. At times, chassis required by the trucks are either not available anywhere in the terminal or are dislocated and need to be repositioned.

Prior to 2014 chassis companies did not work together or have a neutral chassis pool, and shortages and dislocations of chassis occurred frequently. Trucks would often be required to travel between terminals and perform additional trips to pick up or drop off chassis at specific locations in addition to picking up and dropping off the containers for export and import. This was a lengthy and cumbersome process and generated additional queues at each terminal [11].

The shortage of chassis can significantly lengthen truck turn times and cause additional cost for trucking companies and increase emissions at the port. Furthermore, lack of chassis could mean that the container will be kept at the carrier ship for prolonged time and the storage fees will continuously accumulate. The shipper will have to pay additional charge for the failure to discharge a container from the carrier ship within the agreed time frame, known as demurrage charge. Also, when containers are not discharged in a timely manner, the shippers will face a congested space in their area of operation. Such an issue would leave the shippers no choice but to rent additional storage area. This would lead to more expensive carrying cost and delayed delivery time [11]. According to POLA/POLB terminal operators and PierPass officials (2014) one of the core reasons for port congestion is lack of chassis [8].

2.3.2 Traffic Congestion

Traffic congestion around the port is also contributing to the slowdown of port operations. At the POLB and POLA trucks are coming from many locations to drop off or pick up containers and chassis, where the freeways that truck drivers must use to access the port are also used heavily by commuters traveling through the densely populated area surrounding Los Angeles. [12]. The most heavily used freeway to get to and from the POLB and POLA is California Interstate 710 (I-710). I-710 has for the most part, four lanes, heavily packed with trucks and commuter vehicles during rush hours, causing major congestion problems in the vicinity of the ports.

As the American economy expands, there are more demands for commercial operations, increased freight, and increased numbers of foreign commercial partners. These growing

factors give rise to recurring congestion at freight bottlenecks, creating a conflict between freight and passenger service. Moreover, as demands for trading partners increase, more freight ships will be docked to the ports. Handling more transactions also means that the ports will have to increase their processing capacity. This increase will undoubtedly cause the entrance to the port and the areas within the port itself to be heavily congested as well [12].

Congestion in and outside of the port is detrimental to the economy of Southern California, as well as to that of the US as a whole. When there is additional congestion, port operators take much longer to unload cargo ships. Supply chains carrying goods through the POLB and POLA can then become slowed to the point where some retailers find it necessary to redirect their goods. The goods are then redirected by sea or air to other ports on the East Coast where they can be further distributed, resulting in reduced income for the surrounding area as well as additional costs for the retailers themselves [13] [14].

2.4 Chassis Leasing and the Gray Chassis Pool

In late 2014, three chassis leasing companies: Direct Chassis Link, Inc. (DCLI), Trans-Pacific (TRAPAC) Intermodal and Flexi-Van, along with the container terminal operator SSA Marine, (formerly Stevedoring Services in America), decided to develop a solution to the chassis shortage problem. The four companies own about 95% of the total 100,000 chassis in use in the POLA/POLB area. Figure 4 shows the chassis ownership distribution among the four companies, as of 2014. The proposed solution to the chassis shortage problem came in the form of a chassis management model known as “Gray Chassis Pool” or “Pool of Pools (POP)” [8], [10].

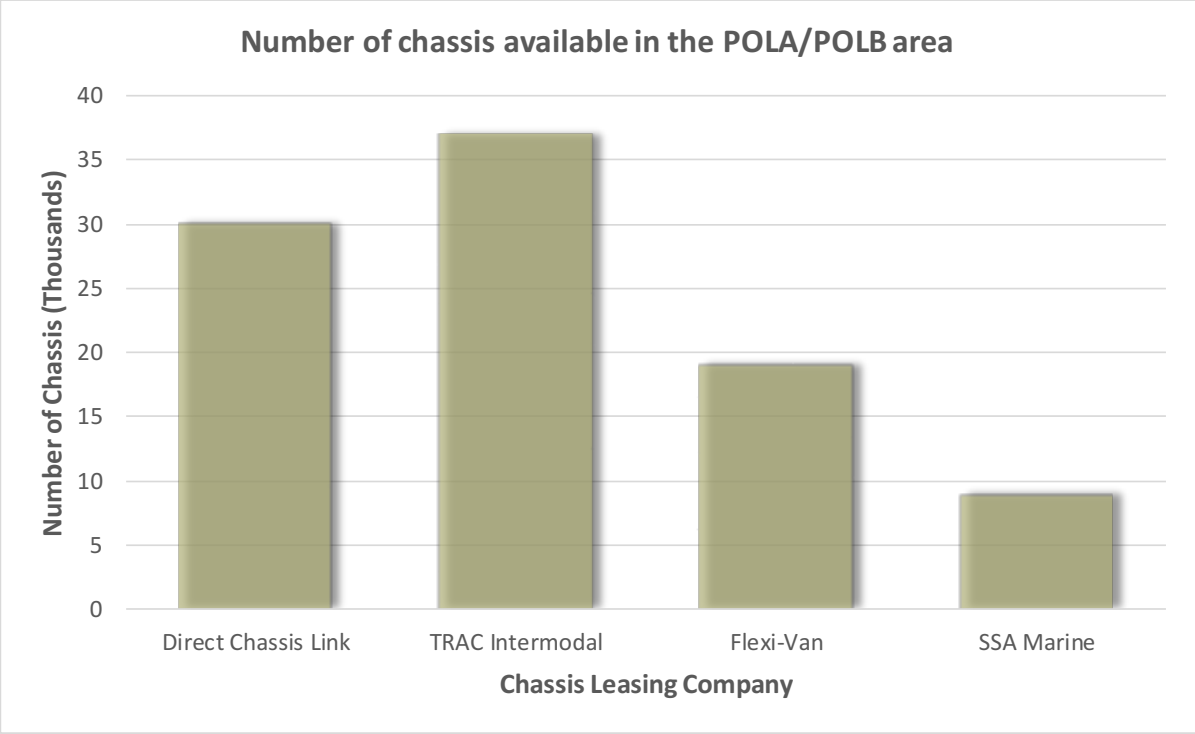

Figure 4. Chassis ownership in the POLA/POLB area

The POP is a neutral, interoperable chassis pool that was launched in February 2015, from DCLI, TRAC Intermodal and Flexi-Van, in cooperation with the POLA, POLB and SSA Marine. Their chassis are pooled together to provide a more efficient way of obtaining chassis for trucking companies, which are able to use the chassis from any of the chassis companies interchangeably. Thus, a trucker can pick any chassis from the POP and drop it off at any designed POP storage area without having to worry about returning chassis to the same exact location. Since truckers have access to any chassis, it allows for a smoother operation at the port and fewer inefficiencies in chassis-related operations. However, the pools still remain commercially independent and are in competition with one another. A third party service provider manages the billing and other proprietary information among these pools [15].

Nonetheless, even with the improved flexibility, interoperability and efficiency which the POP has introduced, the port still suffers some repositioning issues and the heavy traffic congestion problems remain.

2.5 Centralized Processing of Chassis

The concept of Centralized Processing of Chassis was introduced as one method for improving travel times associated with container retrieval. This concept was introduced in Europe as the Chassis Exchange Terminal (CET) [16] . In the CET concept, the centralized processing of chassis was defined as an off-dock terminal (or a number of off-dock terminals) located close to the port, where trucks would go to retrieve imports or drop-off exports instead of unloading and loading containers at the marine terminal. The first step in the operation with the CET involves a container being loaded onto a chassis at the marine terminal. The second step includes the chassis transport to the CET during off-peak hours, for example at night time. The last step in the operation is when a truck carrying a chassis with a container drives into the CET. At this point, the truck exchanges the chassis it brought into the CET with another chassis and container, which has already been transported to the CET during the second step. The exchange operation involves unhooking a chassis and hooking up another one at the CET. This is much simpler, more efficient, and a lot faster operation than the operation of unloading and loading containers and performing chassis exchanges at a regular marine terminal [17] [18] [19].

3 Problem Description

3.1 Problem

The large volume of container trips results in traffic congestion in the areas around and within the ports and is expected to grow even higher in the future. It is clear that any system which helps reducing the total travel time for trucks between their points of origin and their destinations, is worth investigating, since as a consequence it will reduce traffic congestion, noise and emissions, in addition to saving time for both truckers and port operators. Such systems improve the travel time reliability and help the local (and indirectly national) economy to grow. By improving travel time reliability, local businesses require fewer operators and less

equipment to deliver goods on time and need fewer distribution centers and less inventory to account for unreliable deliveries [4].

3.2 Objectives

The main objective of this project is to provide an analytical framework for modeling and optimization of the concept of Centralized Processing of Chassis around marine container terminals, with specific application to the POLB and POLA. This concept builds off of the European Chassis Exchange Terminal (CET) concept and revolves around an off-dock terminal (or a number of off-dock terminals), referred to as Chassis Processing Facilities (CPFs). For the purposes of this report the points of origin are generically referred to as TCs (trucking companies) and the destination points are generically referred to as MTs (marine terminals). A CPF is located close to the port, where trucks will go to exchange chassis, thereby reducing traffic at the MTs, allowing for reduced travel times for trucks and the potential of reduced emissions.

The general concept for the centralized processing of chassis is captured in Figure 5. We assume that there exist J regional TCs which can use any of K potential CPFs as they perform various transactions with the L local MTs. The travel time (cost for the objective function) between each of the possible locations is given by:

- $C_{T_jF_k}$ is the travel time between the j[th] TC, TC_j, and k[th] CPF, CPF_k
- $C_{F_kM_l}$ is the travel time between CPF_k and the l [th] MT, MT_l
- $C_{T_jM_l}$ is the travel time between TC_j and MT_l is given by

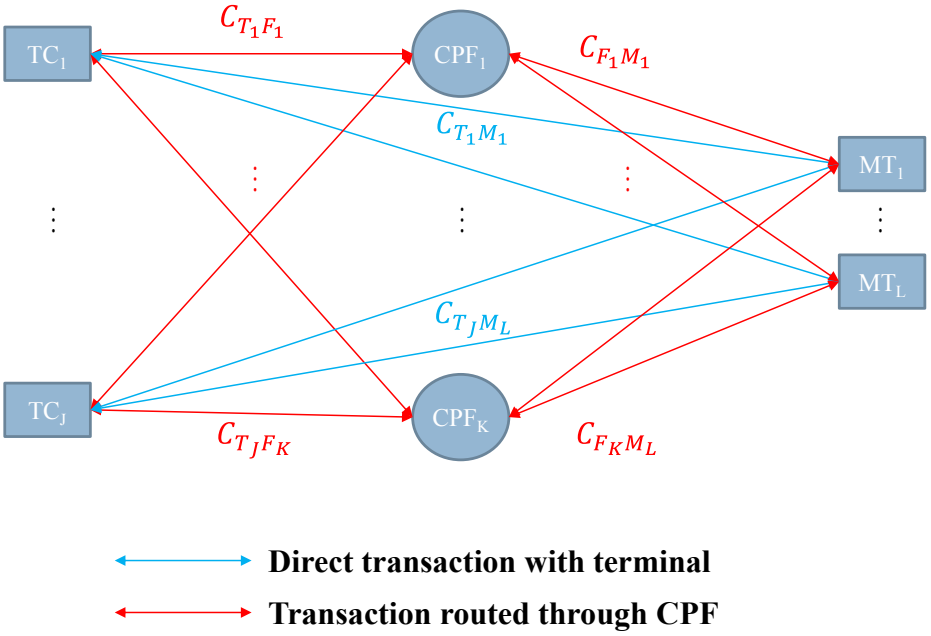

Figure 5. Schematic of centralized processing of chassis concept.

Note that among the types of transactions described in Section 0 (Figure 3) the Type 1 and Type 2 transactions are the only types which would be anticipated to contribute to a noticeable reduction in total transaction time if a CPF was used. In the case of Type 1 transactions, the export container can be dropped off at the desired marine terminal, and then the chassis can be returned to the CPF for storage and later retrieval. In the case of a Type 2 transaction, the chassis for import can be picked up at the CPF before entering the marine terminal to load the import container. In both cases if the chassis exchange transaction can be done more efficiently when it is performed outside of the marine terminal (where it is anticipated that there will be less congestion) this could offer improvements in total time for the transaction. In Type 3 and 4 transactions one can see that no chassis exchange activities are necessary. In a Type 3 transaction the wheeled import includes a container already loaded on a chassis and can simply be picked up by the bobtail. In a Type 4 transaction the chassis used for the export container is the same one onto which the import container can be loaded afterwards. Finally, Type 5 transactions, although they include a chassis exchange, would not be anticipated to have any reduced transaction times using an external CPF. This is due to the fact that after dropping off an export, the bobtail must drop off the chassis used so it can pick up a wheeled import at the same terminal, making in inefficient to travel to an external CPF to drop off the chassis only to return back to the marine terminal to pick up the wheeled import.

3.3 Expected Outcomes

The methodologies developed herein could contribute to improving the traffic conditions in the areas surrounding the ports, by modifying the patterns of truck trips to the ports. They have the potential to reduce traffic congestion on the roads to the terminal gates, air pollution and economic loss resulting from unnecessary delays and truck waiting times.

4 Analytical Models and Optimization

In this section, a general analytical framework for the *Centralized Processing of Chassis* concept is developed. Using this framework, the optimal number and optimal locations of chassis processing facilities will be identified.

Due to the recent changes in chassis leasing policies, such as the introduction of the grey chassis pool in the ports of Long Beach and Los Angeles, it is assumed in this analysis that chassis of similar types are interchangeable and transactions do not need to take into account chassis ownership.

Given:

- the locations and storage capacities of the destination points, MT_l, $l = 1, \dots, L$
- the locations of the points of origin TC_j, $j = 1, \dots, J$
- a set of transactions needed between TC_j, $l = 1, \dots, J$, and MT_l, $l = 1, \dots, L$, during a time interval of interest
- the locations of potential CPF_k sites, $k = 1, \dots, K$,

the objective herein is:

- to minimize the total travel time during the time interval of interest for all transactions by allocating one or more sites (among all potential sites) for *CPF*s, and determining the optimal routing of each of the transactions through CPFs.

4.1 Import-Only Transactions with Unlimited Chassis Processing Facility Usage

For the analytical formulation of the centralized processing of chassis concept, the following notation is used (Table 1).

Table 1. Notation for analytical model (Type 2 transactions)

J	Number of TCs collaborating with the CPFs
K	Number of potential sites for CPFs
L	Number of participating MTs
TC_j	The j^{th} origin point $j \in [1, \dots, J]$
CPF_k	The k^{th} chassis processing facility $k \in [1, \dots, K]$
MT_l	The l^{th} destination point $l \in [1, \dots, L]$
n_{jl}	Number of transactions from TC_j to MT_l
U_k	Storage capacity of chassis at CPF_k
$C_{T_jF_k}$	Cost of transactions between TC_j and CPF_k
$C_{F_kM_l}$	Cost of transactions between CPF_k and MT_l
$C_{T_jM_l}$	Cost of transactions between TC_j and MT_l
x_{jkl}	Number of transactions from TC_j to MT_l routed through CPF_k
y_{jl}	Number of transactions routed directly from TC_j to MT_l

Note that in the initial model, some assumptions have been made in order to simplify the modeling process: The cost of all trips between TCs to CPFs and to MTs has been assumed to be symmetric, i.e. the cost is the same whether the trip is from a TC to CPF or from a CPF to TC, and similarly for MTs. Also, the cost is assumed fixed, based on distance only, without any time varying component that may result from traffic variations at different times of the day. Note also that no specific distinction is given in this problem as to alternate chassis / container sizes or the complete set of transaction types defined above. This problem assumes only Type 2 transaction (grounded imports) using a single common chassis.

These simplifications allow the problem to be defined as an integer linear program where the objective function is given by:

$$\min \quad \sum_{j=1}^{J}\sum_{k=1}^{K} C_{T_jF_k}\left(\sum_{l=1}^{L} x_{jkl}\right) + \sum_{k=1}^{K}\sum_{l=1}^{L} C_{F_kM_l}\left(\sum_{j=1}^{J} x_{jkl}\right) + \sum_{j=1}^{J}\sum_{l=1}^{L} C_{T_jM_l} y_{jl} \tag{1}$$

$$\text{s.t.} \quad \sum_{k=1}^{K} x_{jkl} + y_{jl} = n_{jl} \quad j = 1, \dots, J; \;\; l = 1, \dots, L \tag{2}$$

$$\sum_{j=1}^{J}\sum_{l=1}^{L} x_{jkl} \leq U_k \quad k = 1, \dots, K \tag{3}$$

$$x_{jkl} \in \mathbb{N}^0 \; j = 1, \dots, J; \;\; l = 1, \dots, L; \;\; k = 1, \dots, K \tag{4}$$

$$y_{jl} \in \mathbb{N}^0 \; j = 1, \dots, J; \;\; l = 1, \dots, L \tag{5}$$

In equation (1) the total travel time for completion of all transactions is minimized using the decision variables x_{jkl} (transactions from TC_j to MT_l routed through CPF_k) and y_{jl} (transactions routed directly from TC_j to MT_l). Constraint (2) is the conservation of transactions constraint, forcing the total number of transactions routed directly to MTs and through CPFs to be equal to the total transaction demand. Constraint (3) ensures that the CPF chassis supply is sufficient to meet import demands. Constraints (4)-(5) ensure that the number of transactions routed on any possible path are non-negative integers (i.e. belong to the set of natural numbers including zero).

In order to use a standard solver this was reformulated as an integer linear program below where the objective function is then given by

$$\min \quad f^T x \tag{6}$$

$$\text{s.t.} \quad x \in \mathbb{Z} \tag{7}$$

$$Ax \leq \alpha \tag{8}$$

$$Bx = \beta \tag{9}$$

$$x \geq \gamma \tag{10}$$

where

$$x = \begin{bmatrix} x_{1,1,1} \\ \vdots \\ x_{1,1,L} \\ \vdots \\ x_{1,K,1} \\ \vdots \\ x_{1,K,L} \\ x_{2,1,1} \\ \vdots \\ x_{J,K,L} \\ y_{1,1} \\ y_{1,2} \\ \vdots \\ y_{J,L} \end{bmatrix} \quad f = \begin{bmatrix} C_{T_1F_1} + C_{F_1M_1} \\ \vdots \\ C_{T_1F_1} + C_{F_1M_L} \\ \vdots \\ C_{T_1F_K} + C_{F_KM_1} \\ \vdots \\ C_{T_1F_K} + C_{F_KM_L} \\ C_{T_2F_1} + C_{F_1M_1} \\ \vdots \\ C_{T_JF_K} + C_{F_KM_L} \\ C_{T_1M_1} \\ C_{T_1M_2} \\ \vdots \\ C_{T_JM_L} \end{bmatrix} \tag{11}$$

$$A = \begin{bmatrix} rep_J\left(\left[1_L^T, 0_{(K-1)*L}^T\right]\right), 0_{J*L}^T \\ rep_J\left(\left[0_L^T, 1_L^T, 0_{(K-2)*L}^T\right]\right), 0_{J*L}^T \\ \vdots \\ rep_J\left(\left[0_{(k-1)*L}^T, 1_L^T, 0_{(K-k)*L}^T\right]\right), 0_{J*L}^T \\ \vdots \\ rep_J\left(\left[0_{(K-1)*L}^T, 1_L^T\right]\right), 0_{J*L}^T \end{bmatrix} \quad \alpha = \begin{bmatrix} U_1 \\ U_2 \\ \vdots \\ U_K \end{bmatrix} \tag{12}$$

$$B = \begin{bmatrix} rep_K\left((e_1^L)^T\right), 0_{(J-1)*K*L}^T, \left(e_1^{J*L}\right)^T \\ rep_K\left((e_2^L)^T\right), 0_{(J-1)*K*L}^T, \left(e_2^{J*L}\right)^T \\ \vdots \\ 0_{(j-1)*K*L}^T, rep_K\left((e_l^L)^T\right), 0_{(J-j)*K*L}^T, \left(e_{(j-1)*L+l}^{J*L}\right)^T \\ \vdots \\ 0_{(J-1)*K*L}^T, rep_K\left((e_L^L)^T\right), \left(e_{J*L}^{J*L}\right)^T \end{bmatrix} \quad \beta = \begin{bmatrix} n_{1,1} \\ \vdots \\ n_{1,L} \\ n_{2,1} \\ \vdots \\ n_{2,L} \\ \vdots \\ n_{J,L} \end{bmatrix} \tag{13}$$

$$\gamma = \left[0_{J*K*L+J*L}\right]^T \tag{14}$$

where

$$e_a^b = [e_1, e_2, \dots, e_b]^T, e_a = 1, e_j = 0 \; \forall j \neq a \tag{15}$$

$$rep_b(a) = [a_1, a_2, \dots, a_b], a_j = a \; \forall \, j \tag{16}$$

$$0_b = [\alpha_1, \alpha_2, .., \alpha_b]^T, \alpha_j = 0 \; \forall \, j \tag{17}$$

$$1_b = [\alpha_1, \alpha_2, .., \alpha_b]^T, \alpha_j = 1 \; \forall \, j \tag{18}$$

4.2 Import-Only Transactions with Limited Chassis Processing Facility Usage

The mathematical formulation in the section above assumed that any number of CPFs could be used from within the potential CPFs identified. This may be unrealistic as cost constraints of establishing and maintaining each CPF may prevent some of the sites from being used. One method for putting a constraint on the cost would be to set a limit on the total number of CPFs which can be used. This would require two additional variables (listed below) and the inclusion

of equations (19) and (20) in the original problem formulation equations (1) through equation (5)

N_{cpf} Maximum number of allowable CPFs

z_k Variable identifying if CPF k has any transactions

$$z_k = \begin{cases} 1, & \sum_{j=1}^{J}\sum_{l=1}^{L} x_{jkl} \geq 0 \\ 0, & \text{otherwise} \end{cases}, k = 1, \dots, K \quad (19)$$

$$\sum_{k=1}^{K} z_k \leq N_{cpf} \quad (20)$$

This can be updated further to take into account the potential varying cost of establishing and maintaining the CPFs between each potential site. Assuming that these costs are known, and that the maximum allowable cost for establishing and maintaining the CPFs is also given, the original problem is updated as follows:

$$z_k = \begin{cases} 1, & \sum_{j=1}^{J}\sum_{l=1}^{L} x_{jkl} \geq 0 \\ 0, & \text{otherwise} \end{cases}, k = 1, \dots, K \quad (21)$$

$$\sum_{k=1}^{K} z_k * C_k \leq C_{cpf} \quad (22)$$

where

C_{cpf} Maximum cost allowable for establishing and maintaining CPFs

C_k Cost of establishing and maintaining CPF k

This can be written as an integer program as follows.

$$\min \sum_{j=1}^{J}\sum_{k=1}^{K} C_{T_j F_k}\left(\sum_{l=1}^{L} x_{jkl}\right) + \sum_{k=1}^{K}\sum_{l=1}^{L} C_{F_k M_l}\left(\sum_{j=1}^{J} x_{jkl}\right) + \sum_{j=1}^{J}\sum_{l=1}^{L} C_{T_j M_l} y_{jl} \quad (23)$$

s.t.

$$\sum_{k=1}^{K} x_{jkl} z_k + y_{jl} = n_{jl} \quad j = 1, \dots, J; \; l = 1, \dots, L \quad (24)$$

$$\sum_{j=1}^{J}\sum_{l=1}^{L} x_{jkl} z_k \leq U_k \quad k = 1, \dots, K \quad (25)$$

$$\sum_{k=1}^{K} z_k * C_k \leq C_{cpf} \quad (26)$$

$$x_{jkl} \in \mathbb{N}^0 \; j = 1, \dots, J; \;\; l = 1, \dots, L; \;\; k = 1, \dots, K \quad (27)$$
$$y_{jl} \in \mathbb{N}^0 \; j = 1, \dots, J; \;\; l = 1, \dots, L \quad (28)$$
$$z_k \in \{0, 1\} \; k = 1, \dots, K \quad (29)$$

A comparison of the formulation of Section 0 to the formulation of Section 0, shows that:

- Equations (23), (26), (27), and (28) are identical to equations (1), (4), (22) and (5) respectively.
- Constraints (24), (25) are similar to constraints (2) and (3), representing the conservation of transactions and ensuring that the CPF chassis supply is sufficient to meet import demands, and
- Constraints (29) restrict variables z_k to binary values, as defined in equation (21).

It is noted that the introduction of variables z_k in (24) and (25), results in a set of nonlinear (quadratic) constraints. In the Case Study and simulations presented in Sections 0 and 0, the nonlinear problem has been solved by optimizing a number of linear problems. Further details of the solution are given in Section 0.

4.3 Import and Export Formulation

In this section, the import-only formulation is expanded to include both import and export transactions (i.e. Type 1 and Type 2 transactions). The notation used is as follows:

Table 2. Notation for analytical model (Type 1 & Type 2 transactions)

J	Number of TCs collaborating with the CPFs
K	Number of potential sites for CPFs
L	Number of participating MTs
TC_j	The j^{th} trucking company $j \in [1, \dots, J]$
CPF_k	The k^{th} chassis processing facility $k \in [1, \dots, K]$
MT_l	The l^{th} marine terminal $l \in [1, \dots, L]$
n_{jl}	Number of import transactions from TC_j to MT_l
m_{jl}	Number of export transactions from TC_j to MT_l
U_k	Storage capacity of chassis at CPF_k
$U_{k,0}$	Initial Storage capacity of chassis at CPF_k
$C_{T_jF_k}$	Cost of transactions between TC_j and CPF_k
$C_{F_kM_l}$	Cost of transactions between CPF_k and MT_l
$C_{T_jM_l}$	Cost of transactions between TC_j and MT_l
x_{jkl}	Number of import transactions from TC_j to MT_l routed through CPF_k
y_{jl}	Number of import transactions routed directly from TC_j to MT_l
α_{jkl}	Number of export transactions from TC_j to MT_l routed through CPF_k
β_{jl}	Number of export transactions routed directly from TC_j to MT_l

This can be written as an integer linear program as follows.

$$\min \quad \sum_{j=1}^{J}\sum_{k=1}^{K} C_{T_jF_k}\left(\sum_{l=1}^{L} x_{jkl}\right) + \sum_{k=1}^{K}\sum_{l=1}^{L} C_{F_kM_l}\left(\sum_{j=1}^{J} x_{jkl}\right) + \sum_{j=1}^{J}\sum_{l=1}^{L} C_{T_jM_l} y_{jl} + \sum_{j=1}^{J}\sum_{k=1}^{K} C_{T_jF_k}\left(\sum_{l=1}^{L} \alpha_{jkl}\right) + \sum_{k=1}^{K}\sum_{l=1}^{L} C_{F_kM_l}\left(\sum_{j=1}^{J} \alpha_{jkl}\right) + \sum_{j=1}^{J}\sum_{l=1}^{L} C_{T_jM_l}\beta_{jl} \tag{30}$$

$$\text{s.t.} \quad \sum_{k=1}^{K} x_{jkl} + y_{jl} = n_{jl} \quad j = 1, \dots, J; \;\; l = 1, \dots, L \tag{31}$$

$$\sum_{k=1}^{K} \alpha_{jkl} + \beta_{jl} = m_{jl} \quad j = 1, \dots, J; \;\; l = 1, \dots, L \tag{32}$$

$$\sum_{j=1}^{J}\sum_{l=1}^{L}(x_{jkl} - \alpha_{jkl}) \leq U_{k,0} \quad k = 1, \dots, K \tag{33}$$

$$\sum_{j=1}^{J}\sum_{l=1}^{L}(x_{jkl} - \alpha_{jkl}) \geq U_{k,0} - U_k \quad k = 1, \dots, K \tag{34}$$

$$x_{jkl} \in \mathbb{N}^0 \; j = 1, \dots, J; \;\; l = 1, \dots, L; \;\; k = 1, \dots, K \tag{35}$$

$$y_{jl} \in \mathbb{N}^0 \; j = 1, \dots, J; \;\; l = 1, \dots, L \tag{36}$$

$$\alpha_{jkl} \in \mathbb{N}^0 \; j = 1, \dots, J; \;\; l = 1, \dots, L; \;\; k = 1, \dots, K \tag{37}$$

$$\beta_{jl} \in \mathbb{N}^0 \; j = 1, \dots, J; \;\; l = 1, \dots, L \tag{38}$$

In equation (30) the total travel time for completion of all transactions is minimized using the decisions variables x_{jkl}, y_{jl}, α_{jkl}, and β_{jl}. Constraints (31) and (32) provide the equality constraint forcing the total number of import and export transactions routed directly to MTs and routed through CPFs to be equal to the total transaction demand. Constraints (33) and (34) ensure that the chassis supply and capacity at each CPF is sufficient to meet import and export demands. Constraints (35) through (38) ensure that the number of transactions routed on any possible path are non-negative integers (i.e. belong to the set of natural numbers including zero).

In order to use a standard solver this was once again reformulated as an integer linear program in accordance with equations (6) through (10), giving

$$x = \begin{bmatrix} x_{orig} \\ \alpha_{1,1,1} \\ \vdots \\ \alpha_{1,1,L} \\ \vdots \\ \alpha_{1,K,1} \\ \vdots \\ \alpha_{1,K,L} \\ \alpha_{2,1,1} \\ \vdots \\ \alpha_{J,K,L} \\ \beta_{1,1} \\ \beta_{1,2} \\ \vdots \\ \beta_{J,L} \end{bmatrix} ; \; f = \begin{bmatrix} f_{orig} \\ C_{T_1F_1} + C_{F_1M_1} \\ \vdots \\ C_{T_1F_1} + C_{F_1M_L} \\ \vdots \\ C_{T_1F_K} + C_{F_KM_1} \\ \vdots \\ C_{T_1F_K} + C_{F_KM_L} \\ C_{T_2F_1} + C_{F_1M_1} \\ \vdots \\ C_{T_JF_K} + C_{F_KM_L} \\ C_{T_1M_1} \\ C_{T_1M_2} \\ \vdots \\ C_{T_JM_L} \end{bmatrix} \tag{39}$$

$$A = \begin{bmatrix} rep_J([1_L^T, 0_{(K-1)*L}^T]), 0_{J*L}^T, -rep_J([1_L^T, 0_{(K-1)*L}^T]), 0_{J*L}^T \\ rep_J([0_L^T, 1_L^T, 0_{(K-2)*L}^T]), 0_{J*L}^T, -rep_J([0_L^T, 1_L^T, 0_{(K-2)*L}^T]), 0_{J*L}^T \\ \vdots \\ rep_J([0_{(k-1)*L}^T, 1_L^T, 0_{(K-k)*L}^T]), 0_{J*L}^T, -rep_J([0_{(k-1)*L}^T, 1_L^T, 0_{(K-k)*L}^T]), 0_{J*L}^T \\ \vdots \\ rep_J([0_{(K-1)*L}^T, 1_L^T]), 0_{J*L}^T, -rep_J([0_{(K-1)*L}^T, 1_L^T]), 0_{J*L}^T \\ -rep_J([1_L^T, 0_{(K-1)*L}^T]), 0_{J*L}^T, rep_J([1_L^T, 0_{(K-1)*L}^T]), 0_{J*L}^T \\ -rep_J([0_L^T, 1_L^T, 0_{(K-2)*L}^T]), 0_{J*L}^T, rep_J([0_L^T, 1_L^T, 0_{(K-2)*L}^T]), 0_{J*L}^T \\ \vdots \\ -rep_J([0_{(k-1)*L}^T, 1_L^T, 0_{(K-k)*L}^T]), 0_{J*L}^T, rep_J([0_{(k-1)*L}^T, 1_L^T, 0_{(K-k)*L}^T]), 0_{J*L}^T \\ \vdots \\ -rep_J([0_{(K-1)*L}^T, 1_L^T]), 0_{J*L}^T, rep_J([0_{(K-1)*L}^T, 1_L^T]), 0_{J*L}^T \end{bmatrix} \tag{40}$$

$$\alpha = \begin{bmatrix} U_{1,0} \\ U_{2,0} \\ \vdots \\ U_{k,0} \\ U_1 - U_{1,0} \\ U_2 - U_{2,0} \\ \vdots \\ U_k - U_{k,0} \end{bmatrix} \tag{41}$$

$$B = \begin{bmatrix} rep_K((e_1^L)^T), 0^T_{(J-1)*K*L}, \left(e_1^{J*L}\right)^T, 0^T_{J*K*L+J*L} \\ rep_K((e_2^L)^T), 0^T_{(J-1)*K*L}, \left(e_2^{J*L}\right)^T, 0^T_{J*K*L+J*L} \\ \vdots \\ 0^T_{(j-1)*K*L}, rep_K((e_l^L)^T), 0^T_{(J-j)*K*L}, \left(e^{J*L}_{(j-1)*L+l}\right)^T, 0^T_{J*K*L+J*L} \\ \vdots \\ 0^T_{(J-1)*K*L}, rep_K((e_L^L)^T), \left(e^{J*L}_{J*L}\right)^T, 0^T_{J*K*L+J*L} \\ 0^T_{J*K*L+J*L}, rep_K((e_1^L)^T), 0^T_{(J-1)*K*L}, \left(e_1^{J*L}\right)^T \\ 0^T_{J*K*L+J*L}, rep_K((e_2^L)^T), 0^T_{(J-1)*K*L}, \left(e_2^{J*L}\right)^T \\ \vdots \\ 0^T_{J*K*L+J*L}, 0^T_{(j-1)*K*L}, rep_K((e_l^L)^T), 0^T_{(J-j)*K*L}, \left(e^{J*L}_{(j-1)*L+l}\right)^T \\ \vdots \\ 0^T_{J*K*L+J*L}, 0^T_{(J-1)*K*L}, rep_K((e_L^L)^T), \left(e^{J*L}_{J*L}\right)^T \end{bmatrix} \quad (42)$$

$$\beta = \begin{bmatrix} \beta_{orig} \\ m_{1,1} \\ \vdots \\ m_{1,L} \\ m_{2,1} \\ \vdots \\ m_{2,L} \\ \vdots \\ m_{J,L} \end{bmatrix} \quad (43)$$

$$\gamma = \left[0_{2*(J*K*L+J*L)}\right]^T \quad (44)$$

where $e_a^b = [e_1, e_2, \dots, e_b]^T, e_a = 1, e_j = 0 \; \forall j \neq a$ (45)

$rep_b(a) = [a_1, a_2, \dots, a_b], a_j = a \; \forall \, j$ (46)

$0_b = [\alpha_1, \alpha_2, .., \alpha_b]^T, \alpha_j = 0 \; \forall \, j$ (47)

$1_b = [\alpha_1, \alpha_2, .., \alpha_b]^T, \alpha_j = 1 \; \forall \, j$ (48)

Finally, in order to account for a limited supply of chassis, equations (19) and (21) are updated as shown in equation (49), which results in a quadratic constraint similar to the one presented in Section 0 for the import-only scenario.

$$z_k = \begin{cases} 1, & \sum_{j=1}^{J}\sum_{l=1}^{L}(x_{jkl} + \alpha_{jkl}) \geq 0 \\ 0, & \text{otherwise} \end{cases}, k = 1, \dots, K \quad (49)$$

The general optimization formulations described above have been applied to the analysis of a specific case study created for the POLA and POLB. The following sections describe the set-up of the case study and present results based on a variety of simulation scenarios and conditions.

5 Case Study Set-Up

A case study using the optimization formulation described in Section 4 is performed for the POLB and POLA. The case study uses the MTs in the POLB/POLB complex, and a number of TCs and potential CPF locations in the vicinity of the ports. The selection methods for the TCs and CPF locations are described in greater detail in the following sections.

A general overview of the local POLB and POLA area is shown in Figure 6, which indicates:

- The marine terminal locations (destination points) at the POLB and POLA. The MTs are shown as the color-coded areas on the map.
- The TCs (points of origin) used for the case study. The TCs are distributed in a wide area around the ports, and are shown as yellow dots on the map.
- The potential CPF locations identified for use in the case study, which are distributed in a wide area around the ports and are shown as red areas on the map. For easy identification, the CPFs they are also denoted by the white pins on the map.

The optimization formulations described in Section 4 were applied in the case study to evaluate the use of potential CPF locations. The total travel time for all trucks within a time period of interest is minimized, for an estimated total number of transactions based upon historical data, using estimates of CPF capacities, and estimated travel times between locations taken from Google Maps ©.

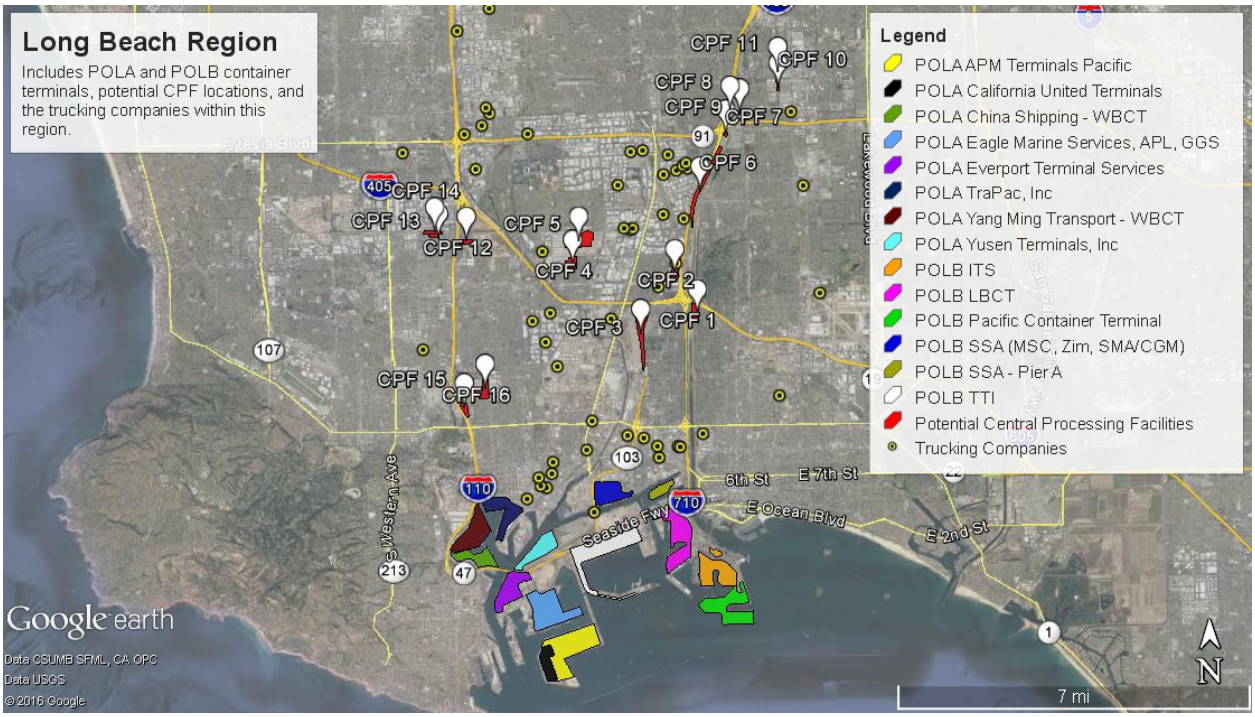

Figure 6. Node locations for the full model used in the simulation.

5.1 Marine Terminals

The POLB and POLA have terminals which cover various categories of imports and exports such as automotive, dry bulk, break bulk, liquid, and containers. This study concentrates on import / export of grounded containers and efficient retrieval and use of their associated chassis by truck. The container terminals at the POLB and POLA are listed in Table 3 and shown in Figure 7.

Table 3. Locations of POLB and POLA marine terminals used in the case study.

MT ID	Name	Address
1	ITS (K-Line)	Pier G E, Long Beach, CA 90802, USA
2	LBCT (OOCL)	Pier F Ave, Long Beach, CA 90802, USA
3	Pacific Container Terminal (COSCO)	Harbor Scenic Way, Long Beach, CA 90802, USA
4	SSA - Pier A	Pier C St, Long Beach, CA 90802, USA
5	SSA (MSC, Zim, SMA/CGM)	Pier A Way, Long Beach, CA 90802, USA
6	TTI (Hanjin)	Hanjin Rd, Long Beach, CA 90802, USA
7	APM Terminals Pacific	Navy Way Terminal Island, CA 90731
8	California United Terminals	Navy Way, Terminal Island, CA 90731
9	China Shipping North America	John S. Gibson Boulevard San Pedro, CA 90731
10	Eagle Marine Services	Terminal Way, Los Angeles, CA 90731
11	Everport Terminal Services	Terminal Island Way Terminal Island, CA 90731

MT ID	Name	Address
12	TraPac, Inc	South Neptune Avenue, Wilmington, CA 90744
13	Yang Ming Marine Transport	John S. Gibson Boulevard, San Pedro, CA 90731
14	Yusen Terminal (Nyk Yusen)	New Dock Street Terminal Island, CA 90731

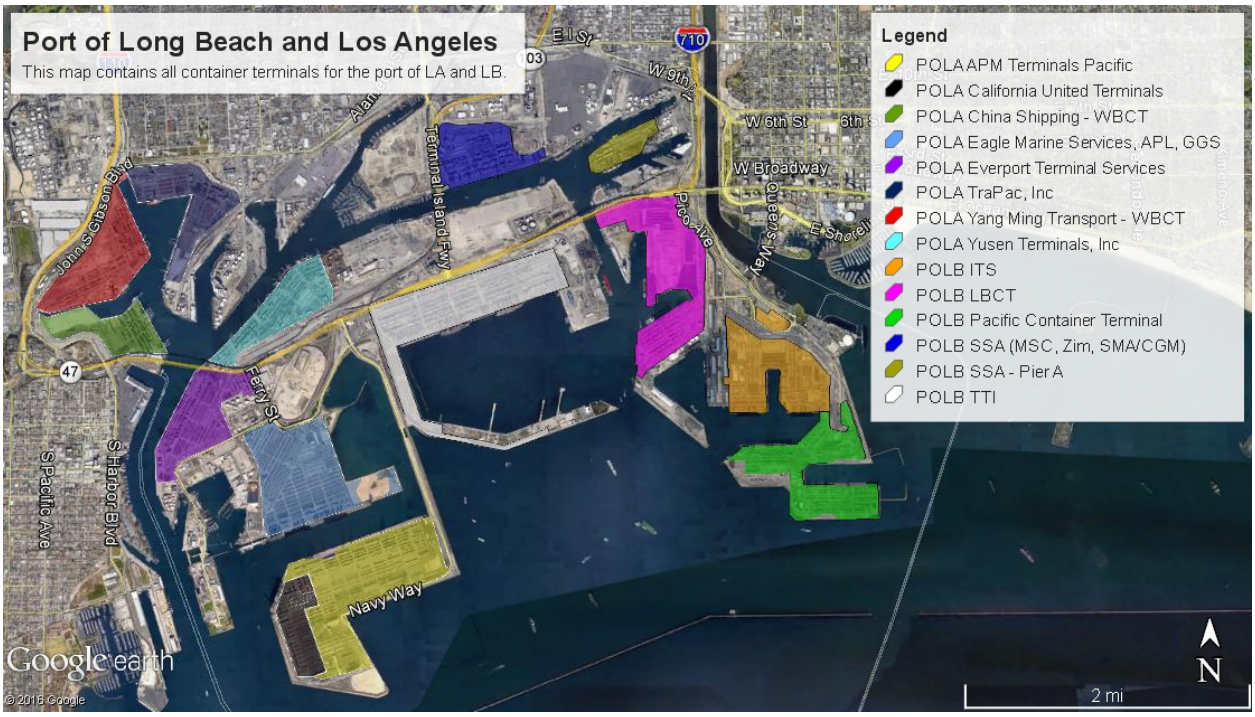

Figure 7. POLB & POLA marine terminal locations

Loaded inbound (import) and outbound (export) quantities through the POLB and POLA for 2015 are included in Table 4 [1], [2].

Table 4. POLB and POLA import and export statistics for 2015.

	loaded import	loaded export
TEU POLB	3,625,263	1,525,560
TEU POLA	4,159,462	1,786,913
TEU Total (Year)	7,784,725	3,312,473
TEU Total Avg (Day)	21,328	9,075

5.2 Trucking Companies

A representative sample of seventy-one trucking companies which service the POLB and POLA is used in this case study. In order to select this sample, an initial list of TCs was created from an internet drayage directory which includes all companies operating within Los Angeles County. Since the location of the TCs is a critical variable for the optimization problem, all companies whose address was not included in the drayage directory were eliminated from the list. The final list contains all companies with known address using chassis. In the analysis herein the number of daily transactions between marine terminals and trucking companies was assumed to be a fixed value between each trucking company and each marine terminal. In the initial analysis, the number of total daily import transactions was set at 50,000 FEU based on forecasts of total daily port trips [20]. Sensitivity analysis results used 10,000 import and 5,000 FEU export daily transactions based on the average daily import and export container traffic provided in Table 1Table 4.

5.3 Central Processing Facilities

Potential CPF locations were identified by searching for vacant land within a 15-mile radius of the POLA and the POLB. The capacities of these locations were estimated by using the Google earth polygon built-in feature to calculate an approximate square footage. Several CPF layout options and chassis stacking methodologies were evaluated as described in 0. Chassis can be stored vertically or horizontally as shown in Appendix A, and each storage method has its advantages and disadvantages. Among the various possibilities that were considered, horizontal storage layout with a maximum of 3 chassis stacked on top of each other was selected for the case study. Using the estimated square footage, the number of forty-foot chassis which could fit in that area was determined using this preferred chassis layout methodology which assumed allocations for access roads; blocks of stacked chassis (stacked three high); and blocks of un-stacked chassis for ease of access, in order to minimize chassis retrieval times. An example of the layout for a 5000×5000 foot area is included in Figure 8 below. For this example, the maximum number of forty-foot chassis which could be stored in this area was estimated at 170,000.

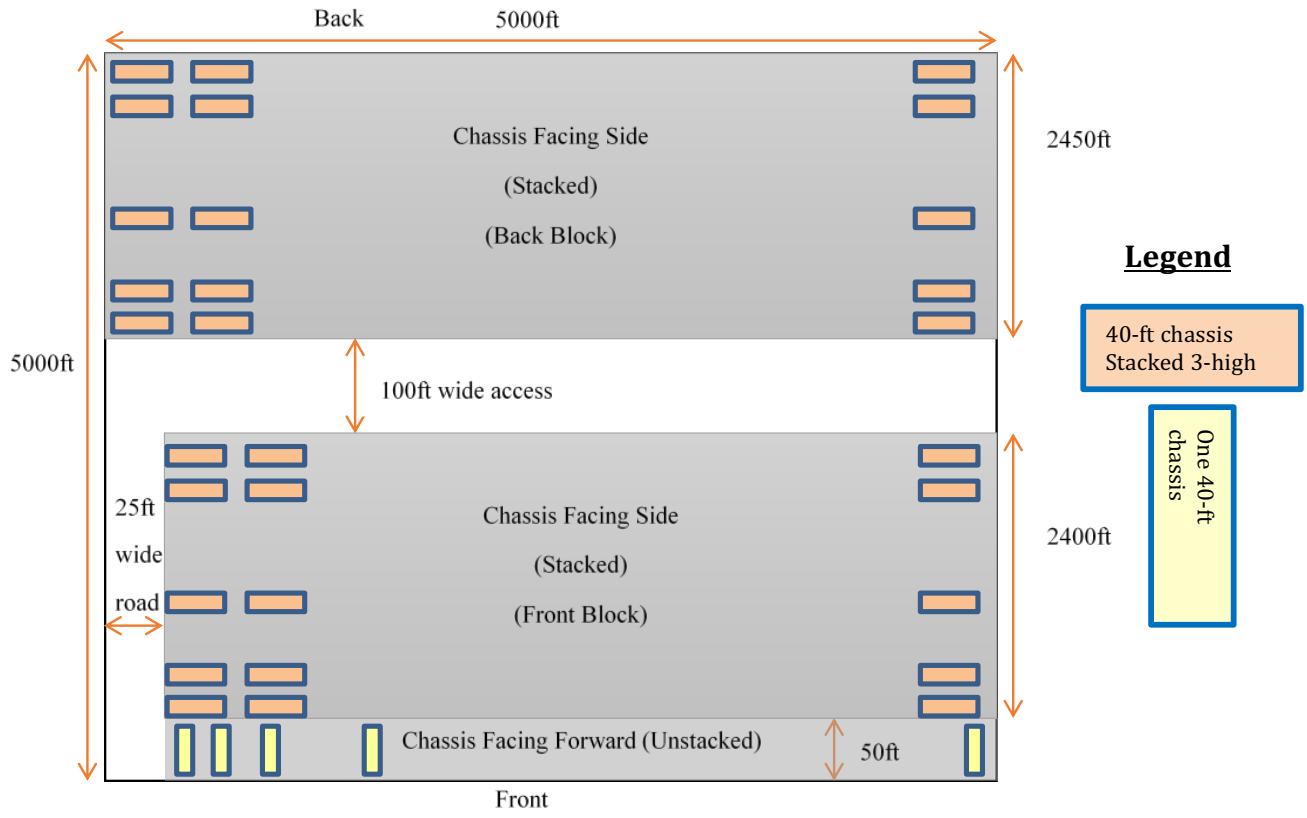

Figure 8. Example of chassis stacking layout within a CPF.

The locations and capacity estimates for each of the CPFs included in the case study are provided in Table 5. The table shows the street name and zip code of the potential CPF locations, but the street address numbers have been removed.

Table 5. Potential CPF locations and capacities for chassis storage.

CPF ID	Address	Estimated Capacity (chassis units)
1	Golden Ave, Long Beach, CA 90806, USA	7467
2	Via Oro Ave, Long Beach, CA 90810, USA	4048
3	River Ave, Long Beach, CA 90810, USA	16779
4	E 213th St, Carson, CA 90746, USA	6350
5	E Del Amo Blvd, Carson, CA 90746, USA	20551
6	Long Beach Blvd, Long Beach, CA 90805, USA	20469
7	Long Beach Blvd, Long Beach, CA 90805, USA	557
8	S Sportsman Dr, Compton, CA 90221, USA	2161
9	Atlantic Ave, Long Beach, CA 90805, USA	757

CPF ID	Address	Estimated Capacity (chassis units)
10	Alondra Blvd, Paramount, CA 90723, USA	2084
11	Alondra Blvd, Paramount, CA 90723, USA	293
12	Torrance Blvd, Carson, CA 90745, USA	3192
13	W Del Amo Blvd, Torrance, CA 90502, USA	1120
14	W Del Amo Blvd, Torrance, CA 90502, USA	1877
15	S Figueroa St, Wilmington, CA 90744, USA	2258
16	Lomita Blvd, Carson, CA 90745, USA	6959

5.4 Travel Time Between Locations

The travel times between all TCs, CPFs and MTs are calculated using the Google Distance Matrix (GDM) Application Program Interface (API). The addresses of each location are given as inputs to the Google API, which in turn provides the travel times between all given locations, under ideal conditions (without traffic congestion). The travel times are used to populate the three matrices identified in Section 0, including the cost (travel time) of transactions between TCs and CPFs (consisting of 1136 individual elements $C_{T_j F_k}$), the cost of transactions between CPFs and MTs (consisting of 224 individual elements $C_{F_k M_l}$), and the cost of transaction between TCs and MTs (consisting of 994 individual elements $C_{T_j M_l}$). In the initial analysis of the case study it is assumed that for any location x and y, the time to travel from location *x* to location *y* (C_{xy}) is equal to the travel time from location y to location x (C_{yx}), i.e.

$$C_{xy} = C_{yx} \quad \forall\, x, y \tag{50}$$

6 Results of the Case Study Simulations

This section presents the results of several simulation scenarios for the case study, based on the optimization formulation described previously. In order to validate the results and assess the developed methodology, the simulations progress from simpler scenarios on a reduced-node model to the more complicated scenarios applied to the full model. In each case, with the exception of Section 6.2.4, a dual simplex algorithm was used, where the optimization was performed using the Matlab (R2016a) function intlinprog with the default settings.

As has been presented in Section 0, the number of potential CPF locations is $= 16$. For this small number of potential CPFs an exhaustive search of linear solutions was performed. This allows the nonlinear problem of Section 0 to be solved through the optimization of a number of linear problems. In particular, for a given value of the maximum number of allowable CPFs, N_{cpf}, the combinations $\binom{16}{N_{\text{cpf}}}$ were generated. For each one of the $\binom{16}{N_{\text{cpf}}}$ combinations, the

optimal linear solution was produced, and the set of $\binom{16}{N_{\text{cpf}}}$ optimal solutions were ranked in terms of the values of the objective function. This process was repeated for $N_{\text{cpf}} = \{1, 2, \cdots 16\}$. For this small value of $K = 16$, the total number of optimal solutions that were investigated was equal to $\sum_{N_{\text{cpf}}=1}^{16} \binom{16}{N_{\text{cpf}}} = 65{,}535$.

6.1 Parameter P: Additional Processing Time

In order to compare the results of different optimization scenarios to each other, an important parameter P has been introduced. This parameter, termed the "Additional Processing Time", is used to provide a measure of the relative advantage of routing a transaction through a CPF over routing the transaction directly to the MT. The parameter P (where $\text{P} \geq 0$) is defined as the difference between the average time it takes to retrieve a chassis stored in a MT and the average time it takes to retrieve a chassis stored in a CPF:

$$P = T_{MT} - T_{CPF} \text{ (sec)} \tag{51}$$

where $T_{MT} =$ (Average chassis retrieval time at a marine terminal, in seconds)
and $T_{CPF} =$ (Average chassis retrieval time at a chassis processing facility, in seconds)

It is noted that in the sequel, many of the results of the simulation scenarios will be plotted against the values of the additional processing time (parameter P).

6.2 Import-Only Transactions with Unrestricted CPF Usage

The case study is performed initially using the import-only integer linear mathematical formulation with no limits on the number of CPFs used, as described in Section 0.

6.2.1 Reduced-Node Model Evaluation: 6 nodes

As an initial assessment of the linear program formulation, a reduced node model is generated utilizing subsets of the TCs, MTs and CPFs. Two nodes from each set of TCs, MTs and CPFs were selected, so that the model used for the initial assessment of the methodology contains a total of six nodes. The selected locations and travel times between them are included in Table 6 through

Table 8. Figure 9 shows the schematic for the reduced node problem.

For this simplified scenario, it is assumed that 12,500 import transactions are required to be completed between each TC and each of the MTs, and that each CPFs has a storage capacity of 50,000 chassis.

Table 6. Travel times (in seconds) from TCs to CPFs without traffic congestion (6-node case).

		CPF Location and CPF ID	
		Golden Ave, Long Beach, CA 90806 CPF ID=1	Via Oro Ave, Long Beach, CA 90810 CPF ID=2
TC Locations	East Del Amo Rancho Dominguez, CA	601	433
	South Susana Road Rancho Dominguez, CA	479	445

Table 7. Travel times (in seconds) from CPFs to TCs without traffic congestion (6-node case).

		MT Locations	
		ITS (K-Line) Pier G E, Long Beach, CA 90802, USA	LBCT (OOCL) Pier F Ave, Long Beach, CA 90802, USA
CPF Locations	Golden Ave, Long Beach, CA 90806 (CPF ID =1)	1044	714
	Via Oro Ave, Long Beach, CA 90810 (CPF ID=2)	1181	850

Table 8. Travel Times (in seconds) from TCs to MTs without traffic congestion (6-node case).

		MT Locations	
		ITS (K-Line) Pier G E, Long Beach, CA 90802, USA	LBCT (OOCL) Pier F Ave, Long Beach, CA 90802, USA
TC Locations	East Del Amo Rancho Dominguez, CA	1179	848
	Road Rancho Dominguez, CA	1057	726

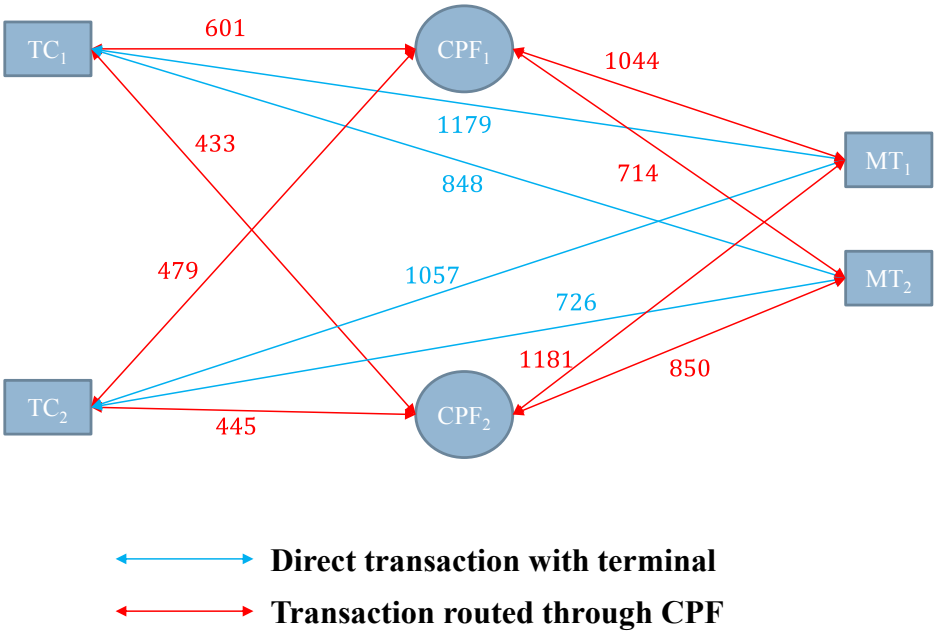

Figure 9. Schematic of centralized processing of chassis concept (6-node case).
Blue arrows: Direct routing to MTs. Red arrows: Routing through CPFs. Labels on each arrow indicate travel time between the two connected nodes (sec).

The optimization process is iterated upon, while the parameter P is varied by steps of 30 seconds. The results are presented in Table 9. The first eight rows of the table show all the possible combinations of two TCs, two CPFs and two MTs (a total of 2x2x2 = 8 combinations). The last four rows of the table show the possible combinations of two TCs and two MTs. The last column in the table shows the average increase in travel time when a truck is routed through a CPF as compared to the truck routed directly to the MT. Routing through CPF will be advantageous only when the average increase in travel time is less than the value of the

parameter *P*. In Table 9 one can see that when $P = 0$ sec, i.e. the chassis average retrieval time at MTs and CPFs is identical, all transactions are routed directly to MTs (bottom four rows in Table 9), since there is no advantage in terms of travel time to route the trucks through any of the CPFs. For the value of $P = 450$ sec, however, all transactions from TC1 are routed through CPF2 (first two green-coded rows in Table 9). This is expected as the difference in average travel time between direct routing from TC1 to the MTs and routing from TC1 to the MTs through CPF2 is 435 seconds. Therefore, as the value of the parameter P increases from 420 to 450 seconds, routing through CPF2 becomes the preferred option over direct routing. In that case, retrieving a chassis at the MT is less efficient, vs. retrieving a chassis at CPF2. Similarly, for the value of $P = 480$ sec, transactions from TC2 are routed through CPF1. This is also expected as the difference average travel time between the direct routing from TC2 to the MTs and routing from TC1 to the MTs through CPF 2 is 466 seconds.

These results are also summarized in Figure 10 which shows the number of transactions routed through each CPF as a function of P. One can see in the figure that when $P = 450$ sec, half of the transactions are routed through CPF2 (rather than being routed directly to the MTs), and when $P = 480$ sec, the other half of the transactions are routed through CPF1, with no more transactions being routed directly to the MTs.

Table 9. Optimal transaction routing (6-node case).

	Location			Number of transactions routed by location vs. parameter P			Increase in average travel time (sec), due to routing through CPFs
	TC	CPF	MT	*P* = 0	*P* = 450	*P* ≥480	
Routing through CPFs	1	1	1	0	0	0	466
	1	1	2	0	0	0	467
	1	2	1	0	12500	12500	435
	1	2	2	0	12500	12500	435
	2	1	1	0	0	12500	466
	2	1	2	0	0	12500	467
	2	2	1	0	0	0	569
	2	2	2	0	0	0	569
Direct Routing to MTs	1		1	12500	0	0	-
	1		2	12500	0	0	-
	2		1	12500	12500	0	-
	2		2	12500	12500	0	-

Note:

$$P = [\text{Average chassis retrieval time at a MT}] - [\text{Average chassis retrieval time at a CPF}] \quad (\text{sec})$$

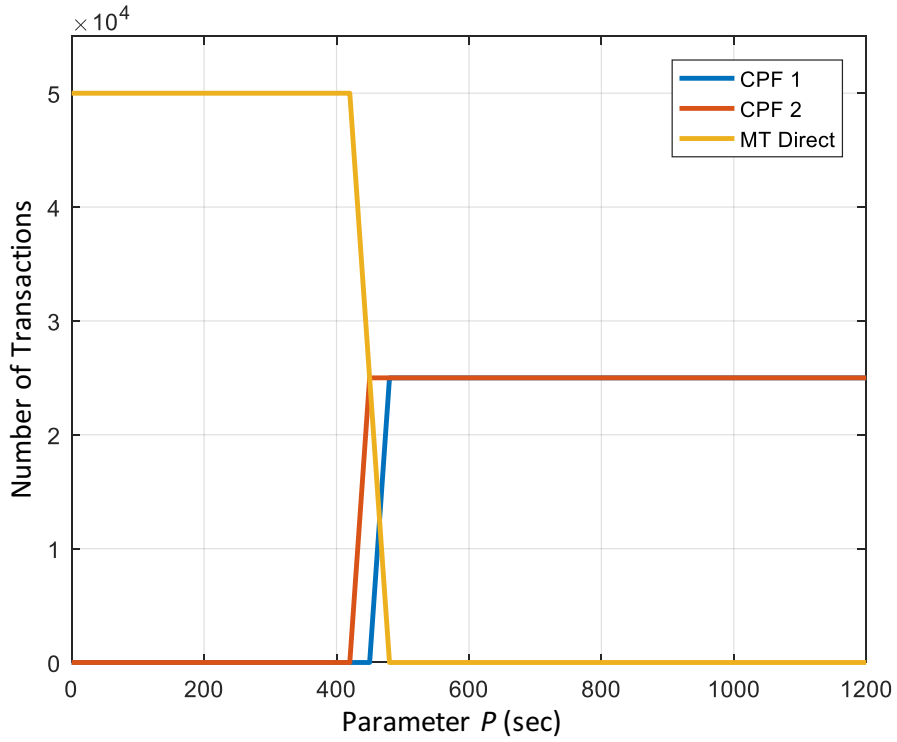

Figure 10. Optimum transaction routing vs. parameter *P* (6-node case). Total number of transactions routed through each CPF or directly to the MT plotted vs. parameter *P*. In this figure: (i) only import transactions are considered; (ii) all CPFs are available in the optimization; (iii) the model is restricted to 6 nodes (2 TCs, 2 CPFs and 2 MTs).

6.2.2 Reduced-Node Model Evaluation: 10 nodes

A second reduced node case is evaluated using a total of 10 nodes (3 TCs, 4 CPFs, and 3 MTs). The selected locations and travel times between them are shown in Table 10 through Table 12. For this simplified scenario, it is assumed that 5,555 import transactions are required to be completed between each TC and each of the MTs, and that each CPF has a storage capacity of 50,000 chassis. The optimization process is iterated upon, while the parameter P is varied in steps of 30 seconds, following the same process as for the 6-node case.

The results are presented in Table 13Table 9. The structure of this table is the same as in Table 9. In Table 13 one can see that when the chassis retrieval time at MTs and CPFs is identical, i.e. $P = 0$ sec, all transactions are routed directly to MTs since there is no advantage in terms of travel time to route the trucks through the CPFs. For the value of $P = 300$ sec, however, all transactions from TC2 are routed through CPF3. This is expected as the difference in average travel time between direct routing from TC2 to the MTs and routing from TC2 to the MTs through CPF3 is more than 287 seconds. Therefore, as the value of P increases from 270 to 300 seconds, routing through CPF3 becomes the preferred option over direct routing to MTs. Similarly, for the value of $P = 330$ sec, transactions from TC1 are routed through CPF6. This is

also expected as the difference in average travel time between direct routing from TC1 to the MTs and routing from TC1 to the MTs through CPF6 is more than 317seconds. Finally, for $P = 780$ sec, none of the transactions are routed directly to MTs, but they are routed through CPFs 1,3, and 5.

These results are summarized in Figure 11Figure 10 which shows the number of transactions routed through each CPF as a function of the parameter P. One can see in the figure that when $P = 300$ sec, one third of the transactions are routed into CPF3 (rather than being routed directly to MTs), and when $P = 330$ sec, another third of the transactions are routed into CPF6. Finally, when $P = 780$ sec, the last third of the transactions are routed through CPF1 with no more transactions being routed directly to the MTs.

Table 10. Travel times (in seconds) from TCs to CPFs without traffic (10 node case).

		CPF Locations & CPF ID			
		Golden Ave, Long Beach, CA 90806 CPF ID =1	Via Oro Ave, Long Beach, CA 90810 CPF ID =2	River Ave, Long Beach, CA 90810 CPF ID = 3	Long Beach Blvd, Long Beach, CA 90805 CPF ID = 6
TC Locations	Brookhollow Circle Riverside, CA	3817	3782	3855	3494
	S. Main Street Los Angeles, CA	1035	1026	900	890
	W 17th St, Long Beach, CA	493	499	572	446

Table 11. Travel times (in seconds) from CPFs to TCs without traffic (10 node case).

		MT Locations		
		Pacific Container Terminal (COSCO) Harbor Scenic Way, Long Beach, CA 90802	SSA - Pier A Pier C St, Long Beach, CA 90802	SSA (MSC, Zim, SMA/CGM) Pier A Way, Long Beach, CA 90802
CPF Locations	Golden Ave, Long Beach, CA 90806, CPF ID = 1	1108	748	775
	Via Oro Ave, Long Beach, CA 90810, CPF ID = 2	1244	885	886
	River Ave, Long Beach, CA 90810, CPF ID = 3	1085	726	774
	Long Beach Blvd, Long Beach, CA 90805 CPF ID = 6	1280	921	947

Table 12. Travel times (in seconds) from TCs to MTs without traffic (10 node case).

		MT Locations		
		Pacific Container Terminal (COSCO) Harbor Scenic Way, Long Beach, CA 90802	SSA - Pier A Pier C St, Long Beach, CA 90802	SSA (MSC, Zim, SMA/CGM) Pier A Way, Long Beach, CA 90802
TC Locations	Brookhollow Circle Riverside, CA	4458	4098	4125
	S. Main Street Los Angeles, CA	1698	1338	1384
	W 17th St, Long Beach, CA	837	477	504

Table 13. Optimal transaction routing (10-node case).

	Location			Number of transactions routed by location vs. parameter P				Increase in average travel time (sec), due to routing through CPFs
	TC	CPF	MT	P = 0	P = 300	P = 330	P ≥780	
Routing through CPFs	1	1	1	0	0	0	0	467
	1	1	2	0	0	0	0	467
	1	1	3	0	0	0	0	467
	1	2	1	0	0	0	0	568
	1	2	2	0	0	0	0	569
	1	2	3	0	0	0	0	543
	1	3	1	0	0	0	0	482
	1	3	2	0	0	0	0	483
	1	3	3	0	0	0	0	504
	1	6	1	0	0	5555	5555	316
	1	6	2	0	0	5555	5555	317
	1	6	3	0	0	5555	5555	316
	2	1	1	0	0	0	0	445
	2	1	2	0	0	0	0	445
	2	1	3	0	0	0	0	426
	2	2	1	0	0	0	0	572
	2	2	2	0	0	0	0	573
	2	2	3	0	0	0	0	528
	2	3	1	0	5555	5555	5555	287
	2	3	2	0	5555	5555	5555	288
	2	3	3	0	5555	5555	5555	290
	2	6	1	0	0	0	0	472
	2	6	2	0	0	0	0	473
	2	6	3	0	0	0	0	453
	3	1	1	0	0	0	5555	764
	3	1	2	0	0	0	5555	764
	3	1	3	0	0	0	5555	764
	3	2	1	0	0	0	0	906
	3	2	2	0	0	0	0	907
	3	2	3	0	0	0	0	881
	3	3	1	0	0	0	0	820
	3	3	2	0	0	0	0	821
	3	3	3	0	0	0	0	842
	3	6	1	0	0	0	0	889
	3	6	2	0	0	0	0	890
	3	6	3	0	0	0	0	889

	Location			Number of transactions routed by location vs. parameter P				Increase in average travel time (sec), due to routing through CPFs
	TC	CPF	MT	P = 0	P = 300	P = 330	P ≥780	
Direct Routing to MT	1		1	5555	5555	0	0	
	1		2	5555	5555	0	0	
	1		3	5555	5555	0	0	
	2		1	5555	0	0	0	
	2		2	5555	0	0	0	
	2		3	5555	0	0	0	
	3		1	5555	5555	5555	0	
	3		2	5555	5555	5555	0	
	3		3	5555	5555	5555	0	

Note:

$$P = [\text{Average chassis retrieval time at a MT}] - [\text{Average chassis retrieval time at a CPF}] \quad (\text{sec})$$

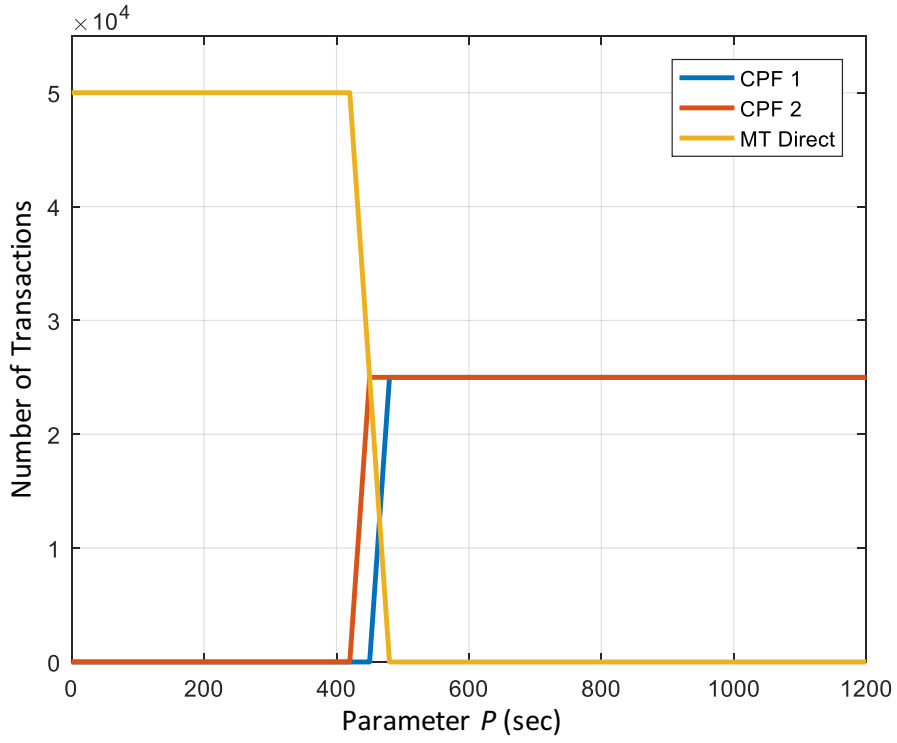

Figure 11. Optimum transaction routing vs. parameter *P* (10-node case).
The total number of transactions routed through each CPF or directly to the MT vs. parameter *P*. In this figure: (i) only import transactions are considered; (ii) all CPFs are available in the optimization; (iii) the model is restricted to 10 nodes (3 TCs, 4 CPFs and 3 MTs).

6.2.3 Full model (101-node model)

After verifying that the linear program behaved as expected for the two simplified models used in the reduced-node cases, the full model was analyzed using the same approach. In this case, all of the 16 potential CPF locations were included, each with its the estimated chassis storage capacities provided in Table 5. All 71 TCs and 14 MTs are also included with ~50,000 transactions distributed evenly between them (corresponding to approximately 50 transactions between each TC and each MT). The results are summarized in Figure 12, where it can be seen that when $P = 0$ seconds, all of the transactions are routed directly from the TCs to the MTs. However, even with a 5-minute increase in efficiency at the CPFs in terms of average chassis retrieval time (corresponding to $P = 300$ seconds), approximately half of the transactions are routed through CPFs. The number of transactions that are routed directly from TCs to MTs is decreasing rapidly as the value of the parameter P increases. Figure 12 shows that when P=1200 sec, virtually no transactions are routed directly to marine terminals. Table 14 shows the percent utilization of the CPFs for $P = 1200$ seconds. One can see in this case that several of the candidate CPFs are underutilized (e.g. CPFs with ID numbers 5, 10 and 11). This underutilization indicates that these CPFs are not the best candidates for any of the TCs when there are other choices (i.e. when all of the CPFs are available for use). However, it should be noted these CPFs may still be good candidates when only a limited number of CPF sites are available due to cost or other constraints.

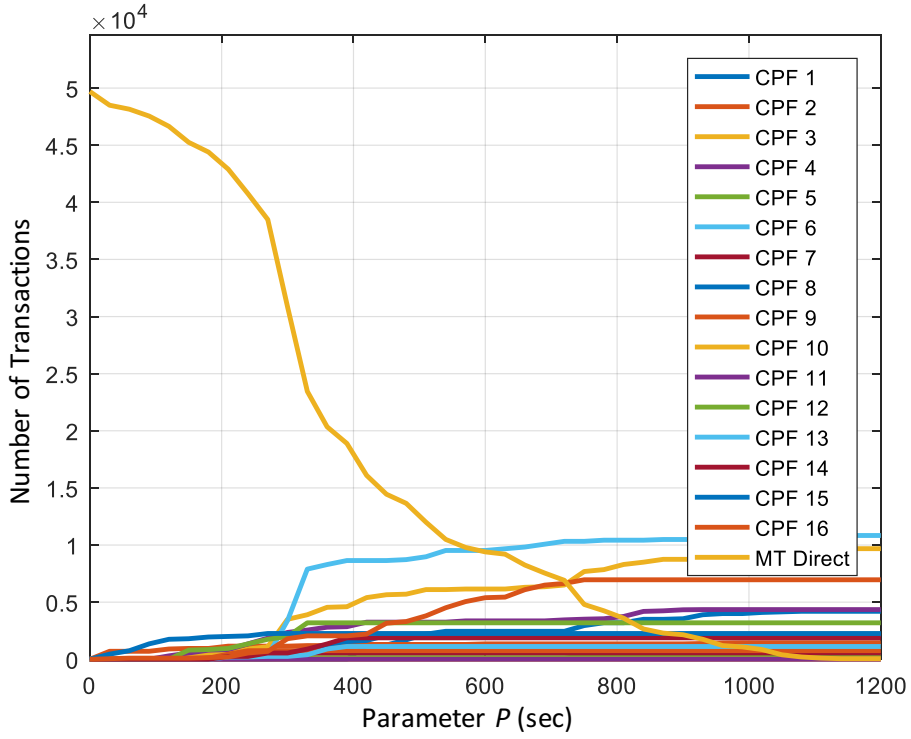

Figure 12. Number of transactions routed through CPFs at optimality, as a function of *P*. Total number of transactions routed through each CPF or directly to the MT for the optimal solution. In this figure: (i) only import transactions are considered; (ii) all CPFs are available; (iii) the full model is used (including all 101 nodes of TCs, CPFs and MTs).

Table 14. CPF capacity utilization (*P*=1200 sec)

CPF ID	Capacity	Number of transactions routed through CPF	Percent of CPF capacity utilized
1	7467	4182	56%
2	4048	1457	36%
3	16779	9732	58%
4	6350	4382	69%
5	20551	206	1%
6	20469	10849	53%
7	557	557	100%
8	2161	2161	100%
9	757	757	100%
10	2084	0	0%
11	293	0	0%
12	3192	3192	100%
13	1120	1120	100%
14	1877	1877	100%
15	2258	2258	100%
16	6959	6959	100%

Note:
(i) Only import transactions are considered
(ii) All CPFs are available
(iii) The full 101-node model is used

6.2.4 Evaluation of the Optimal Solution: With and Without Integer Constraints

In order to evaluate the performance of the solver used to generate the results provided in Figure 12 and Table 14, the program is re-run while the integer constraint is relaxed. The goal is to assess if the same solution would be generated, and determine if performing the optimization without the integer constraint would be more efficient. The integer solution was once again generated using the Matlab (R2016a) function intlinprog and the default settings. The solution without integer constraints was generated using the Matlab (R2016a) function linprog with its default settings. It is noted that while the intlinprog function used a dual simplex algorithm, the linprog function defaulted to an integer-point-legacy algorithm. The results are included in Figure 13 through Figure 15. Figure 13 shows the difference between the number of transactions routed to each potential CPF location when the integer constraint is used, and when the integer constraint is relaxed. From Figure 13 it can be seen that the difference is negligible. The total number of transactions routed is the same using either solver, if the number is rounded to the nearest integer value. Figure 14 shows the change in the final solution when run without integer constraints as a percentage of the original solutions with

integer constraints. The maximum difference for any of the solutions negligible, indicating the solution quality is identical with and without the integer constraint. Finally, Figure 15 shows the percent increase in computational time for the solver without integer constraints over that with integer constraints. The increase in computational time was typically between 50% and 100%. Given the fact that the solutions were equivalent and the computational time for the solver with integer constraints is less, the solver with integer constraints is used in all of the following analysis.

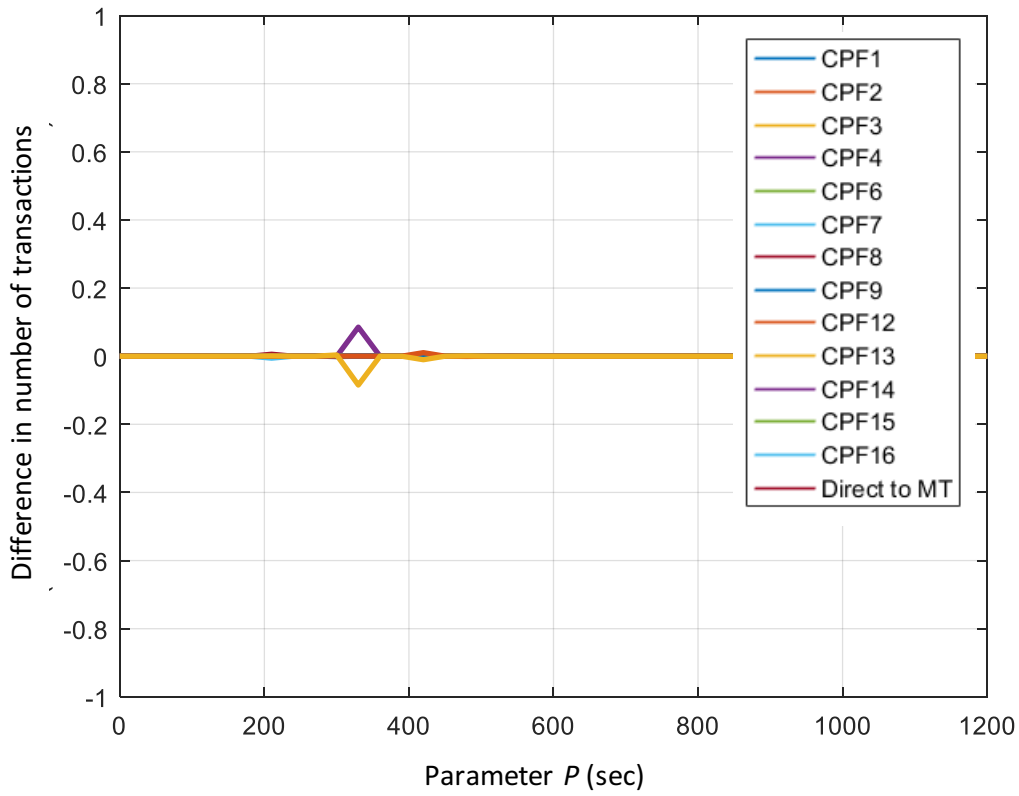

Figure 13. Evaluation of Optimal Solution: Difference in the Number of Transactions.
The difference in the number of transactions routed through each CPF at optimality, found when: (a) the integer constraint is present and (b) the integer constraints is relaxed. In this figure: (i) only import transactions are considered; (ii) all CPFs are available; (iii) the full model is used (including all 101 nodes of TCs, CPFs and MTs).

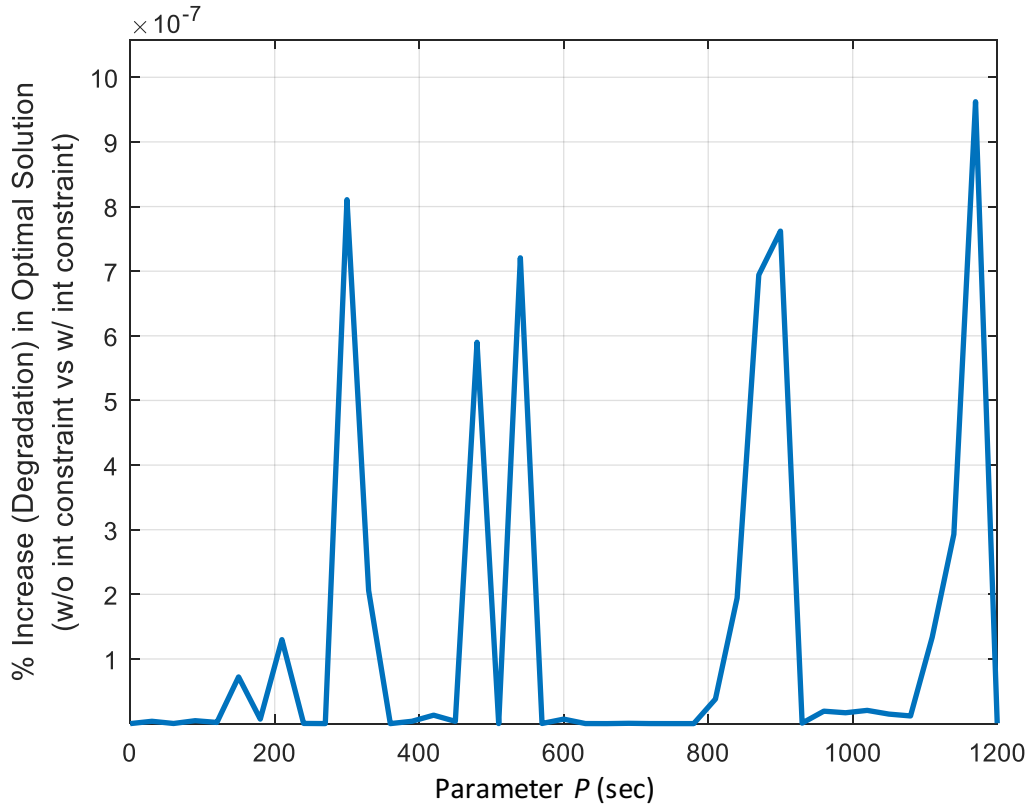

Figure 14. Evaluation of Optimal Solution: Percent difference in the Value of the Objective Function. Percent difference in the optimal value of the objective function between case (a) when the solver with integer constraints is present, and case (b) when the integer constraint is relaxed.

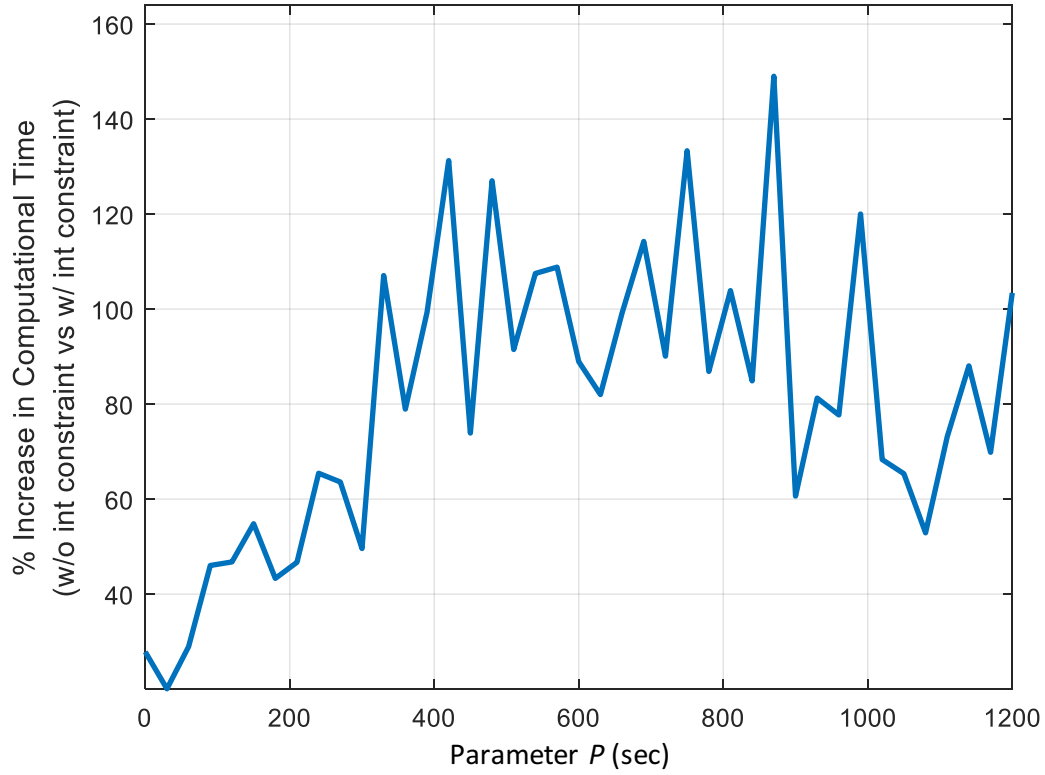

Figure 15. Evaluation of Optimal Solution: Percent Difference in Computational Time.

Percent difference in computational time to reach the optimal solution: $\Delta = \left(\frac{T_{ICR} - T_{ICP}}{T_{ICP}}\right)\%$,

where:

T_{ICR} = (Computational time when the integer constraint is relaxed)

T_{ICP} = (Computational time required when integer constrained is present).

6.3 Import-Only Transactions with Restricted CPF Availability

The next phase in the process is to evaluate the degree of preferential usage for each of the potential CPF candidates. This is an important consideration if the number of potential CPFs is limited due to unavailability. First, it is assumed that only one CPF is available. In order to identify the preferred CPF if only a single CPF location can be used, the problem is solved 16 times, using only a single different CPF at a time. This is equivalent to the original mathematical formulation with the additional constraints of equations (19) and (20) applied for the case when $N_{\text{cpf}} = 1$. The configuration used for TCs and MTs is the same as the one in the original problem, with the exception that a single CPF was included at a time. The results are shown in Figure 16 and Figure 17.

Figure 16 shows the number of transactions routed through each of the candidate CPFs as a function of the parameter *P*, assuming that only one CPF is available to be used. It can be seen from Figure 16 that the number of transactions routed through a CPF eventually saturates at

the capacity of each of the potential CPFs. From this figure, it is seen that value of the parameter *P* and the total number of transactions are key drivers in the selection of a single CPF location. For $P \geq 300$ seconds and a total number of transactions greater than 5000, CPFs 3 and 6 begin to have more transactions routed through them. At this point it becomes more efficient to route some transactions through CPFs 3 & 6, rather than direct routing to marine terminals. CPF 5, on the other hand, does not have the same number of chassis routed through it as CPFs 3 and 6 until *P* increases by several hundred more seconds.

Figure 17 shows the total travel time for the optimal solution as a function of *P*, assuming that only one CPF is available to be used. In Figure 17 the optimal solution is shown for each of the CPF routing options. When $P = 500$ seconds the figure shows an observable improvement to the total travel time if trucks are routed through CPF 3 and 6 as compared to any of the other options. For $P \geq 800$ seconds CPFs 3, 6 and 5 are clearly superior to all the other CPFs in terms of optimal total travel time.

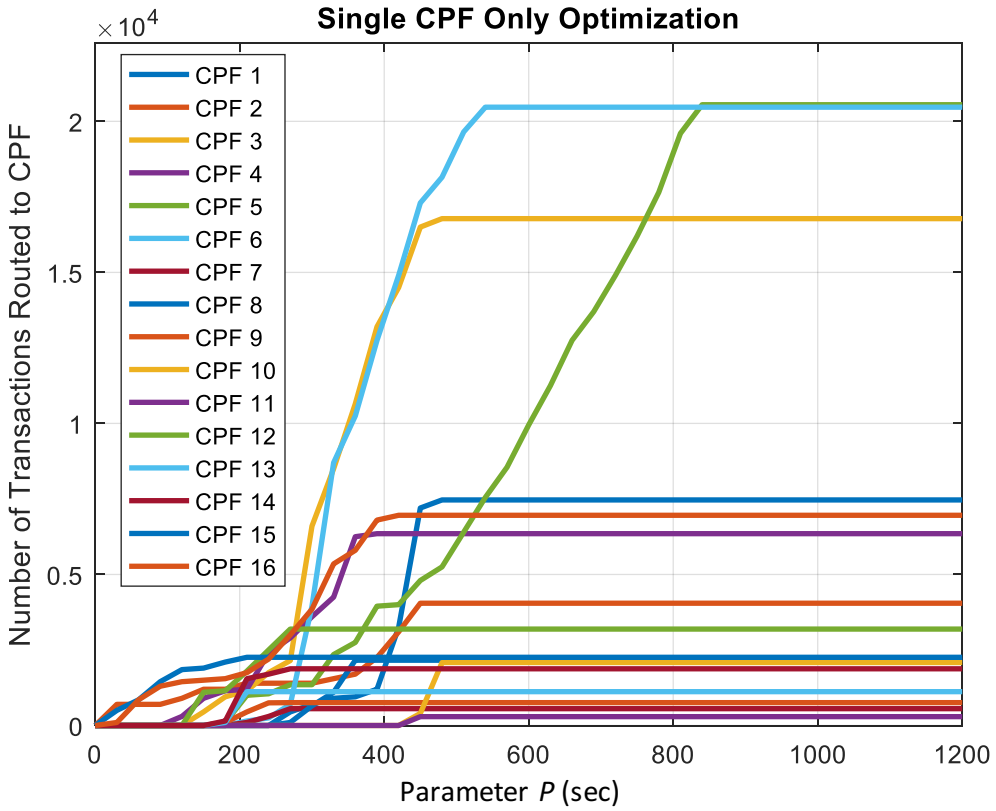

Figure 16. Optimum transaction routing vs. parameter *P*: one CPF available. The total number of transactions routed through a CPF is plotted against parameter *P*. In this figure: (i) only import transactions are considered; (ii) only one CPF is are available at a time; (iii) the full model is used (including all 101 nodes of TCs, CPFs and MTs).

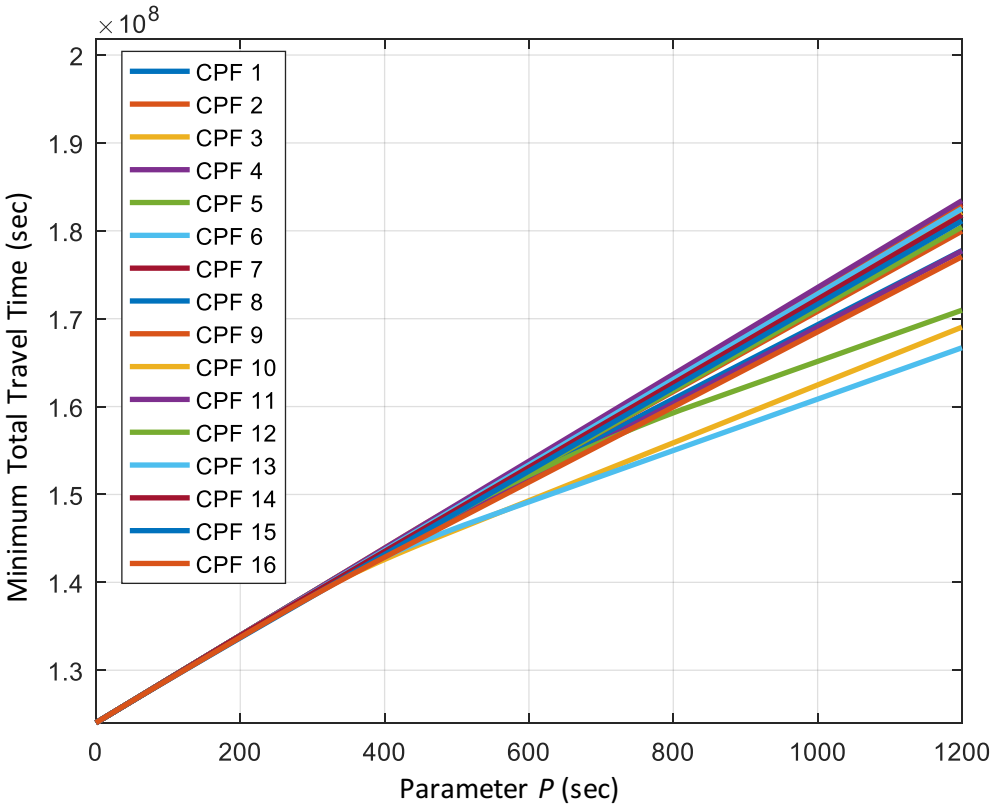

Figure 17. Optimal value of the objective function vs. parameter *P*: one CPF available. The minimum total travel time vs. parameter *P* at optimality. In this figure: (i) only import transactions are considered; (ii) only one CPF is are available at a time; (iii) the full model is used (including all 101 nodes of TCs, CPFs and MTs).

Table 15 shows the complete ranking of all CPFs, if only one CPF can be used. The rankings for

Table 15 are obtained with the value of the parameter *P* set at $P = 1200$ seconds. It is apparent that CPFs 6 and 3 are good candidates to be used as CPFs if financial resources for only a single CPF are available.

Table 15. Ranking of potential CPF locations if only CFP is available.

CPF ID	Address	Ranking
6	Long Beach Blvd, Long Beach, CA 90805, USA	1
3	River Ave, Long Beach, CA 90810, USA	2
5	E Del Amo Blvd, Carson, CA 90746, USA	3
16	Lomita Blvd, Carson, CA 90745, USA	4
4	E 213th St, Carson, CA 90746, USA	5
1	Golden Ave, Long Beach, CA 90806, USA	6
2	Via Oro Ave, Long Beach, CA 90810, USA	7
12	Torrance Blvd, Carson, CA 90745, USA	8
15	S Figueroa St, Wilmington, CA 90744, USA	9
8	S Sportsman Dr, Compton, CA 90221, USA	10
14	W Del Amo Blvd, Torrance, CA 90502, USA	11
10	Alondra Blvd, Paramount, CA 90723, USA	12
13	W Del Amo Blvd, Torrance, CA 90502, USA	13
9	Atlantic Ave, Long Beach, CA 90805, USA	14
7	Long Beach Blvd, Long Beach, CA 90805, USA	15
11	Alondra Blvd, Paramount, CA 90723, USA	16

6.4 Import/Export Integer Linear Formulation with the Full Model

In this section the full 101-node model, including both import and export transactions, is analyzed and the preferred CPF locations are identified. Figure 18 shows the percent improvement in the total travel time when using routing through CPFs as compared to direct routing to the MTs. The optimal solution has been obtained for two values of the parameter *P*: (a) when $P = 600$ seconds, and (b) when $P = 1200$ seconds, assuming that the total number of import transactions is $\cong 10{,}000$ and that the total number of export transactions is $\cong 5{,}000$.

Figure 18 shows that when there are no CPFs available (i.e. the number of CPFs is 0), then direct routing through the MTs is obviously the only option. As the number of available CPFs increases from 0 to 3, the figure shows that there is a significant improvement in using the CPFs as compared to routing directly to the MTs. The improvement is more dramatic for the higher value of the parameter *P* ($P = 1200$) as expected. Figure 18 also shows that there is no significant improvement to the total travel time if more than three CPFs are utilized, independently of the value of the parameter *P*.

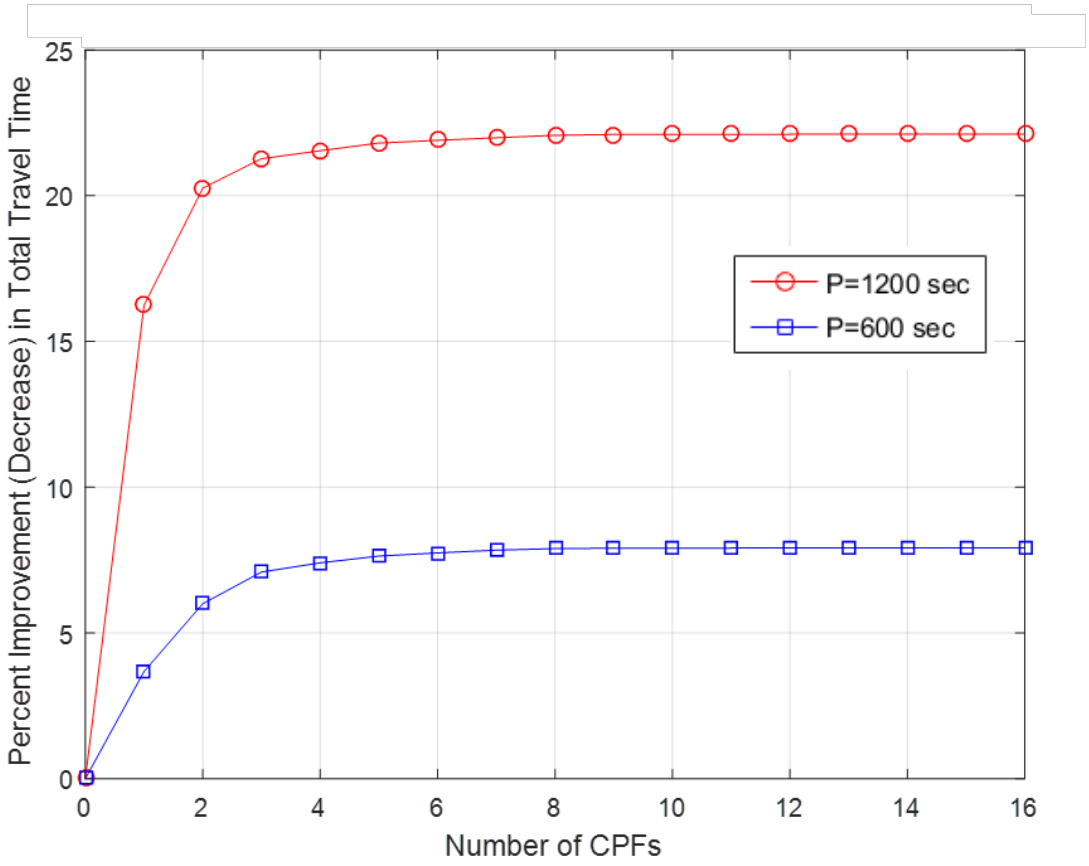

Figure 18. Number of CPFs used vs. total travel time. Percent improvement in total travel time at optimality. The improvement is calculated as the percent decrease in total travel time from the case (a) When all transactions are routed to the MTs; to the case (b) When transactions are routed to optimally. The percent improvement is plotted against the number of available CPFs. In this Figure: (i) both import and export transactions are considered; (ii) two values of the parameter P are studied (P=600 sec, and P=1200 sec); (iii) the full model is used (including all 101 nodes of TCs, CPFs and MTs).

Table 16 and
Table 17 show the complete list of the top 5 CPF options as a function of the number of CPFs used.

In Table 16, $P = 1200$ sec. If only one CPF is used, the top three options are CPFs $\{3\}$, $\{6\}$ and $\{16\}$. However, as the number of CPFs used increases from one to two, and to three, the highest ranked options become $\{3, 15\}$ and $\{3, 6, 15\}$ respectively.

Similarly, in

Table 17, where $P = 600$ sec, if only one CPF is used, the top three options are CPFs $\{3\}$, $\{15\}$ and $\{6\}$. However, as the number of CPFs used increases from one to two, and to three, the highest ranked options become $\{6, 15\}$ and $\{3, 6, 15\}$ respectively.

The fact that a difference exists between the individually ranked CPFs and the rankings if combinations of CPFs are used is not surprising. Inclusion of several CPFs allows for the opportunity to select locations spread out in such a way as to offer regional hubs, each of which can be targeted to certain areas. On the other hand, if a single CPF is used, the top rankings when are determined in such a way as to minimize the distance from all of the trucking companies. In addition, the top ranking CPFs also tend to be located closer to the primary freeways such as the I-710 and the I-110. The optimal CPF locations are shown on the maps of **Error! Reference source not found.** and

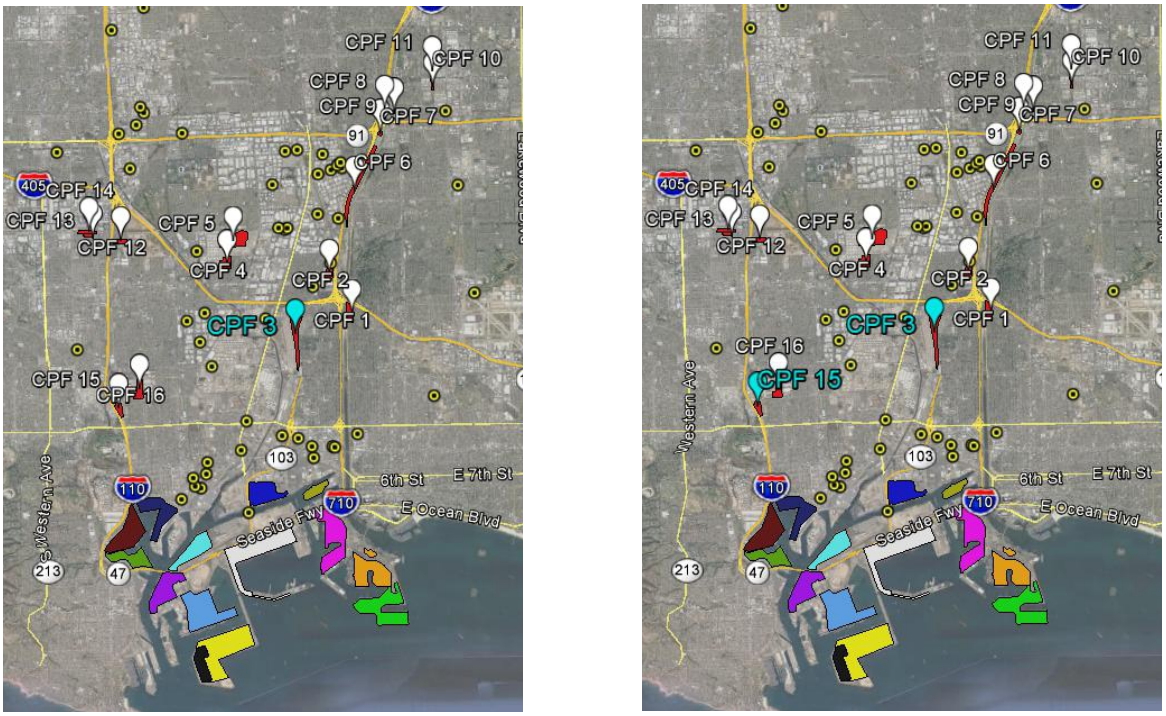

(a) (b)

Figure 19. Map of the optimal CPF locations (*P* = 1200 sec). (a) One CPF is used (optimal location denoted by the blue pin). (b) Two CPFs are used (optimal locations denoted by the two blue pins).

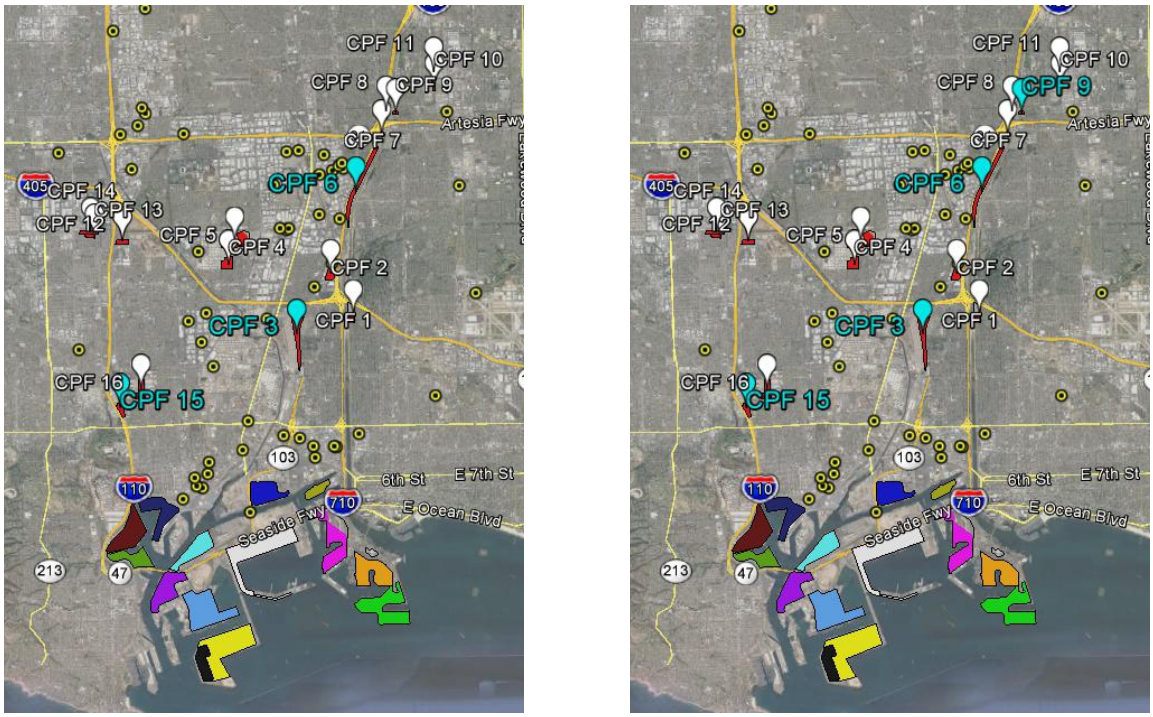

(a) (b)

Figure 20.

As seen in Figure 18, if the number of CPFs used is more than three, there is no significant additional benefit in terms of total travel time. Hence, for the following analysis a maximum number of there CPFs will be used. To determine which CPFs should be selected to be used in the analysis, the results of Table 16 and Table 17 have been utilized. The CPFs which are at the top for each case in Table 17, were ranked by the times of occurrence within the optimal set. Figure 21. Ranking of CPF candidate locationsFigure 21 shows the number of inclusions in the optimal set for each candidate CPF. It is clear that CPFs $\{3\}$, $\{6\}$, and $\{15\}$ are ranked higher than all other options. The results of Figure 21 are obtained for the value $P = 600$ seconds. The same top rankings are obtained when $P = 1200$ seconds. Table 18 summarizes the rankings of all CPFs for both cases, when $P = 600$ sec, and when $P = 1200$ sec.

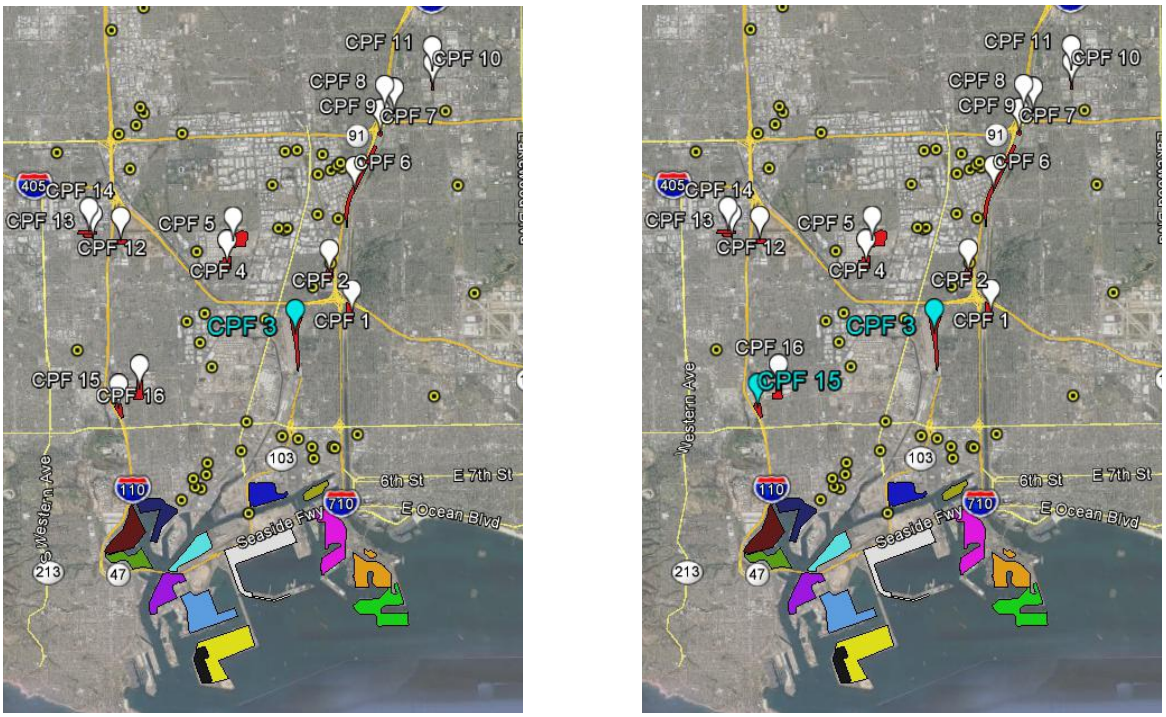

(a) (b)

Figure 19. Map of the optimal CPF locations (*P* = 1200 sec). (a) One CPF is used (optimal location denoted by the blue pin). (b) Two CPFs are used (optimal locations denoted by the two blue pins).

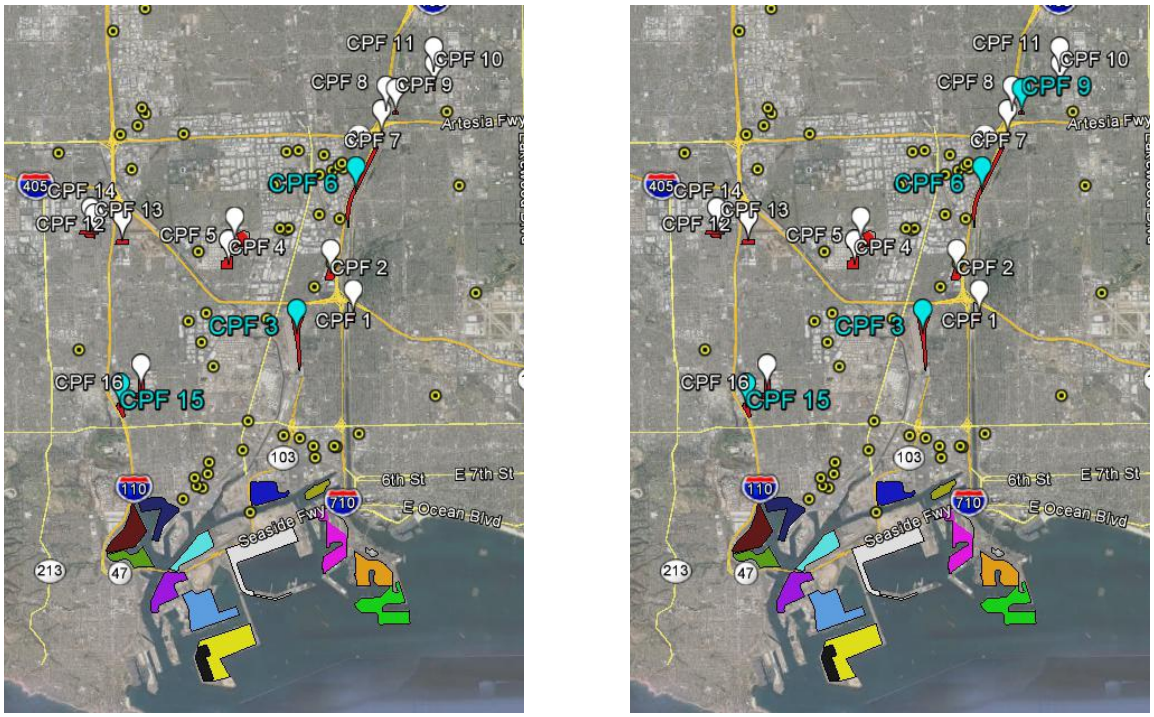

(a) (b)

Figure 20. Map of the optimal CPF locations (*P* = 1200 sec). (a) Three CPFs are used (optimal locations denoted by the three blue pins). (b) Four CPFs are used (optimal locations denoted by the four blue pins).

Table 16. Top CPF ranking vs. number of CPFs used: *P* = 1200 sec.

Number of CPFs used	CPF IDs for the top 5 options ($P = 1200$ sec)
1	3 6 16 1 15
2	3 15 6 15 3 16 1 15 6 16
3	3 6 15 3 7 15 3 9 15 3 8 15 4 6 15
4	3 6 9 15 3 6 12 15 3 7 9 15 3 4 6 15 3 7 12 15
5	3 6 9 12 15 3 7 9 12 15 3 4 6 9 15 3 6 9 14 15 3 6 9 13 15
6	1 3 6 9 12 15 2 3 6 9 12 15 3 4 6 9 12 15 3 4 6 9 14 15 3 4 6 9 13 15

Number of CPFs used	CPF IDs for the top 5 options ($P = 1200$ sec)
7	1 2 3 6 9 12 15 1 3 4 6 9 12 15 1 3 4 6 9 14 15 2 3 4 6 9 12 15 2 3 4 6 9 14 15
8	1 2 3 4 6 9 12 15 1 2 3 4 6 9 14 15 1 2 3 4 6 9 13 15 1 2 3 4 7 9 12 15 1 2 3 4 7 9 14 15
9	1 2 3 4 6 9 12 14 15 1 2 3 4 6 9 12 13 15 1 2 3 4 6 9 12 15 16 1 2 3 4 6 8 9 12 15 1 2 3 4 6 8 9 14 15
10	1 2 3 4 6 8 9 12 14 15 1 2 3 4 6 8 9 12 13 15 1 2 3 4 5 6 9 12 14 15 1 2 3 4 5 6 9 12 13 15 1 2 3 4 6 9 12 14 15 16
11	1 2 3 4 5 6 8 9 12 14 15 1 2 3 4 5 6 8 9 12 13 15 1 2 3 4 6 8 9 12 14 15 16 1 2 3 4 6 8 9 12 13 15 16 1 2 3 4 6 7 8 9 12 14 15
12	1 2 3 4 5 6 8 9 12 14 15 16 1 2 3 4 5 6 8 9 12 13 15 16 1 2 3 4 5 6 7 8 9 12 14 15 1 2 3 4 5 6 7 8 9 12 13 15 1 2 3 4 6 7 8 9 12 14 15 16
13	1 2 3 4 5 6 7 8 9 12 14 15 16 1 2 3 4 5 6 7 8 9 12 13 15 16 1 2 3 4 5 6 8 9 12 13 14 15 16 1 2 3 4 5 6 8 9 11 12 14 15 16 1 2 3 4 5 6 8 9 10 12 14 15 16
14	1 2 3 4 5 6 7 8 9 12 13 14 15 16 1 2 3 4 5 6 7 8 9 11 12 14 15 16 1 2 3 4 5 6 7 8 9 10 12 14 15 16 1 2 3 4 5 6 7 8 9 11 12 13 15 16 1 2 3 4 5 6 7 8 9 10 12 13 15 16

Number of CPFs used	CPF IDs for the top 5 options ($P = 1200$ sec)
15	1 2 3 4 5 6 7 8 9 10 12 13 14 15 16 1 2 3 4 5 6 7 8 9 11 12 13 14 15 16 1 2 3 4 5 6 7 8 9 10 11 12 14 15 16 1 2 3 4 5 6 7 8 9 10 11 12 13 15 16 1 2 3 4 5 6 8 9 10 11 12 13 14 15 16

Table 17. Top CPF ranking vs. number of CPFs used: *P* = 600 sec.

Number of CPFs used	CPF IDs for the top 5 options ($P = 600$ sec)
1	3 15 6 12 7
2	6 15 3 15 7 15 6 16 3 16
3	3 6 15 3 7 15 3 9 15 4 6 15 3 8 15
4	3 6 9 15 3 7 9 15 3 4 6 15 3 6 12 15 3 7 12 15
5	3 4 6 9 15 3 6 9 12 15 3 4 7 9 15 3 7 9 12 15 3 6 9 14 15

Number of CPFs used	CPF IDs for the top 5 options ($P = 600$ sec)
6	2 3 4 6 9 15 2 3 6 9 12 15 3 4 6 9 12 15 3 4 6 9 14 15 3 4 6 9 13 15
7	2 3 4 6 9 12 15 2 3 4 6 9 14 15 2 3 4 6 9 13 15 2 3 4 7 9 12 15 1 2 3 4 6 9 15
8	1 2 3 4 6 9 12 15 1 2 3 4 6 9 14 15 1 2 3 4 6 9 13 15 1 2 3 4 7 9 12 15 2 3 4 6 9 12 14 15
9	1 2 3 4 6 9 12 14 15 1 2 3 4 6 9 12 13 15 1 2 3 4 6 8 9 12 15 1 2 3 4 5 6 9 12 15 1 2 3 4 6 7 9 12 15
10	1 2 3 4 6 8 9 12 14 15 1 2 3 4 6 8 9 12 13 15 1 2 3 4 5 6 9 12 14 15 1 2 3 4 5 6 9 12 13 15 1 2 3 4 6 7 9 12 14 15
11	1 2 3 4 5 6 8 9 12 14 15 1 2 3 4 5 6 8 9 12 13 15 1 2 3 4 6 7 8 9 12 14 15 1 2 3 4 6 7 8 9 12 13 15 1 2 3 4 5 6 7 9 12 14 15
12	1 2 3 4 5 6 7 8 9 12 14 15 1 2 3 4 5 6 7 8 9 12 13 15 1 2 3 4 5 6 8 9 12 14 15 16 1 2 3 4 5 6 8 9 12 13 14 15 1 2 3 4 5 6 8 9 11 12 14 15
13	1 2 3 4 5 6 7 8 9 12 14 15 16 1 2 3 4 5 6 7 8 9 12 13 14 15 1 2 3 4 5 6 7 8 9 11 12 14 15 1 2 3 4 5 6 7 8 9 10 12 14 15 1 2 3 4 5 6 7 8 9 12 13 15 16

Number of CPFs used	CPF IDs for the top 5 options ($P = 600$ sec)
14	1 2 3 4 5 6 7 8 9 12 13 14 15 16
	1 2 3 4 5 6 7 8 9 11 12 14 15 16
	1 2 3 4 5 6 7 8 9 10 12 14 15 16
	1 2 3 4 5 6 7 8 9 11 12 13 14 15
	1 2 3 4 5 6 7 8 9 10 12 13 14 15
15	1 2 3 4 5 6 7 8 9 10 12 13 14 15 16
	1 2 3 4 5 6 7 8 9 11 12 13 14 15 16
	1 2 3 4 5 6 7 8 9 10 11 12 14 15 16
	1 2 3 4 5 6 7 8 9 10 11 12 13 14 15
	1 2 3 4 5 6 7 8 9 10 11 12 13 15 16

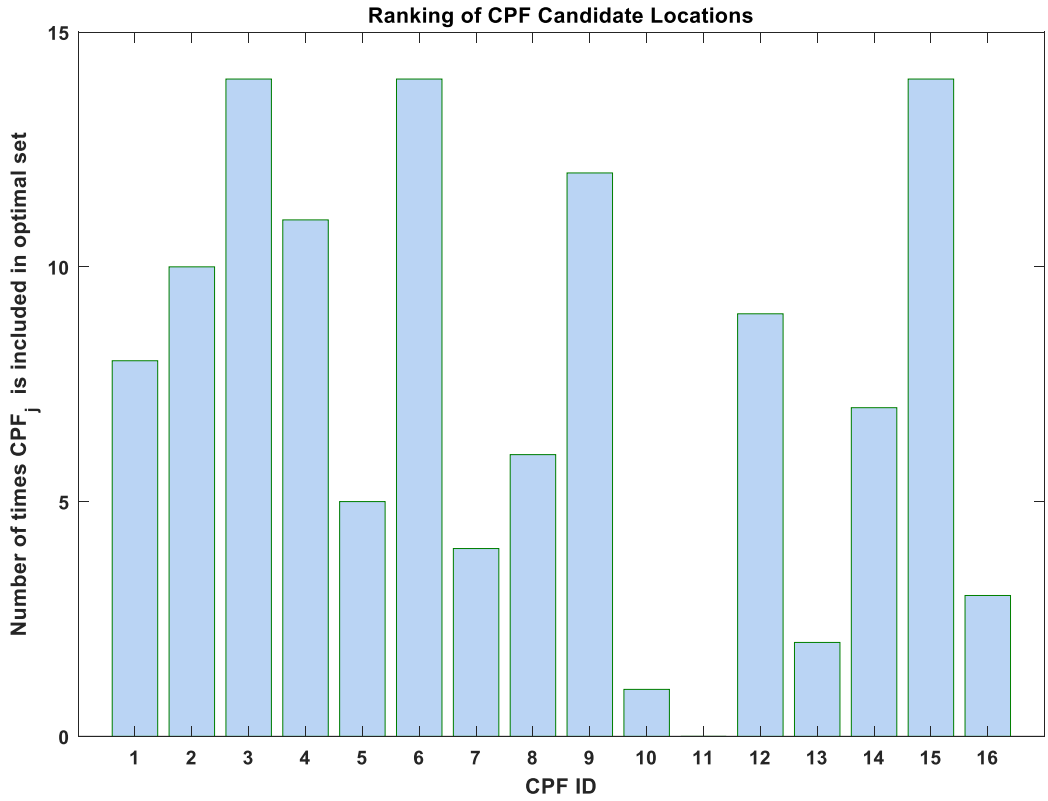

Figure 21. Ranking of CPF candidate locations (*P* = 600 sec). The CPFs are ranked by the number of times each one has been included in the optimal set (based on the results of Table 16 and Table 17). In this figure CPFs {3, 6, 15} are the three highest-ranked CPFs.

Table 18. Top CPF ranking for import / export transactions.

CPF ID	Address	CPF Ranking	
		P= 1200 sec	*P*=600 sec
3	River Ave, Long Beach, CA 90810, USA	1	1
15	S Figueroa St, Wilmington, CA 90744, USA	2	1
6	Long Beach Blvd, Long Beach, CA 90805, USA	3	1
9	Atlantic Ave, Long Beach, CA 90805, USA	4	4
4	E 213th St, Carson, CA 90746, USA	8	5
2	Via Oro Ave, Long Beach, CA 90810, USA	7	6
12	Torrance Blvd, Carson, CA 90745, USA	5	7
1	Golden Ave, Long Beach, CA 90806, USA	6	8
14	W Del Amo Blvd, Torrance, CA 90502, USA	9	9
8	S Sportsman Dr, Compton, CA 90221, USA	10	10
5	E Del Amo Blvd, Carson, CA 90746, USA	11	11
7	Long Beach Blvd, Long Beach, CA 90805, USA	13	12
16	Lomita Blvd, Carson, CA 90745, USA	12	13
13	W Del Amo Blvd, Torrance, CA 90502, USA	14	14
10	Alondra Blvd, Paramount, CA 90723, USA	15	15
11	Alondra Blvd, Paramount, CA 90723, USA	16	16

6.5 Linear Program Sensitivity Analysis

In this section, a sensitivity analysis is performed. The analysis presents the effects on the total travel time of variations in the following quantities:

- The number of CPFs used
- Limitations on CPF capacity
- Total number of transactions
- The ratio of import to export transactions

Table 19 (import transactions only) shows the effect that the number of CPFs used and the CPF capacity limitations have on the total travel time. The results of the table are for the import-only situation, when $P = 1200$ sec. The table presents several comparisons between cases where the following quantities are varied:

(a) Varying the number of CPFs used (presented in the rows of Table 19). Here comparisons are performed only for the cases when 1, 2, or 3 CPFs are used, since using more than 3 CPFs does not provide significant improvements. All these results are compared to the baseline results of using 0 CPFs, which is the case of direct routing to the marine terminals. The comparisons include the following CPF sets:

- When a single CPF is used, the top 5 single CPFs are included in the comparison set;
- When two CPFs are used, the top 5 CPF pairs are included in the comparison set;
- When three CPFs are used, the top 5 CPF triplets are included in the comparison set;

(b) Varying the capacity of the CPFs (presented in the columns of Table 19). Here comparisons are performed between the cases of unlimited and limited CPF capacity, as estimated previously (Table 5).

The last two columns of Table 19 present the improvements in total travel time when using the CPFs as compared to the baseline scenario (direct routing to the marine terminals). It is seen that the improvements range from 11% to 21%. When the selected CPFs are restricted to the top ranked only, the improvements are in the range of 16% to 21%. The difference in improvements between the limited CPF capacity and unlimited CPF capacity cases are relatively small, for the top ranked CPFs.

Table 19. CPF rankings vs CPF capacity: import transactions only.

Number of CPFs Used	**CPF ID**		**Value of the objective function Total travel time (sec x 10^7)**		**Percent improvement over baseline**	
	Limited CPF capacity	Unlimited CPF capacity	Limited CPF capacity	Unlimited CPF capacity	Limited CPF capacity	Unlimited CPF capacity
0 (Baseline)			3.6731	3.6731		
1	3 6 1 16 4	3 15 7 6 16	3.0765 3.1522 3.1992 3.2011 3.2524	3.0765 3.1146 3.1521 3.1522 3.1543	16% 14% 13% 13% 11%	16% 15% 14% 14% 14%
2	3 16 3 15 6 16 1 16 3 12	3 15 7 15 6 15 1 15 3 16	2.9604 2.9637 2.9650 2.9922 2.9960	2.9251 2.9311 2.9311 2.9536 2.9604	19% 19% 19% 19% 19%	20% 20% 20% 20% 19%
3	3 12 15 3 6 15 3 6 16 6 12 15 3 14 15	3 7 15 3 6 15 3 9 15 3 8 15 4 7 15	2.9205 2.9207 2.9225 2.9234 2.9238	2.8888 2.8889 2.8898 2.9004 2.9104	20% 20% 20% 20% 20%	21% 21% 21% 21% 21%

Similarly, Table 20 (import and export transactions) shows the effect that the number of CPFs used and the CPF capacity limitations have on the total travel time. The results of the table correspond to $P = 1200$ sec. The table presents several comparisons between cases where the following quantities are varied:

(a) Varying the number of CPFs used (presented in the rows of Table 20). Here comparisons are performed only for the cases when 1, 2, or 3 CPFs are used (since using more than 3 CPFs does not provide significant improvements). All these results are compared to the baseline results of using 0 CPFs, which is the case of direct routing to the marine terminals. The comparisons include the following CPF sets:
- When a single CPF is used, the top 5 single CPFs are included in the comparison set;
- When two CPFs are used, the top 5 CPF pairs are included in the comparison set;
- When three CPFs are used, the top 5 CPF triplets are included in the comparison set;

(b) Varying the capacity of the CPFs (presented in the columns of Table 20). Here comparisons are performed between the cases of unlimited and limited CPF capacity, as estimated previously (Table 5).

The last two columns of Table 20 present the improvements in total travel time when using the CPFs as compared to the baseline scenario (direct routing to the marine terminals). It is seen that the improvements range from 11% to 21%. When the selected CPFs are restricted to the top ranked only, the improvements are in the range of 16% to 21%. The difference in improvements between the limited CPF capacity and unlimited CPF capacity cases are relatively small, for the top ranked CPFs.

Table 21 shows the CPF ranking when the number of total transactions varies, for $P = 1200$. The table shows the results for the case when 2 CPFs with limited capacity are used. From Table 21 it can be seen that as the total number of transactions grows beyond 30,000, CPF6 passes CPF3 as the best possible candidate. This is due to the fact that the capacity of CPF6 is larger than that of CPF3, and as the difference between export and import transactions grows beyond 10,000 the benefit of routing transactions to the more optimally located CPF3 is eventually out-weighed by the higher capacity of CPF6.

Table 20. CPF rankings vs CPF capacity: import and export transactions.

Number of CPFs Used	CPF ID		Value of the objective function Total travel time (sec x 10^7)		Percent improvement over baseline	
	Limited CPF capacity	Unlimited CPF capacity	Limited CPF capacity	Unlimited CPF capacity	Limited CPF capacity	Unlimited CPF capacity
0 (Baseline)			5.5097	5.5097		
1	3	3	4.6147	4.6147	16%	16%
	6	15	4.7283	4.6719	14%	15%
	16	7	4.7384	4.7282	14%	14%
	1	6	4.7614	4.7283	14%	14%
	15	16	4.7640	4.7315	14%	14%
2	3 15	3 15	4.3934	4.3877	20%	20%
	6 15	7 15	4.4047	4.3966	20%	20%
	3 16	6 15	4.4406	4.3966	19%	20%
	1 15	1 15	4.4437	4.4303	19%	20%
	6 16	3 16	4.4475	4.4406	19%	19%
3	3 6 15	3 7 15	4.3378	4.3333	21%	21%
	3 7 15	3 6 15	4.3447	4.3333	21%	21%
	3 9 15	3 9 15	4.3458	4.3348	21%	21%
	3 8 15	3 8 15	4.3561	4.3506	21%	21%
	4 6 15	4 7 15	4.3702	4.3655	21%	21%

Table 21. CPF rankings vs total number of transactions: import and export transactions.

Total number of transactions	Number of import transactions	Number of export transactions	Difference between import and export transactions	CPF ID	Value of the objective function Total travel time (sec x 10^7)
7500	2500	5000	2500	3 15 6 15 1 15 3 16 6 16	2.0481 2.0529 2.0700 2.0723 2.0755
15000	5000	10000	5000	3 15 6 15 3 16 1 15 6 16	4.3934 4.4047 4.4406 4.4437 4.4475
22500	7500	15000	7500	3 15 6 15 3 16 6 16 3 12	6.4534 6.4756 6.5129 6.5235 6.5946
30000	10000	20000	10000	3 15 6 15 3 16 6 16 3 12	8.8058 8.8292 8.8837 8.8992 8.9944
37500	12500	25000	12500	6 15 3 15 3 16 6 16 3 12	10.9243 10.9705 10.9824 10.9842 11.1492
45000	15000	30000	15000	6 15 6 16 3 15 3 16 3 12	13.3293 13.3774 13.4015 13.4182 13.6036
52500	17500	35000	17500	6 15 6 16 3 15 3 16 3 6	15.5100 15.5408 15.6107 15.6182 15.7774

60000	20000	40000	20000	6 15 6 16 3 15 3 16 3 6	17.9485 17.9864 18.0569 18.0770 18.2081

Figure 22 shows the percent change in total travel time as a function of the ratio of exports and imports for a fixed total number of transactions (~15,000). The results in the figure correspond to the case when 2 CPFs with limited capacity are used, for $P = 1200$. From Figure 22 it can be seen that a 1:1 export/import ratio provides an optimal point, where the allowed reuse of the chassis returned after dropping off exports as chassis for retrieving imports eliminates the impact of the effect of CPF capacity. In addition, one can see that as would be expected changing the export/import ratio from 2:1 to 1:1 in this plot shows the same improvement as removing any capacity restrictions on CPFs as noted in Table 18 for the 2 CPF case.

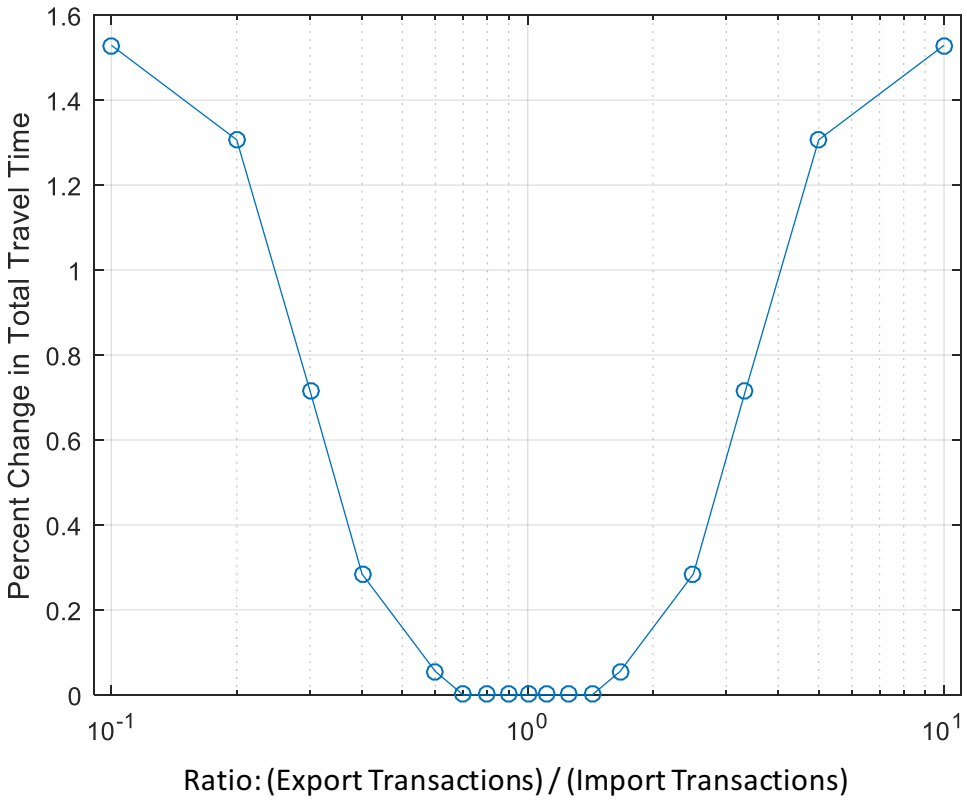

Figure 22. Percent change in total travel time vs. ratio of (export/import) transactions. Percent change in total travel time for optimal solution vs. different values of the ratio of (export transactions)/(import transactions). The zero value in the vertical axis corresponds to the case when this ratio is equal to 1.0.

7 Discrete Event Simulation Model (DESM)

A discrete event simulation model (DESM) of the transaction routing process has been developed and presented in this section. The discrete event model is used to simulate details which have not been included in the analytical model, such as daily traffic variations, queuing at the marine terminal or queuing at the CPFs, and other variations which are used to represent a more realistic environment. The tool selected for building the DESM was Simulink's SimEvents, a discrete event simulation toolbox from the MathWorks. The development of the DESM follows the development of the simulation scenarios presented in Section 0. Initially the DESM shown in Figure 23 is developed to match the "import-only transactions" scenario described in Section 0. The DESM was subsequently enhanced to simulate the full analytical model, which includes import and export transactions through 16 potential CPF locations. The optimal results for chassis routing from the points of origin through the CPFs to the marine terminals were provided as inputs to the model. The assignments in the discrete model, however, were randomized.

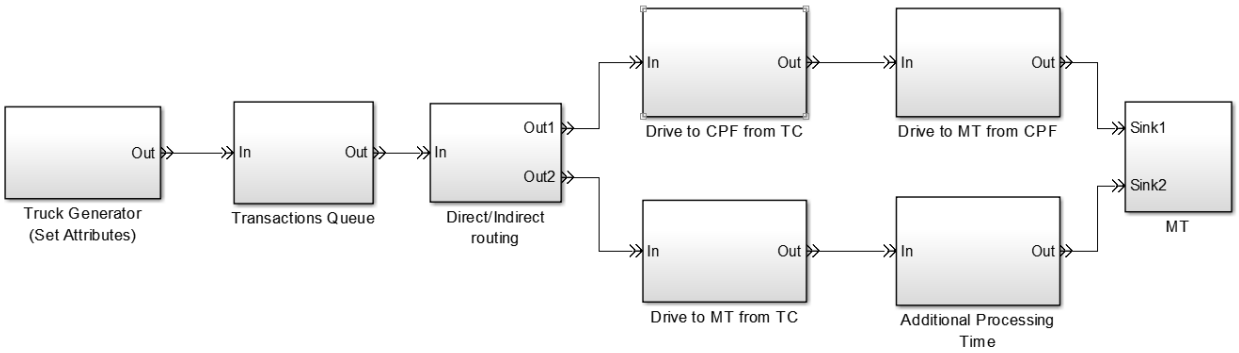

Figure 23. Discrete event simulation model of the transaction routing process.

In the DESM shown in Figure 23. Discrete event simulation model of the transaction routing process.Figure 23, trucks are generated at a specific point of origin (TC) and then are randomly assigned to different destination points (MTs). The trucks then are routed based on the analytical results of Section 0. For example, consider a case when the analytical optimal results show that half of the transactions between TC_1 and MT_2 are routed through CPF_3 and the remaining transactions are routed directly to MT_2. Then, any time a truck traveling between TC_1 and MT_2 is generated in the discrete model, it has a 50% chance of being routed through CPF_3 and a 50% chance of being routed directly to MT_2.

Once the routing of trucks is determined, the DESM uses the travel time between points as described in Section 0, in order to simulate the process. The parameter *P* (page **Error! Bookmark not defined.**) used in the simulation scenarios is implemented in the DESM as an additional delay added to the processing time required to complete a transaction.

7.1 Validation of the discrete event simulation model

For validation purposes, the DESM was first set up to run with the same simulation parameters as the full analytical model of Section 0. In order to obtain statistical data regarding the validity of the DESM, one hundred simulations were performed and the results are presented in Table 22 and Figure 24.

Figure 24 as well as the second column of Table 22 show the average number of transactions through each CPF, averaged over one hundred simulation runs. These averages match the second column of Table 14 very closely.

Table 22. CPF routing with the DESM (*P* = 1200 sec).

CPF ID	Average number of transactions routed through CPF
1	4227
2	1452
3	9710
4	4288
5	259
6	10712
7	582
8	2182
9	771
10	0
11	0
12	3180
13	1109
14	1868
15	2344
16	7016
Note: (i) Only import transactions are considered (ii) All CPFs are available (iii) The full 101-node model is used	

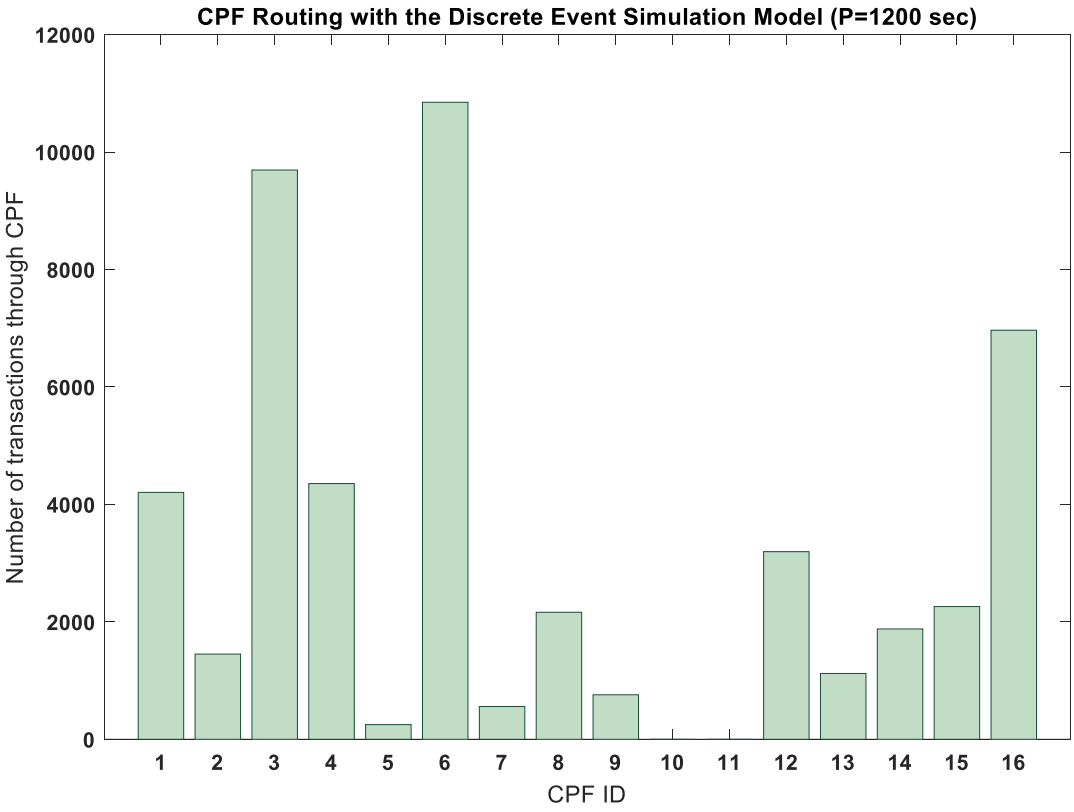

Figure 24. Average number of transactions routed through each CPF. In this figure: (i) only import transactions are considered; (ii) all CPFs are available; (iii) the full 101-node model is used (model includes all TCs, CPFs and MTs)

The percent difference in the value of the objective function between the optimal solution and the DESM, for all one hundred simulation runs is shown in Figure 25. This difference is less than ± 2%. Figure 26 presents the same difference, plotted as a running average over one hundred simulations. From these figures, it is seen that the DESM approximates the analytical model very well. The DESM will be used for further experimentation, in cases where the analytical model is not available, such as when heuristic techniques are used and evaluated.

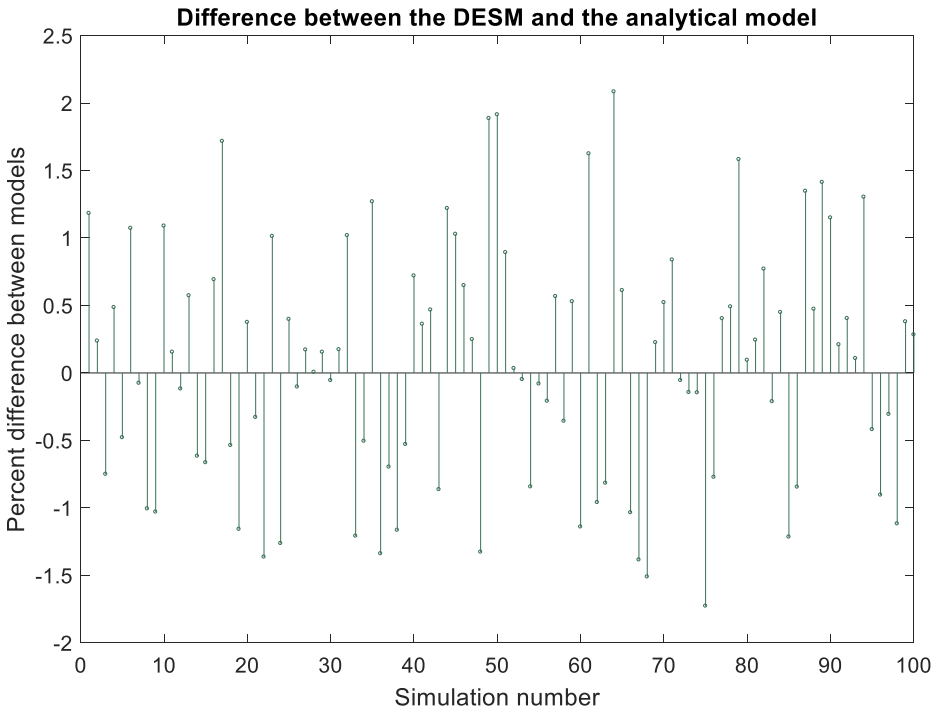

Figure 25. Percent difference in the value of the objective function between the DESM and the analytical model plotted for each simulation run.

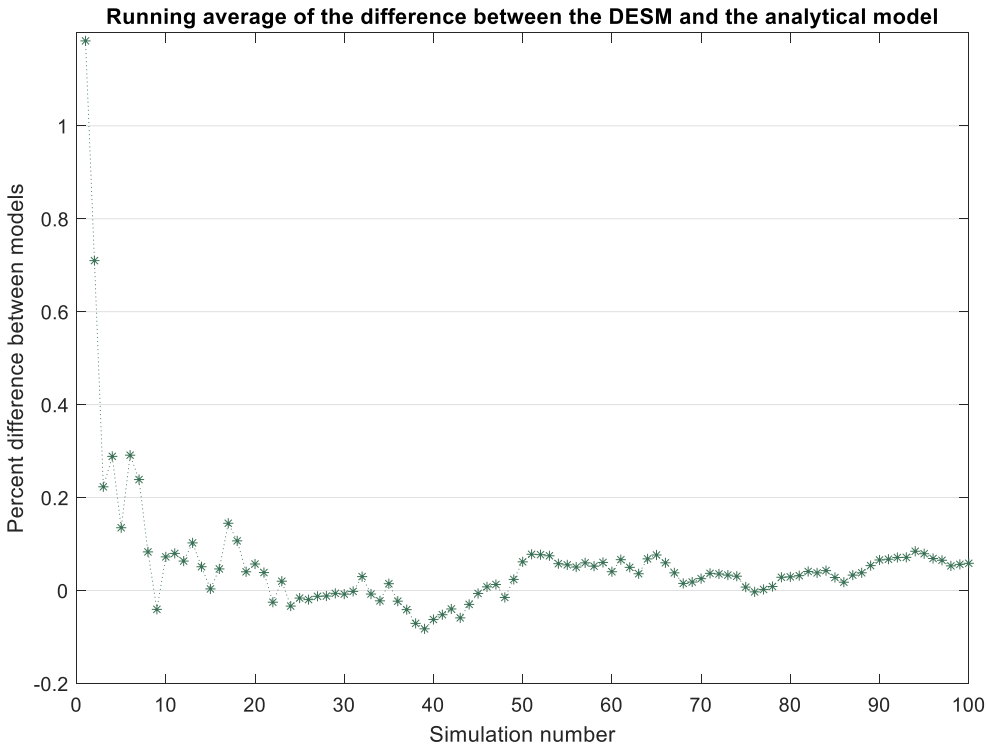

Figure 26. Running average of the percent difference in the value of the objective function between the DESM and the analytical model, plotted over 100 simulations.

7.2 Comparison of Optimal Solution to the Baseline Case using the DESM

The baseline case is defined as the situation when all transactions are routed directly to the marine terminals without using any of the CPFs. The DESM shown in Figure 27 is developed to simulate the baseline case, and compare it to the optimal solution.

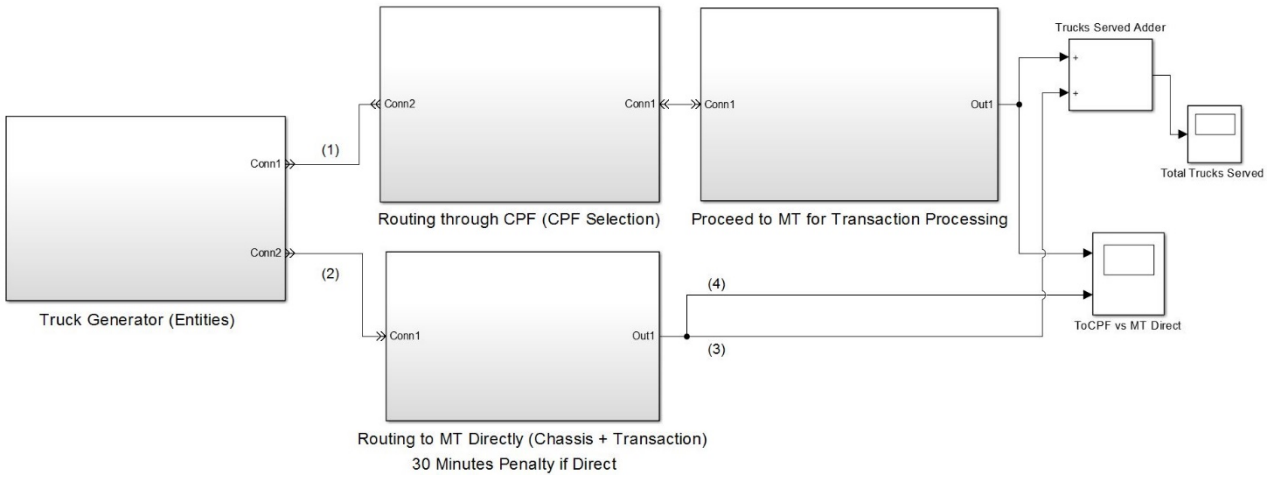

Figure 27. DSEM for baseline case

Figure 28 and

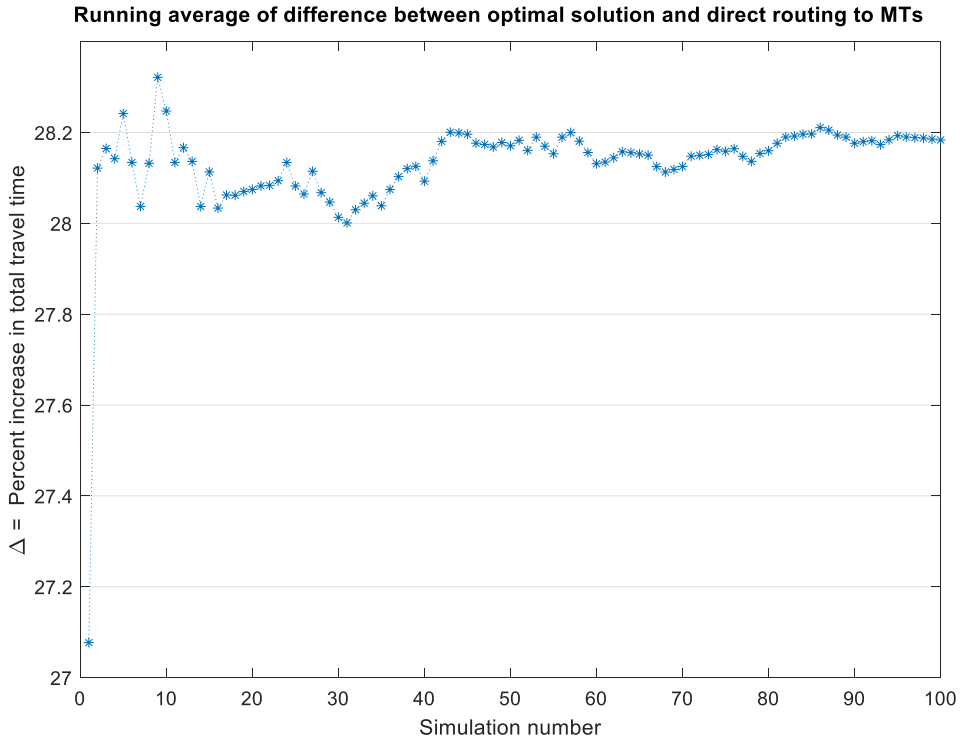

Figure 29 present the results of one hundred simulations. Figure 28 shows the percent increase in total travel time if direct routing to MTs is used for all transactions, as compared to routing performed by the optimization algorithm when all CPFs are available.

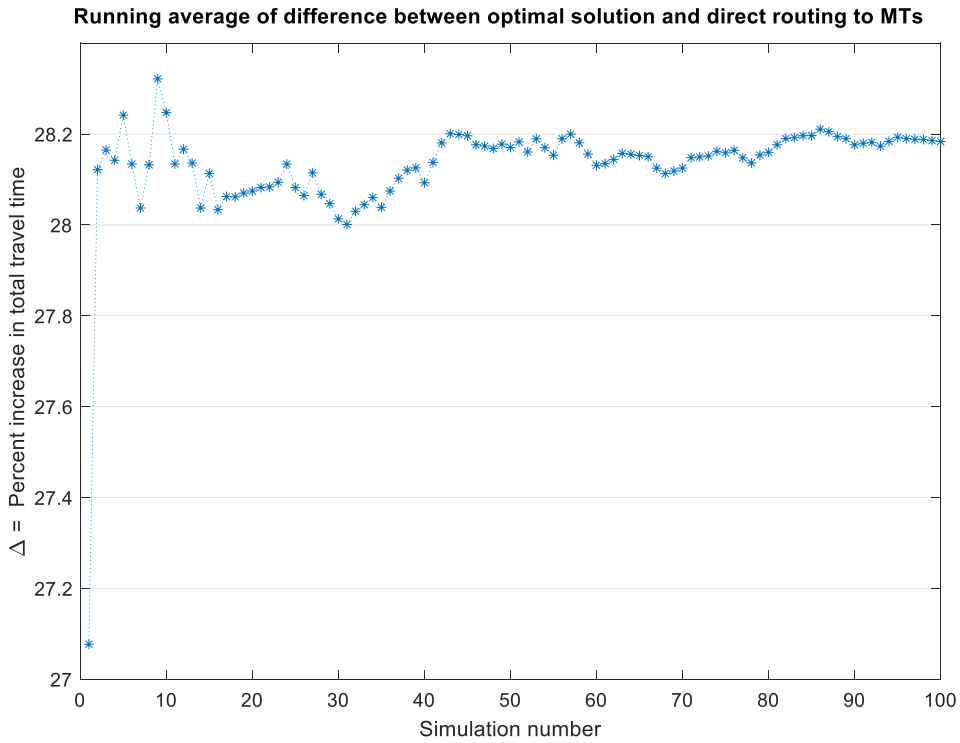

Figure 29 presents the running average of the increase, averaged over one hundred simulations. In both figures the percent increase (Δ) in total travel time is defined as:

$$\Delta = \left(\frac{T_{DR} - T_{OPT}}{T_{OPT}}\right)\%$$

Where:

T_{DR} = (Total travel time for direct routing to marine terminals)
T_{OPT} = (Total travel time for optimal solution routing through CPFs**)**

It is seen that routing directly to marine terminals suffers by an average increase of 28.2% in total travel time as compared to the optimal solution.

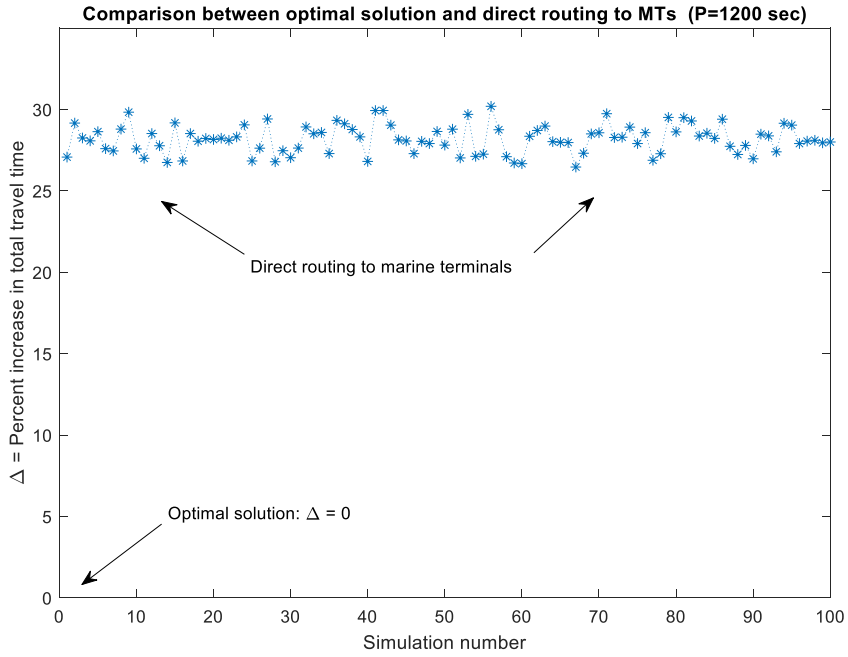

Figure 28. Comparison between the optimal solution and direct routing to MTs
In this figure: (i) only import transactions are considered; (ii) all CPFs are available; (iii) the full 101-node model is used (model includes all TCs, CPFs and MTs)

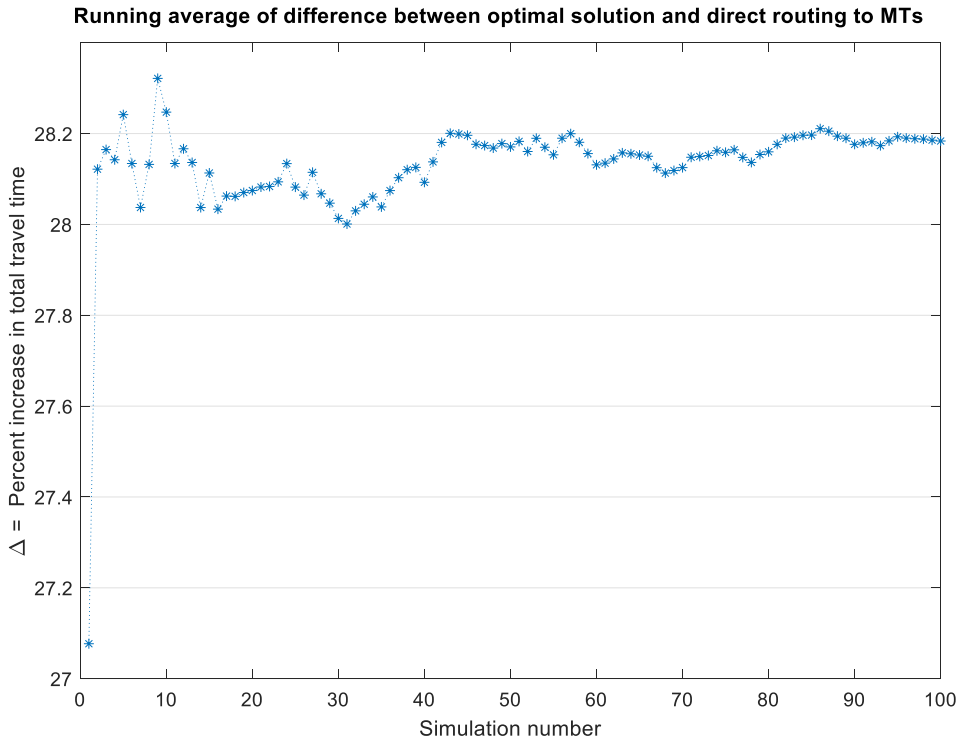

Figure 29. Running average of percent difference between optimal solution and direct routing to MTs

7.3 Heuristic Methods

In addition to the previous simulations, the DESM has been used to simulate and evaluate two heuristic routing methods, termed H1 and H2 in this report.

The number of available chassis at a CPF at a given time is an important variable for the simulation of heuristics H1 and H2. This variable is denoted by $N_{ACj}(t)$ and defined as:

$$N_{ACj}(t) = \text{Number of available chassis at CPF}_j \text{ at time } t$$

7.3.1 Heuristic Method H1

In the first heuristic method (H1), a truck is routed to the CPF that is the closest geographically (for example CPF_{j1}) to the truck's point of origin. The routing algorithm in heuristic H1 uses only local information, (i.e. uses only geographical proximity between the point of origin and the CPF, but does not use global considerations, which are applied over the totality of the nodes). The routing algorithm does not, therefore, take into account the number $N_{ACj1}(t)$ of chassis available at CPF_{j1}, at a given time t.

It is possible that a truck may be routed to pick up a chassis from the closest CPF_{j1}, when in fact CPF_{j1} is depleted of chassis at that time (i.e. $N_{ACj1}(t) = 0$). The heuristic strategy for H1, in such a case, will send the truck to the next closest CPF, e.g. CPF_{j2}. If CPF_{j2} is also depleted of chassis at that time, then the heuristic strategy will send the truck to the next closest CPF, etc.

Figure 30 presents the simulation results of applying Heuristic H1 to the full 101-node model using the DESM. The horizontal axis in Figure 30 is related to $N_{ACj}(t)$, the number of available chassis at CPF_j. For the purposes of this simulation, it is assumed that at the beginning of a simulation run, each CPF has an initial inventory of chassis available, proportional to the CPF's capacity. For simplicity, the proportionality constant, C_0, is the same for each CPF, and is defined as:

$$C_0 = \left(\frac{N_{ACj}(0)}{C_{ACj}} \right) \% \ ,$$

Where:

$N_{ACj}(0)$= (Number of available chassis at CPF_j at the beginning of the simulation)

C_{ACj}= (Capacity of CPF_j)

Thus, the total number of available chassis at the beginning of the simulation run will be:

$$\sum_{j=1}^{16} N_{ACj}(0) = \sum_{j=1}^{16} C_0 C_{ACj}$$

The horizontal axis of Figure 30 represents values of the proportionality constant C_0. The vertical axis is the percent increase (Δ_{H1}) in total travel time when heuristic H1 is used, as compared to the optimal solution, and is defined as

$$\Delta_{H1} = \left(\frac{T_{H1} - T_{OPT}}{T_{OPT}}\right)\%$$

Where:

T_{H1} = (Total travel time when heuristic H1 is used)
T_{OPT} = (Total travel time for optimal solution routing through CPFs**)**

The three lines in Figure 30**Error! Reference source not found.** represent calculations for three different values of the parameter *P, i.e.,* P = {300, 600, 900} seconds. From Figure 30, it can be seen that:

- When C_0 is small, the solution given by heuristic H1 is far from the optimal, especially for large values of *P.* When C_0 is small there are not enough chassis available at the CPFs, hence many transactions will be routed directly to the marine terminals.
- As C_0 increases, fewer transactions will be routed to the MTs. More and more transactions are routed through CPFs. If $C_0 \geq 60\%$, the three lines converge to the same value, independently of the parameter *P*.
- Heuristic H1 is a good suboptimal method, which can be implemented using only local information, as mentioned previously.
- Further analysis needs to be performed to determine whether heuristic H1 will still be a good suboptimal alternative, in the case that only a few CPFs are available, as was done with the analytical model.

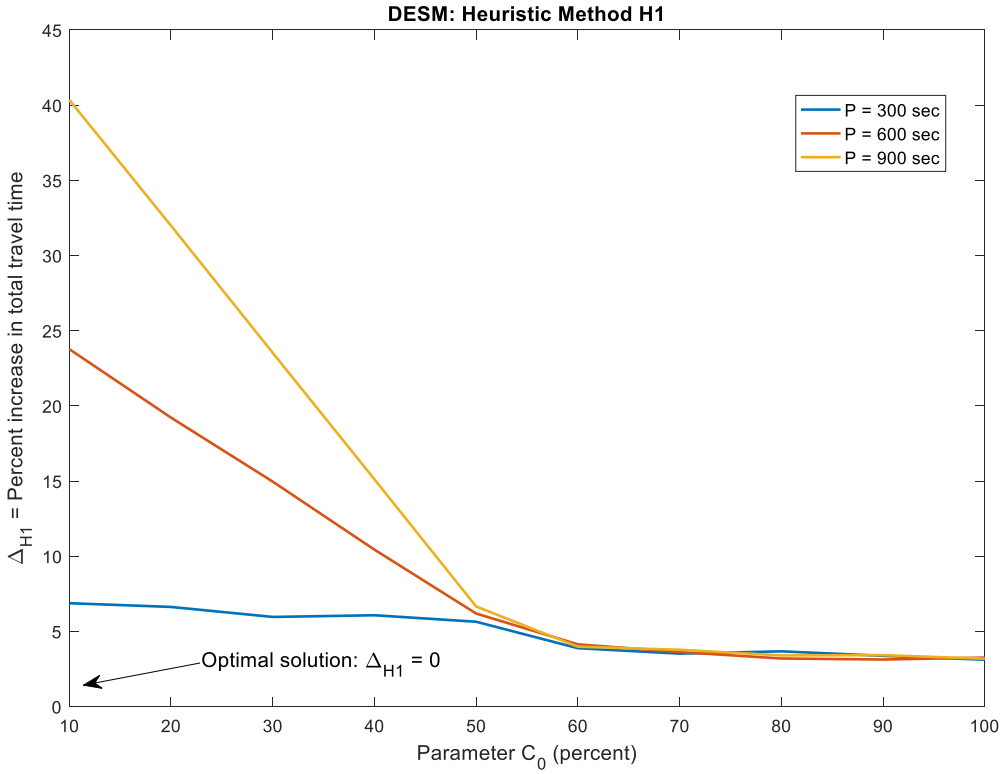

Figure 30. Percent increase in the value of the objective function between Heuristic H1 and the optimal solution. In this figure: (i) only import transactions are considered; (ii) all CPFs are available; (iii) the full 101-node model is used (model includes all TCs, CPFs and MTs)

7.3.2 Heuristic Method H2

In the second heuristic method (H2), a truck is routed to the CPF that lies on the shortest path from the truck's point of origin (TC) to its point of destination (MT). For every origin/destination pair {TC_j, MT_k} all paths through all available CPFs are calculated.

The same considerations as those of Heuristic H1, regarding the initial number of available chassis, apply to Heuristic H2 as well.

Error! Reference source not found. Figure 31 presents the simulation results of applying Heuristic H2 to the full 101-node model using the DESM. The horizontal axis in Figure 31 is the same proportionality constant C_0 as defined for Heuristic H1. The vertical axis of Figure 31 shows the percent increase (Δ_{H2}) in total travel time when heuristic H2 is used, as compared to the optimal solution, and is defined as:

$$\Delta_{H2} = \left(\frac{T_{H2} - T_{OPT}}{T_{OPT}}\right)\%$$

Where:

T_{H2} = (Total travel time when heuristic H2 is used)
T_{OPT} = (Total travel time for optimal solution routing through CPFs**)**

The three lines in Figure 31 represent calculations for three different values of the parameter *P, i.e., P* = {300, 600, 900} seconds. From Figure 31, it can be seen that:

- When C_0 is small, the solution given by heuristic H2 is far from the optimal, especially for large values of *P.* When C_0 is small there are not enough chassis available at the CPFs, hence many transactions will be routed directly to the marine terminals.
- As C_0 increases, fewer transactions will be routed to the MTs. More and more transactions are routed through CPFs. If $C_0 \geq 60\%$, the three lines converge to the same value, independently of the parameter *P*.
- Heuristic H2 is a good suboptimal method, which can be implemented using only local information.
- Further analysis needs to be performed to determine whether heuristic H2 will still be a good suboptimal alternative, in the case that only a few CPFs are available, as was done with the analytical model.

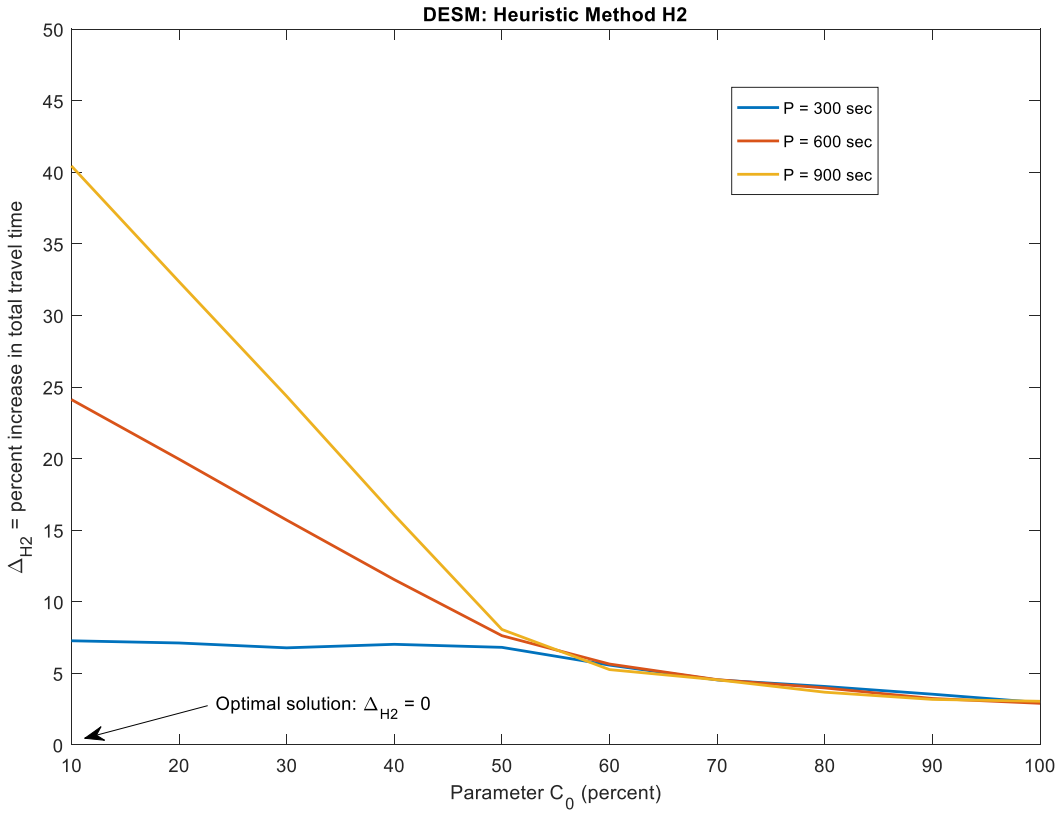

Figure 31. Percent increase in the value of the objective function between Heuristic H2 and the optimal solution. In this figure: (i) only import transactions are considered; (ii) all CPFs are available; (iii) the full 101-node model is used (model includes all TCs, CPFs and MTs)

7.3.3 Relation of Heuristic H1 to Heuristic H2

Figure 32 presents the percent increase in total travel time for the two heuristics H1 and H2. From Figure 32 it can be seen that:

- The two heuristics are close to each other, and exhibit similar behavior for varying values of the parameter C_0.
- When $C_0 \geq 85\%$, the two heuristics converge to the same values, independently of the parameter *P*.
- Both H1 and H2 are good suboptimal methods, and can be implemented using only local information.
- Heuristic H1 performs slightly better than heuristic H2, although the total path length between origin/destination pairs for H2 is always shorter or equal to the total path length for H1. This is due to the fact that the selection of H2 is based on distance, whereas the vertical axis in Figure 32 is based on time. It is possible that a path can have shorter length, but the truck may take longer to reach the destination, depending on average travel speed along the path.
- Further analysis needs to be performed to determine whether the two heuristics will stay close to each other, and whether they remain good suboptimal alternatives, in the case that only a few CPFs are available.

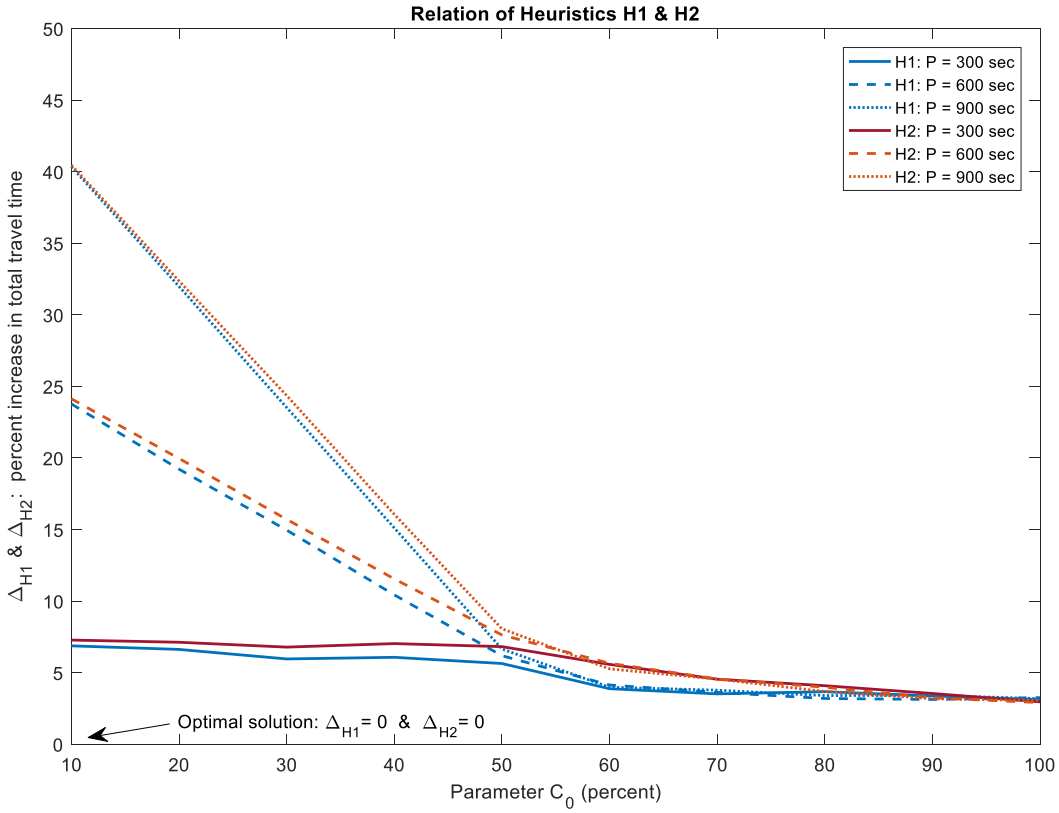

Figure 32. Comparison of Heuristics H1 & H2. In this figure: (i) only import transactions are considered; (ii) all CPFs are available; (iii) the full 101-node model is used (model includes all TCs, CPFs and MTs)

7.4 Simulations with Varying Traffic Conditions Using the DESM

The simulations presented in the previous sections calculate the travel times between points on the map using average speed data. The average speeds for each individual path on the map are obtained from Google maps and used in the discrete event simulation model. In this section speed data from the PeMS database [21] for the Long Beach region are used, differentiating between times of little or no congestion and times of higher traffic congestion.

Figure 33 presents the total travel time for the optimal solution, under varying traffic conditions: (a) no traffic congestion, and (b) typical traffic congestion. The results of twenty simulation runs of the DESM are presented. It is seen that under typical traffic congestion conditions the optimal solution is approximately higher by 25% as compared to conditions under no traffic congestion.

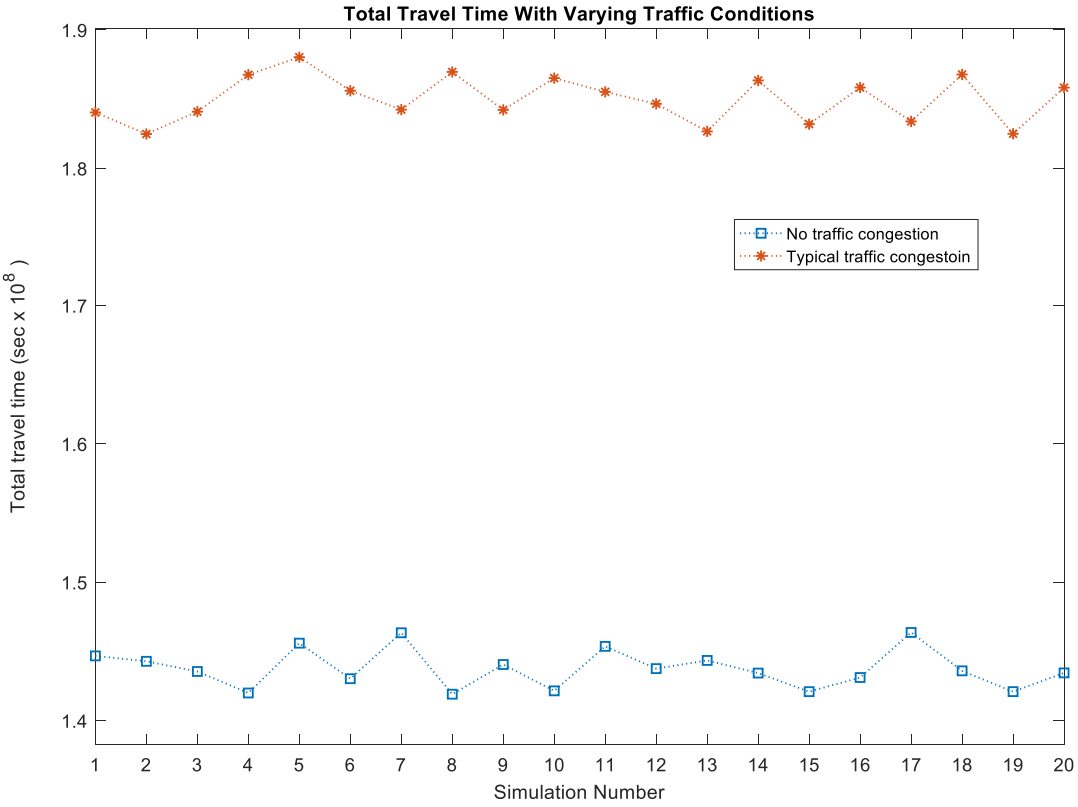

Figure 33. Total travel time with varying traffic conditions at optimality. In this figure: (i) only import transactions are considered; (ii) all CPFs are available; (iii) the full 101-node model is used (model includes all TCs, CPFs and MTs)

7.5 Preliminary Model for Calculations of CO2 Emissions

This section presents a simplified model of CO_2 emissions to determine any possible benefits when routing through the CPFs vs. direct routing to the MTs (baseline). The emissions calculations are performed for the full analytical model with import and export transactions, for a value of the parameter *P* = 1200 sec, as described in Section 0. Based on the results of Section 0, only the three top-ranked CPFs = $\{3, 6, 15\}$ are used for truck routing, since using more than three CPFs does not improve the objective function significantly.

For the simplified emissions model used here, two travel modes are considered: cruise and creep, as defined by the FHWA [22]. The cruise mode is the typical driving pattern while a truck is travelling from its point of origin towards a CPF or towards a marine terminal. The creep mode refers to vehicle driving patterns operating at a very low speed, at an average of 1.77 mph. The creep mode is the typical driving pattern while a truck is waiting in queue to enter a marine terminal, or while it is waiting to pick up a chassis inside the marine terminal. Assuming

that there is no queue while the truck is entering a CPF, or while the truck is picking up a chassis at the CPF, then the creep mode is not relevant in cases when a CPF is used.

For heavy duty trucks in cruise mode an average rate of CO_2 emissions of 2,100 grams/mile is used; in the creep mode an average rate of 6,900 grams/mile is used [22]. Based on this model and using10,000 import transactions and 5,000 export transactions, the CO_2 emissions for the optimal solution of Section 0 are calculated. When there is no creep at the marine terminals, then there is no benefit in using the CPFs from the emissions perspective, since all calculations in that case will be based on miles travelled in cruise mode. When there is creep for an average length of two miles at the marine terminals, then routing through CPFs will reduce the CO_2 emissions by approximately 4%, when compared to the baseline. In the future, the discrete event simulation system can be enhanced to include a detailed emissions model for each simulated vehicle.

8 Conclusions

In this project, the concept of Centralized Processing of Chassis is studied, and the possibility of using this concept to reduce total travel time to/from ports is explored. A mathematical optimization framework is defined for minimizing the total travel time for trucks which are picking up or dropping off containers from/at marine terminals. An analytical model of the chassis exchange process is developed, and the optimization results are applied to a case study using the ports of Long Beach and Los Angeles. Central to the methodology of centralized processing of chassis is the concept of a "Chassis Processing Facility" (CPF), an area close to the port where the trucks will go to exchange chassis outside of the marine terminals.

The case study identifies sixteen locations in the vicinity of the ports that can be potentially used as CPFs, and evaluates several scenarios of container pickup/drop-off transactions. The case study uses the geographic locations of the sixteen potential CPFs, the locations of the fourteen container terminals at the ports, and the locations of seventy-one trucking companies in the vicinity of the ports. Simulation scenarios using typical traffic patterns between locations, and typical chassis-related transactions are studied. The simulation scenarios are first validated on a reduced-size model, and then are applied to the full-size model which includes all marine terminals, all potential CPFs and all points of origin for trucks (a total of 101 nodes in the optimization model).

A major advantage of using a CPF for chassis exchange is that the CPF offers a reduced chassis retrieval time, as compared to chassis retrieval time at a marine terminal (this difference between the chassis retrieval times when using the CPFs vs. when using the marine terminals directly is termed the parameter P in the report). The simulation results show that using the CPFs can provide improvement (reduction) of the total travel time by 5%-10% if the parameter P=600 sec, whereas improvements of 20%-25% in total travel time can be expected if the parameter P=1200 sec. A sensitivity analysis with respect to the number of CPFs employed for chassis exchange, shows that the optimal solution does not improve after more than three CPFs are used. In addition, a discrete event simulation model has been implemented, which is used as a tool for performing a more detailed study, taking into account items not included in the analytical model such as daily traffic variations, queuing at the marine terminal and chassis retrieval locations, and other random variations which represent a more realistic environment. The discrete event simulation model has also been used to simulate two heuristic methods for chassis exchange. The performance of the heuristic methods is far from the optimal when the chassis availability is limited, but it converges to within 5% of the optimal when chassis availability is close to the CPF capacity.

Potential follow-on activities for the current project include further development of the discrete simulation model and characterization of total travel time over a wider variety of real-life scenarios, further development of the analytical model to include some of these same stochastic processes, assessment of the impact on emissions, and other updates to linear program such as modification to optimize for total cost including actual cost of establishing and maintaining CPFs.

9 References

[1] "Port of Los Angeles Statistics," 2015. [Online]. Available: https://www.portoflosangeles.org/Stats/stats_2015.html.

[2] "Port of Long Beach Statistics," 2015. [Online]. Available: http://www.polb.com/economics/stats/yearly_teus.asp.

[3] The Tioga Group, "Empty Ocean Logistics Study," Technical Report, Submitted to the Gateway Cities Council of Governments, 2002.

[4] Cambridge Systematics, "Traffic Congestion and Reliability," Technical Report, Prepared for Federal Highway Administration, 2005.

[5] H. Jula, A. Chassiakos and P. Ioannou, "Port Dynamic Empty Container Reuse," *Transportation Research Part E: Logistics and Transportation, TRE,* vol. 42, no. 1, pp. 43-60, 2006.

[6] J. Zhang, P. Ioannou and A. Chassiakos, "Automated Container Transport System between Inland Port and Terminals," *ACM Transactions on Modeling and Computer Simulation,* vol. 16, no. 2, p. 2006, 95-118.

[7] H. Jula, A. Chassiakos and P. Ioannou, "Increasing the Efficiency of Empty Container Interchange," Final Report and Optimization Software. Center for Commercial Deployment of Transportation Technologies, California State University, Long Beach, 2003.

[8] T. O'Brien, T. Reeb and A. Kunitsa, "Mitigating Urban Freight through Effective Management of Truck Chassis," METRANS Transporation Center, 2014.

[9] H. D. Le-Griffin, L. Mai and M. Griffin, "Impact of container chassis management practices in the United States on terminal operational efficiency: An operations and mitigation policy analysis," *Research in Transportation Economics,* no. 32, pp. 90-99, 2011.

[10] Z. Izmirli, "The Gray Chassis Pool and What it Means to You," 5 January 2015. [Online]. Available: http://www.morethanshipping.com/the-gray-chassis-pool-and-what-it-means-to-you/.

[11] Bailey, Mollie; Hewitt, Sheila, "The Long-Term Effects of Chassis Shortages," BNP Media, 2014.

[12] "Freight Management and Operations," U, 20 November 2015. [Online]. Available: http://ops.fhwa.dot.gov/freight/freight_analysis/freight_story/congestion.htm.

[13] A. Kouri, "Congestion at ports of L.A., Long Beach is putting a damper on economy," December 2014. [Online]. Available: http://www.latimes.com/business/la-fi-port-traffic-20141226-story.html.

[14] S. van der Heide, "Truck Congestion Problems at Seaport Container Terminals: Analyzing innovative solutions," Erasmus School of Economics, Erasmus University, Rotterdam, 2010.

[15] W. Jew, "3 Things Happening to get Shippers' Cargo Moving at the LA & LB Ports," 10 March 2015. [Online]. Available: http://www.universalcargo.com/3-Things-Happening-to-Get-Shippers-Cargo-Moving-at-the-LA-LB-Ports/. [Accessed 17 February 2016].

[16] R. Dekker, S. van der Heide, E. van Asperen and P. Ypsilantis, "A Chassis Exchange Terminal to Reduce Truck Congestion at Container Terminals," *Flexible Services and Manufacturing Journal,* p. 528–542, 2013.

[17] I. Vis and R. de Koster, "Transshipment of containers at a container terminal: an overview," *European Journal of Operation Research,* vol. 147, no. 1, p. 1–16, 2003.

[18] T. E. Notteboom, "Container shipping and ports: an overview," *Review of Network Economics,* vol. 3, no. 2, p. 86–106, 2004.

[19] D. Steenken, S. Voss and R. Stahlbock, "Container terminal operation and operations research a classification and literature review," *OR Spectrum,* vol. 26, p. 3–49, 2004.

[20] D. Weikel, "Los Angeles Times," 17 March 2015. [Online]. Available: http://www.latimes.com/local/california/la-me-california-commute-20150317-story.html.

[21] California Department of Transportation, "Caltrans Performance Measurement System," [Online]. Available: http://pems.dot.ca.gov/. [Accessed September 2016].

[22] FHWA, "Improving Vehicle Fleet, Activity, and Emissions Data for On-Road Mobile Sources Emissions Inventories," [Online]. Available: https://www.fhwa.dot.gov/environment/air_quality/conformity/research/improving_data/taqs05.cfm. [Accessed January 2017].

[23] Chassis System Inc. , "Stacker," [Online]. Available: http://www.chassissystems.com/. [Accessed May 2016].

Appendix

In order to support the analysis and optimization presented in this report, chassis storage and stacking arrangements are examined, based upon the two most common chassis lengths: 20ft and 40ft. This Appendix includes estimates of the area required to store chassis, and examines the time it takes to stack and unstack the chassis. The purpose of this investigation is to look into what the best storage models for a CPF may be, estimate the square footage requirement, and calculate the approximate chassis storage capacities of the potential CPFs based upon a common storage model. Three possible arrangements for CPFs are explored, including arrangements using two different methods for vertical storing of chassis as well as one arrangement in which chassis are stored horizontally.

A.1 Vertical Chassis Storing

This configuration, also known as parallel stacking, is an arrangement in which chassis are stacked upside down, parallel to one another and are supported by racks. Each rack can hold up to 8 chassis per side (see **Error! Reference source not found.**Figure 1). The tool that is used to stack chassis vertically is a side handler, a specialized stacker which uses hydraulics to rotate a chassis from horizontal to almost completely vertical. The stacker is shown in Figure 3. The process is relatively simple and a single chassis can be stacked or unstacked in about half a minute [23].

Figure Error! No text of specified style in document.**-1. Chassis racks.**

Figure Error! No text of specified style in document.**-2. Specialized hydraulic stacker lifting a chassis.**

Figure Error! No text of specified style in document.**-3. Example of vertical chassis storing.**

A.2 Chassis Storage Model 1

The first of the vertical storing models considered in this section is based upon the arrangement used in the Port of Virginia, shown in Figure Error**! No text of specified style in document.**-4 (a). Each block denoted by "A" in Figure Error**! No text of specified style in document.**-4 (b) can store up to 16 chassis stored vertically. A detailed view of a typical block "A" is presented in Figure Error**! No text of specified style in document.**-5. This model contains additional areas for chassis to be stored horizontally, located in-between the vertically stored chassis blocks. These additional areas serve as a temporary storage location for chassis ready to be picked up by a bobtail in order to allow for easier and faster access.

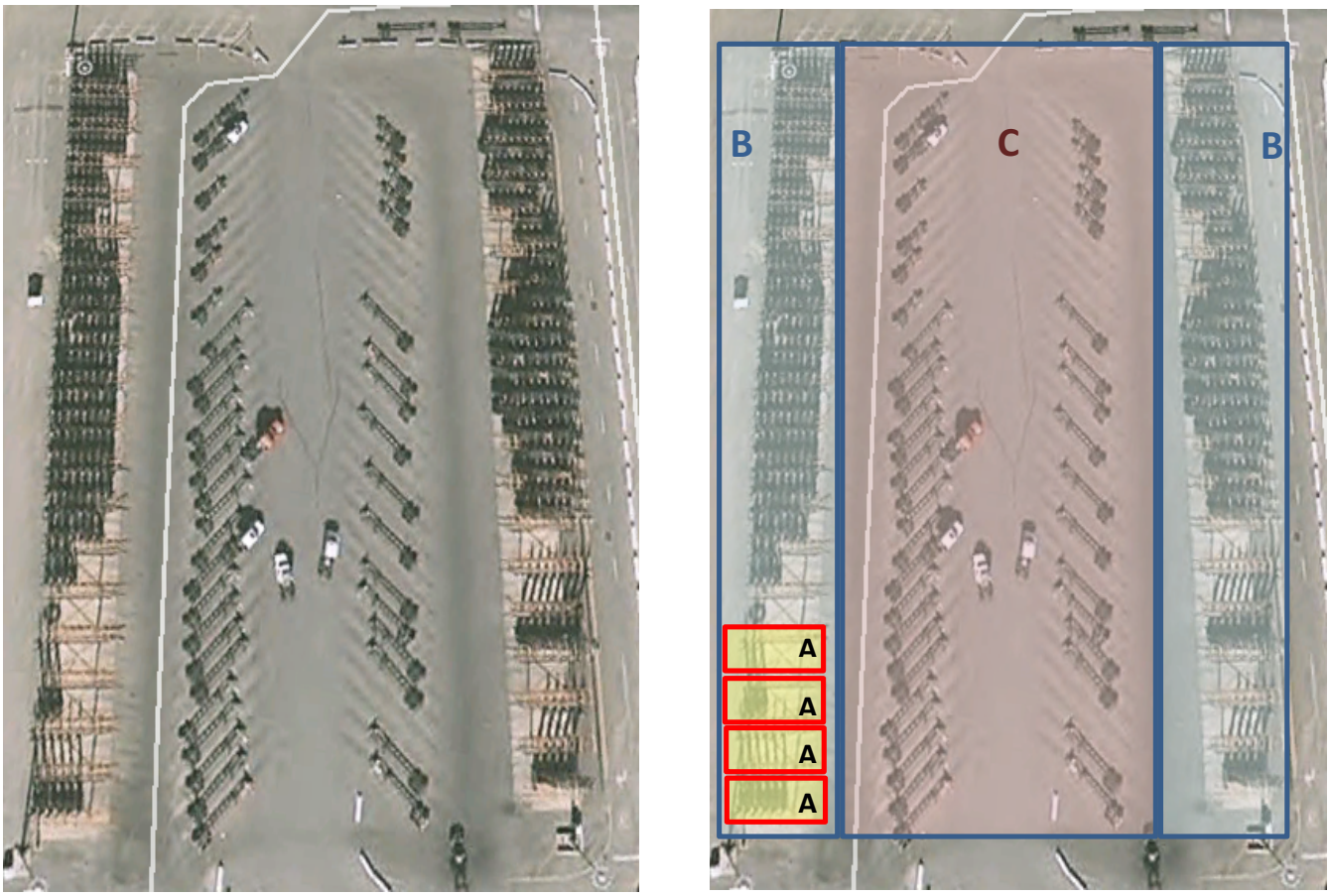

(a) **(b)**

Figure Error! No text of specified style in document.**-4. Port of Virginia arrangement of chassis storage. (a) The arrangement as captured by Google Images (2011). (b) Each block "A" can store up to 16 vertically stored chassis. A detailed view of block "A" is shown in Figure Error**! No text of specified style in document.**-5. Each block "B" consists of several "A" blocks arranged in parallel. Block "C" consists of horizontally arranged single chassis, ready to be picked up.**

Measurements of the relative distances for this layout were done using Google Earth. As viewed from above, a completely occupied rack block area contains 16 vertically stored chassis as illustrated in Figure A-5. In the figure, the rack of 16 vertically stored chassis occupies a footprint of approximately 40 ft x 21.5 ft. It is noted that an empty rack plus the space around it will have almost the same footprint as a fully occupied rack because the rack's upper axle that locks the chassis, extends to almost the same length as the chassis width.

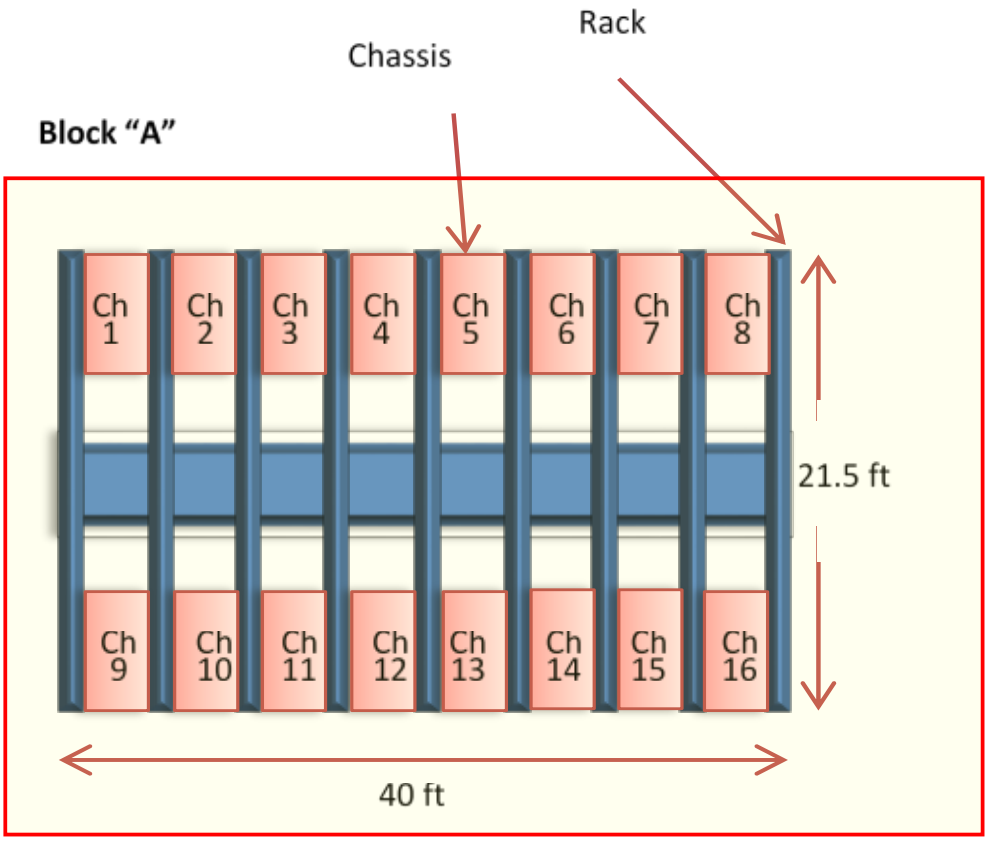

Figure Error! No text of specified style in document.**-5. (Top View) Chassis rack with 16 vertically stacked chassis.** Expanded and detailed view of block "A" shown in Figure Error! No text of specified style in document.**-4**. The rack stores 16 vertically stored chassis, denoted by $\{Ch1, Ch2, \cdots, Ch16\ \}$.

A front view of the rack is shown in Figure 0. The only difference between the 40ft and 20ft stored chassis volume is the additional height for the 40ft chassis, but the overall required footprint of the rack is the same for the two chassis sizes.

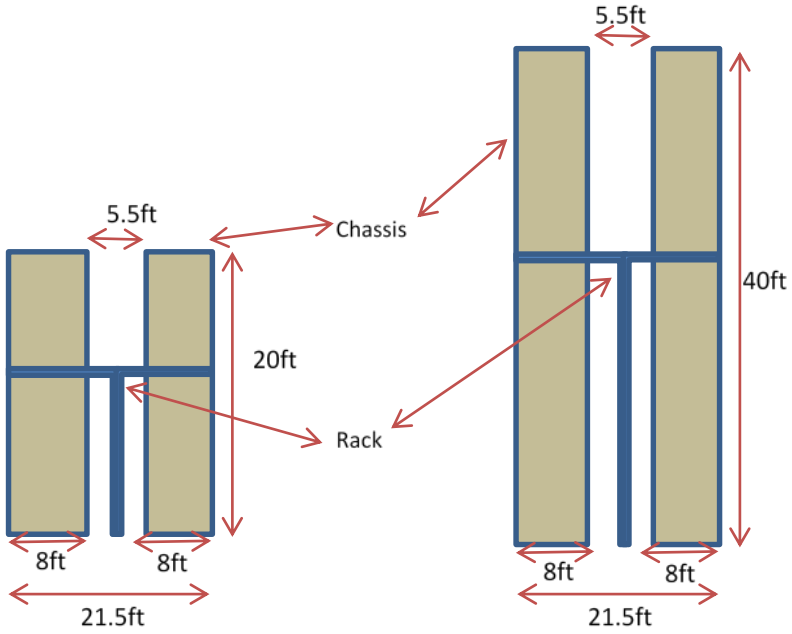

Figure Error! No text of specified style in document.**-6. Chassis rack (front view) with 20ft chassis (left) and 40ft chassis (right).**

Figure A-7 shows a generic layout of the chassis racks for a storage lot of different dimensions. In this figure, the pattern of blocks “B” and “C” which is outlined in Figure Error**! No text of specified style in document.**-4 (b), is repeated to fill the available storage area. The number of chassis which could be stored in a lot with a given footprint using Model 1, is calculated in Table Appendix A-1, for different lot sizes.

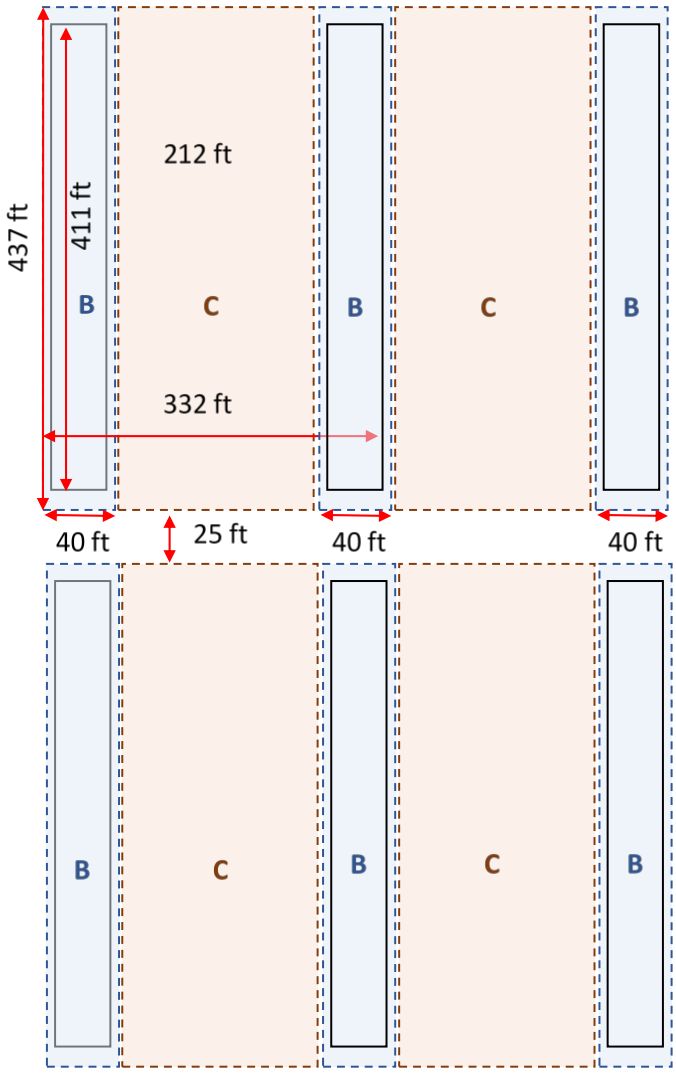

Figure Error! No text of specified style in document.**-7. Schematic of a generic chassis storage Model 1.**

A.3 Chassis Storage Model 2

The second chassis storing model is a simplified version of Model 1. The new model, termed Model 2 includes vertically stored chassis (bock “B”) and a peripheral access road, however it does not include a lot for temporary storage (block “C”). Instead, it employs a 150ft access area in-between each rack space as illustrated in Figure Error**! No text of specified style in document.**-8. The sub-block area in this model is, therefore, significantly smaller than that of Model 1. The number of chassis which could be stored in a lot with a given footprint using Model 2, is calculated in Table Appendix A-1, for different lot sizes.

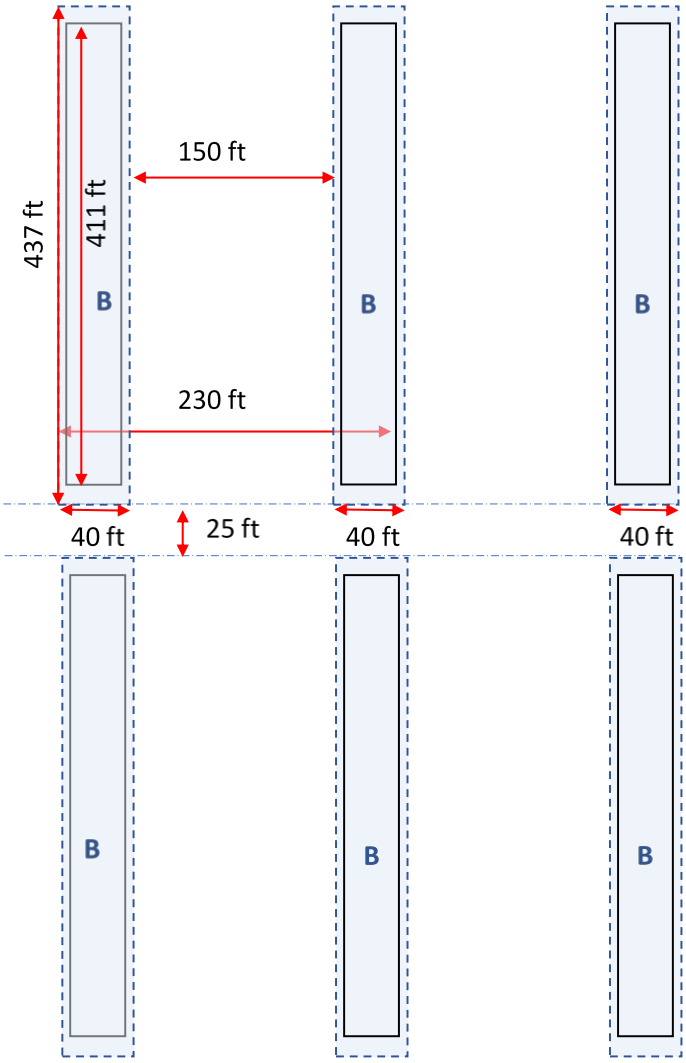

Figure Error! No text of specified style in document.**-8. Schematic of a generic chassis storage Model 2.**

A.4 Chassis Storage Model 3

This model is emulating the most commonly used chassis storage arrangement for the POLB and POLA. In this model, the chassis storage area is divided into two main blocks. Along the side of the front block, there is a 25ft wide road that provides access to both the front and back blocks of chassis. Within the front block the first row contains unstacked chassis that face outward and are ready to be picked up. In all other rows in the front and back blocks, the chassis are horizontally arranged, stacked on top of each other up to 3-high. The separation between each chassis is set at 2 feet in order to match typical measurements of spaces between stacked chassis. In-between the front and back blocks there is a 100 ft-wide road in which the chassis-handling equipment can operate. The equipment is stacking and unstacking chassis as necessary, in order to maintain the front row with chassis available for pickup, as well as with spaces ready for chassis drop-off (Figure **Error! No text of specified style in document.**-9. Schematic of a generic chassis storage Model 3.Figure Error**! No text of specified style in document.**-9). The spacing between chassis, the dimensions of the access roads and other parameters of interest for Model 3, are estimated based on current practice (Figure Error**! No text of specified style in document.**-10). The number of chassis which could be stored in a lot with a given footprint using Model 3, is calculated in Table Appendix A-1, for different lot sizes.

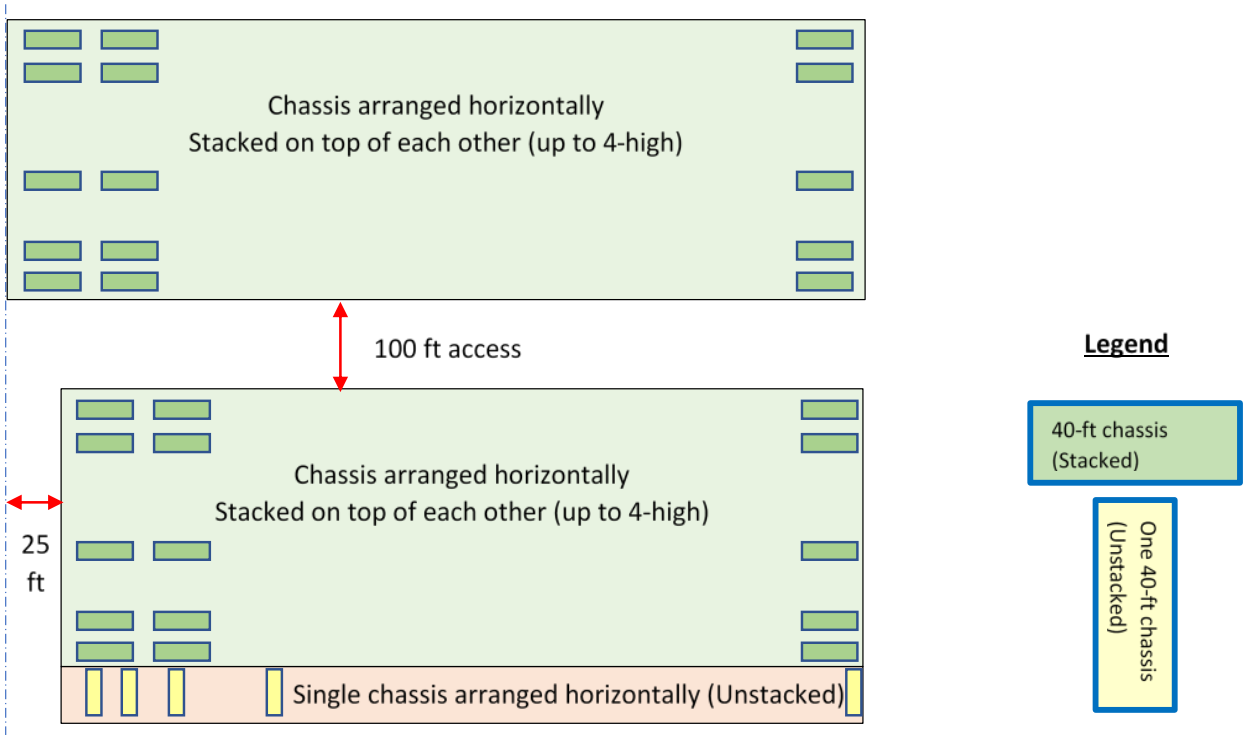

Figure Error! No text of specified style in document.**-9. Schematic of a generic chassis storage Model 3.**

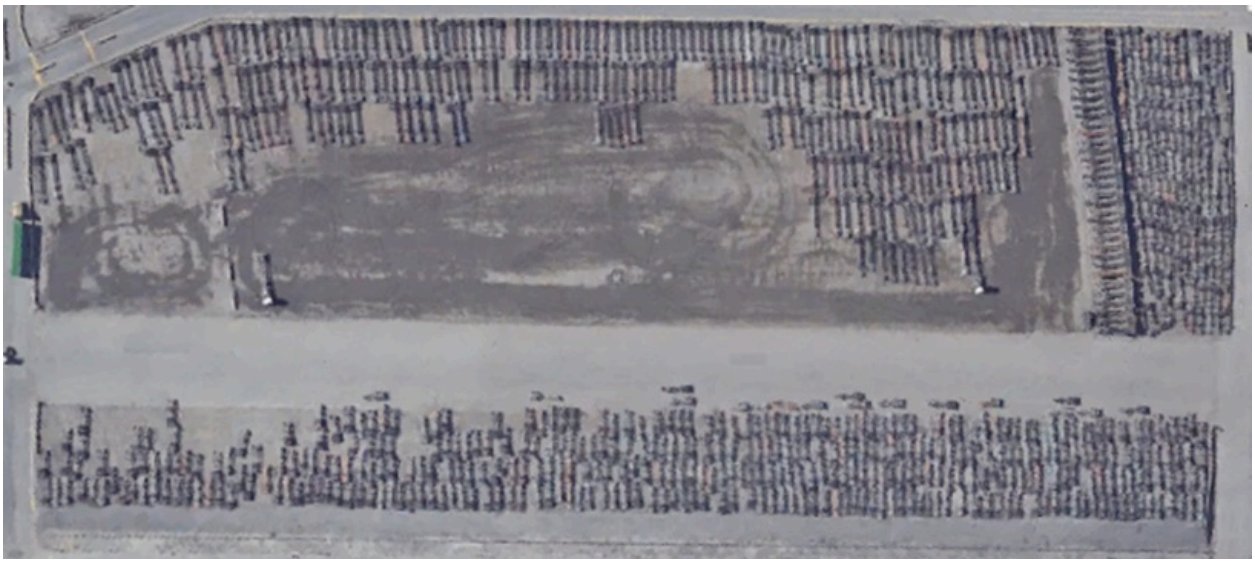

Figure Error! No text of specified style in document.**-10. Example of chassis storage Model 3 (Google Earth).**

A.5 Wheeled Containers (Model 4)

In this model containers are loaded directly onto chassis for storage. This approach at a chassis processing facility could be used to facilitate the pick-up process by minimizing pick-up time, hence reducing congestion within the ports. The import containers could be brought to the chassis processing facility during the night or at other off-peak hours and then they would be ready for a bobtail to pick them up during the day. Similarly, a trucking company could drop a container (on its chassis) for export at the facility, and the container and chassis could be brought to the port during off-peak hours. The storage model itself is similar to Model 3; however, in Model 4 there are roads in-between each row of chassis to allow for access for the bobtails to pick up the trailers (Figure Error**! No text of specified style in document.**-11).

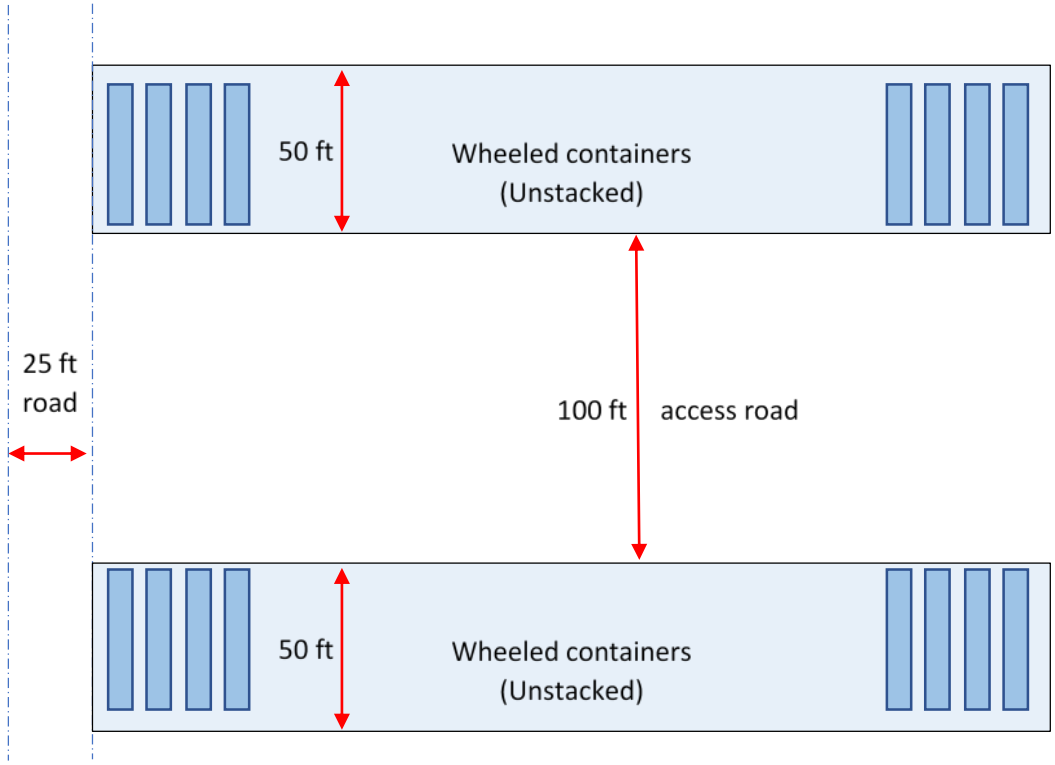

Figure Error! No text of specified style in document.**-11. Schematic of a generic chassis storage Model 4 (wheeled containers).**

A.6 Estimated CPF Storage Capacities

The estimated CPF storage capacities for the different storage arrangements (storage models 1-4) are calculated for various CPF footprints. The capacity calculations are based on the geometries presented in the previous sections, considering the areas required for chassis stacking plus the access roads. The results are presented in **Error! Reference source not found.** for different CPF footprints. The vertical stacking of chassis allows for faster stacking and unstacking times. The number of chassis which can fit in a given area, however, is larger when the horizontal arrangement is used, with chassis stacked on top of each other 3-high. The times to stack a chassis are estimated as approximately 60 seconds (model 3), or 35 seconds (models 1 & 2). The times to unstack a chassis are estimated as approximately 90 seconds (model 3), or 40 seconds (models 1 & 2). The configuration used in the current project is storage Model 3 (horizontal arrangement, with chassis stacked up to 3-high).

Table Appendix Error! No text of specified style in document.**-1. CPF capacity estimates for different stacking configurations.**

Storage Model	Lot size (ft^2)	Height of horizontal chassis stacks	Chassis storage capacity at location
Model 1	300x600	N/A	304
Model 1	1000x1000	N/A	1,824
Model 1	2500x2500	N/A	13,680
Model 1	5000x5000	N/A	57,760
Model 2	300x600	N/A	304
Model 2	1000x1000	N/A	3040
Model 2	2500x2500	N/A	18,240
Model 3	300x600	1	322
Model 3	1000x1000	1	2,052
Model 3	2500x2500	1	13,997
Model 3	5000x5000	1	57,972
Model 3	300x600	2	617
Model 3	1000x1000	2	4,007
Model 3	2500x2500	2	27,747
Model 3	5000x5000	2	115,447

Storage Model	Lot size (ft^2)	Height of horizontal chassis stacks	Chassis storage capacity at location
Model 3	300x600	3	912
Model 3	1000x1000	3	5,962
Model 3	2500x2500	3	41,497
Model 3	5000x5000	3	172,922
Model 3	5000x5000	4	230,397
Model 4	1000x1000	1	880
Model 4	5000x5000	1	22,600